A BALLOON-BORNE INTERFEROMETER

for

INFRA-RED AERONOMY

Thesis presented for the degree

of Doctor of Philosophy

by

Keith Harwood, B.Sc. Hons.

UNIVERSITY OF ADELAIDE

1 9 7 2

ACKNOWLEDGEMENTS

I would like to thank my supervisors, Professor J.H. Carver and Doctor A.G. Gregory, for their help and encouragement during the preparation of the work described herein. I would also like to thank Mr. K. Merry who constructed the interferometer, Doctor P. Davidson for his valuable advice on the design and execution of balloon experiments, Mr. J. Hillier and the staff of the Balloon Launching Station for their assistance in the preparation of the two balloon flights and performing the flights, Doctor R. Clay whose assistance before the second flight was invaluable and Mr. J. Bibbo who also assisted during the second flight.

A BALLOON-BORNE INTERFEROMETER

for

INFRA-RED AERONOMY

This thesis contains no material which has been accepted for the award of any other degree or diploma in any University and, to the best of my knowledge and belief, contains no material previously published or written by any other person, except where due reference is made in the test of the thesis.

AN INTERFEROMETER FOR INFRA-RED AERONOMY

This thesis describes the design and construction of an infra-red interferometer used as a Fourier transform spectrometer. The interferometer is intended for a specific experiment to measure the vertical distribution of water vapour and carbon dioxide. Water vapour, carbon dioxide and some minor constituents of the atmosphere absorb infra-red radiation strongly in a number of broad bands. The total absorption in a band is not directly related to the amount of absorber. The amount of the absorber can be deduced from the shape of the absorption spectrum. Every band in the sun's spectrum is the result of the overlap of bands of two or more atmospheric constituents. A technique called spectrum stripping is used to separate the spectrum of each constituent from the observed spectrum. Estimates of the amounts of each absorber are made and their spectra calculated. These spectra are subtracted from that observed and the difference gives improved estimates. The process is repeated until the difference between observed and calculated spectra is zero. A wide-band spectrometer is required to measure the amount of absorber. If such a spectro-

meter is mounted on a balloon and spectra are taken at increasing altitudes, the spectra can be analysed to give the amounts of absorber above each altitude. This gives the vertical distribution of the different constituents of the atmosphere. All possible types of spectrometer were considered. The one chosen for this experiment was a single channel interferometer used as a Fourier transform spectrometer. This interferometer is of a class not previously used for this work - a wave-front division instrument based on Young's double slit interferometer. It contains no refracting or absorbing components and is an inherently broad-band instrument. It covers the band from 500 to 5000 cm^{-1} with a maximu resolution of 10 cm^{-1}. It is also capable of absolute intensity measurements.

The full advantage of Fourier transform spectroscopy can only be realised if the data is recovered accurately and reliably. A telemetry system has been developed for this experiment which transmits one data point every 1.6 seconds, together with extensive calibration and engineering data. The data channels have an accuracy of better than 0.1% and are digitally encoded with sufficient redundancy for error checking and correcting. This data can be recorded on paper tape for subsequent computer processing.

CONTENTS

		Page
CHAPTER ONE	Introduction	1
1.1	The Infra-red Interferometer	3
1.2	History of Fourier Transform Spectroscopy	4
CHAPTER TWO	Nature of the Atmospheric Absorption	10
2.1	The Minor Constituents	10
2.2	Theoretical Studies	11
2.3	Measurements of the Absorption	19
2.4	Measurement of the Amount of Absorber	23
CHAPTER THREE	Spectrometry	25
3.1	Classification of Spectrometers	26
3.2	Fourier Theory of Diffraction	27
3.3	Specific Spectrometers	29
CHAPTER FOUR	The Interferometer	44
4.1	Theory of the Interferometer	44
4.2	The Optical Path	49
4.3	The Mechanical Construction	51
4.4	Aligning the Interferometer	63
4.5	Testing the Interferometer	68
4.6	Comparison with other Instruments	73

CONTENTS (Cont.)

		Page
CHAPTER FIVE	The Telemetry Unit	76
5.1	Requirements of the Telemetry	77
5.2	Overall Design	80
5.3	Circuit Description	86
CHAPTER SIX	Data Processing	104
6.1	The Data Link	104
6.2	The Punching Convention	107
6.3	The Computer Program	109
CHAPTER SEVEN	Results	123
7.1	The First Flight	124
7.2	The Second Flight	130
CHAPTER EIGHT	Conclusion	138

CHAPTER ONE

INTRODUCTION

The radiation from celestial objects carries a great deal of information about the chemical and physical properties of the objects. Most of this information is lost when the radiation is absorbed by the Earth's atmosphere. In the past, instruments have been developed to recover as much information as possible from the radiation which does reach the surface of the Earth. The most important instrument for measuring the quality of the radiation is the spectrometer. Many different forms of spectrometer have been developed to analyse the visible and radio radiation which penetrates the atmosphere. Recently it has become possible to perform measurements with experiments flown on balloons, rockets and satellites. Many of the techniques developed for spectroscopy in ground based experiments are inappropriate, inapplicable or impossible in a space environment.

Spectrometers intended for use in space will differ in many ways from one which is used on the ground. Firstly, they will analyse wavelengths which are substantially different from those studied from the ground. Detectors suitable for the wavelengths which are absorbed in the atmosphere have not been developed to the same extent as those for wavelengths which are transmitted. Optical materials may not be available for the unusual wavelengths and sometimes a method which is well known and understood at one wavelength may be physically impossible at another. Secondly, the instrument must operate in an unfamiliar environment. All instruments which measure radiation which is absorbed by the atmosphere must operate in a vacuum. They must be able to withstand shocks and vibration, extremes of temperature and often high energy radiation. Thirdly, they must operate automatically or by remote control without fault for periods from minutes, in rocket experiments, to months in the case of satellite experiments. They must be capable of self-calibration or be extremely stable in calibration. They must be capable of recording their results, or of transmitting them to the ground. Sometimes they must be capable of repairing themselves. Fourthly, their physical realisation is constrained by matters which have nothing to do with the experiment. Almost invariably they must be light in weight. They must either be small in size or capable of erecting themselves.

1.1 The Infra-red Interferometer.

This thesis describes an interferometer which is designed for use as a Fourier transform spectrometer. It covers the wavelength range from two to twenty microns. These wavelengths are strongly absorbed by the water vapour and carbon dioxide in the atmosphere. The instrument was designed to measure the concentrations and distributions of these in the atmosphere. The interferometer is carried by a balloon and measures the spectrum of the sun at different altitudes during the ascent.

1.1.1. Outline of the Theory.

The interferometer is developed from Young's double slit interferometer. The wave-front of the light entering the interferometer is split into two beams by two slits. The light from the slits is focussed onto an infra-red detector. There is a variable path difference between the beams from the two slits. By varying the path difference, the interference pattern at the detector changes and the intensity measured as a function of the path difference, called the interferogram, is the Fourier transform of the spectrum of the radiation.

1.1.2. Detectors.

Many detectors are available for the wavelength range covered by this interferometer. They fall into two classes, thermal and photon detectors. The photon detectors measure individual photons. Those which cover only the shorter wave-lengths need liquid neon

or liquid air cooling. These detectors were rejected for use in the interferometer on the grounds of both cost and difficulty of maintaining the coolant in a low pressure environment. The thermal detectors integrate the energy of many photons to produce a rise in temperature of a sensitive element. These are far less sensitive than the photon detectors, but they operate without special cooling. They are readily available, robust and the Barnes thermistors chosen for this experiment have been used in space experiments before. The nature and properties of infrared Detectors are reviewed by Potter and Eisenman (1962).

1.1.3. Components.

The interferometer has been designed so that the only optical components are either slits or mirrors. There are no refracting or absorbing components so that the interferometer can operate over the whole wavelength range for which the diffraction theory of chapter three, below, is valid. The mirror surfaces are aluminium which has 99% reflectivity over the two to twenty micron band.

The interferometer is mechanically robust since there are only four moving parts, the rotor of an electric motor, a micrometer screw, a lever and a mirror.

1.2 History of Fourier transform spectroscopy.

The first use of interferometry as a means of spectrometry was made by Fizeau in 1862. Fizeau set up a Newton's rings apparatus

in which the spacing between a lens and flat plate was variable. He measured the visibility of the rings at increasing separations. He found that the visibility of the rings in sodium light varied approximately with the cosine of the separation and deduced that the D line of sodium was a doublet with a separation of about six Angstroms.

In 1890, Michelson used the interferometer which he had designed to measure the motion of the Earth through the aether, to test for hyperfine structure in spectral lines. Michelson's immediate purpose was not the measurement of the structure of the spectra, but the search for a very narrow line for use as a standard of length. The interferometer consisted of a pair of mirrors and a beam splitter. The degree of interference depended on the difference in the path lengths from the beam splitter to the two mirrors. The path difference could be made very large, so that the method could measure very narrow lines. Michelson defined the visibility as the ratio of the intensities of the bright rings and dark rings. He was able to measure the separations of several doublets and to show that other lines had complex fine structures, but was not able to interpret the visibility curves. He found that the red line of cadmium was a single line and chose it as his standard of length. In 1892, Raleigh showed that it was possible to determine the spectrum from visibility curves only if the spectrum was symmetrical. He showed that the intensities of the maxima and minima of the interference pattern contained a great

deal of information about the spectrum. The visibility curve is the envelope of the extrema of the interference pattern and contains far less information.

The first direct use of the interference pattern was made by Rubens and Wood in 1910. They were measuring the properties of various infra-red sources at long wavelengths where the sources were weak. Their interferometer was similar to Fizeau's, consisting of a pair of flat plates with a variable separation. By measuring the intensity of the radiation transmitted by the plates at different separations they obtained the first interferogram to be published. They did not show that the interferogram was the Fourier transform of the spectrum. Nor did they use the inverse Fourier transform to recover the spectrum. They assumed the shape of the spectrum and constructed the interferogram that this would produce. They then compared the calculated interferogram with that actually measured and adjusted the spectrum until the two interferograms were the same.

The measurement of spectra by interferometry remained a seldom used and specialised technique until after the Second World War. It was devoted to the measurement of the hyperfine structure of spectral lines. In 1948 Jaquinot showed that the Michelson interferometer had a substantial advantage over the grating spectrometer and the prism. The Michelson interferometer can accept radiation from a large area. The other two must pass the radiation to be analysed through a slit which restricts the acceptance angle to one dimension. In Chapter three, below, all

spectrometers are considered to be interferometers. The Jaquinot advantage is common to all amplitude division interferometers.

In 1952, Fellgett applied the name 'Fourier transform spectroscopy' to the technique of measuring spectra with an interferometer. He discovered that the method has an advantage which is not as general as the Jaquinot advantage, but is of more value in practice. He showed that the spectrum is multiplexed in the measurement. That is, all spectral elements are present in the measured signal at all times. When the intensity of the radiation is measured by a detector which generates a constant amount of noise the signal to noise ratio of the spectrometer is increased over that of a spectrometer in which the spectrum is not multiplexed. If the spectrum has N spectral elements, the signal to noise ratio is greater by a factor of $\sqrt{N}$. Rubens and Wood evidently achieved the multiplex advantage, but they did not appreciate its value. Later workers with interferometry were dealing with spectra with only a few spectral elements so that they did not gain much from the advanatage. To demonstrate his theories, Fellgett used a very simple interferometer. One optical flat rested on another with a thin wedge of air between them. Light was passed through the wedge to form a thin film interference pattern. A detector was passed across the pattern from the point of contact of the flats, the zero path difference position, to the thick end of the wedge. The output of the detector was a measure of the intensity of the light as a function of path difference, that is, an interferogram. This inter-

ferogram was the Fourier transform of the spectrum of the light and Fellgett recovered the spectrum using the inverse Fourier transform. In order to combine the advantages of the diffraction grating Strong, 1956, developed a lamellar grating interferometer. Like the instrument described in chapter four, below, Strong's interferometer was constructed without any refracting or absorbing components. Unlike the instrument of chapter four, however, it did not produce the Fourier transform of the spectrum, so that the spectrum was not multiplexed and the instrument did not have the Fallgett advantage. It did have the Jaquinot advantage and it was used for infra-red astronomical studies.

The first astronomical use of Fourier transform spectroscopy was made by Gebbie, Delbouille and Roland during the years 1957 to 1964. They obtained high resolution spectra of Venus and Jupiter. During the same period, P and J Connes were developing a Michelson interferometer with a maximum path difference of two meters. This was designed for a very high resolution spectroscopy (resolution better than $10^{-2}cm^{-1}$.) It was used at the Jungfraujoch Observatory to produce very high resolution spectra of Venus in the wave-band from one to three microns.

The first time a Fourier transform spectrometer was flown in a balloon was in 1964. Gush obtained spectra of the sun in the one to three micron region with a resolution of about 10 cm^{-1}. Later interferometers flown concentrated on the far infra-red, that is between twenty and two hundred microns. Each instrument obtained

spectra over only part of this region. So far the only celestial object studied by balloon borne interferometers has been the sun.

A Michelson interferometer has been flown in the Nimbus 3 satellite. The investigators, Hanel and Conrath have published spectra obtained with this instrument, which covers the waveband from five to twenty-five microns.

One of the most important contributions to Fourier transform spectroscopy was made by the mathematicians Cooley and Tukey. In 1958 they developed an algorithm for calculating the Fourier transform. In previous methods of performing the Fourier transform numerically, the number of calculations was proportional to the square of the number of data points transformed. Even with the use of digital computers, the cost of performing the calculations prevented the use of Fourier transform spectroscopy when the spectrum to be found contained many spectral elements. The fast Fourier transform algorithm developed by Cooley and Tukey required $N \log_2 N$ calculations where N is the number of data points. Thus for a spectrum of one thousand elements, the conventional method of performing the Fourier transform required a million calculations whereas the fast Fourier transform required only ten thousand.

CHAPTER TWO

THE NATURE OF THE ATMOSPHERIC ABSORPTION

2.1 Nitrogen and oxygen together make up ninety-nine percent of the Earth's atmosphere and absorb less than one percent of the sun's radiation. The minor constituents, chiefly water vapour, carbon dioxide and ozone, absorb about twenty percent of the radiation. Over the past several years, members of the University of Adelaide, Physics Department have been measuring the distribution of oxygen and ozone in the atmosphere using the absorption of the sun's ultra-violet radiation. Ultra-violet detectors are mounted on a balloon, rocket or satellite and the intensity of the sun's radiation measured as the vehicle ascends. The absorption is found from the intensities and the amount of absorber at the different altitudes computed. It is proposed to use the infra-red absorption of water vapour and carbon dioxide in a similar manner to measure their distributions. This chapter considers the nature of the absorption and the relation between the amount of absorption and the amount of absorber. The discussion follows approximately that of Goody (1964).

2.2 Theoretical Studies.

2.2.1. Definitions.

Lambert's law of absorption states that equal amounts of a given absorber absorbs equal fractions of incident radiation. At a given frequency ν the transmission, the ratio between incident and transmitted intensities, is given by $T(\nu) = \exp(-k(\nu)a)$ where a is the amount of absorber in the beam and $k(\nu)$ is the absorption coefficient. The absorption is given by $A(\nu) = 1-T(\nu)$. The transmission cannot be measured at one frequency and so the mean transmission over a finite band of frequencies must be measured. The mean transmission is in general a function of both the amount of absorber and the bandwidth $\Delta\nu$ of the measurement. It is given by $\bar{T}(\nu_o) = \frac{1}{\Delta\nu} \int_{\Delta\nu} \exp(-k(\nu)a)d\nu$.
The mean absorption is given by

$$\bar{A}(\nu_o) = 1-\bar{T}(\nu_o) = \frac{1}{\Delta\nu} \int_{\Delta\nu} \{1-\exp(-k(\nu)a)\}d\nu$$

The total absorption of a spectrum is given by

$$W(a) = \int_{-\infty}^{\infty} A(\nu)d\nu = \int_{-\infty}^{\infty} \{1-\exp(-k(\nu)a)\}d\nu$$

The relation between the total absorption and the amount of absorber is called the curve of growth. The total absorption cannot be measured over the whole electro-magnetic spectrum, but it is possible to measure it over a band-width which includes the whole of a line or band and for which the absorption at the band limits is zero. The total absorption of a band is defined as

$$\int_{\nu_1}^{\nu_2} A(\nu)d\nu$$

The total absorption of a band can be measured by the integral of the mean absorption

$$\int_{\nu_1}^{\nu_2} \bar{A}(\nu)d\nu = \int_{\nu_1}^{\nu_2} \frac{1}{2h} \int_{\nu-h}^{\nu+h} A(\nu^1)d\nu^1 \, d\nu$$

$$= \int_{\nu_1}^{\nu_2} \frac{1}{2h} \int_{-h}^{h} A(\nu+\delta)d\delta \, d\nu$$

where $\nu^1 = \nu+\delta$

Expanding the absorption as a Taylor series

$$\int_{\nu_1}^{\nu_2} \bar{A}(\nu)d\nu = \int_{\nu_1}^{\nu_2} \frac{1}{2h} \int_{-h}^{h} (A(\nu)+\delta A'(\nu)+\frac{\delta^2}{2} A''(\nu)+\ldots)d\delta \, d\nu$$

$$= \int_{\nu_1}^{\nu_2} \frac{1}{2h} (2hA(\nu)+0+\frac{h^3}{3} A''(\nu)+\ldots)d\nu$$

$$= \int_{\nu_1}^{\nu_2} A(\nu)d\nu+\frac{h^2}{6} \int_{\nu_1}^{\nu_2} A''(\nu)d\nu+\ldots$$

$$= \int_{\nu_1}^{\nu_2} A(\nu)d\nu+\frac{h^2}{6} (A'(\nu_2)-A'(\nu_1))+\ldots$$

If the absorption is zero over a finite bandwidth at ν_1 and ν_2 then the second and higher terms vanish. The integral of the mean absorption over a band is equal to the total absorption of the band provided that the mean absorption at the band limits is zero. Thus, the total absorption of a band can be measured by an instrument with any bandwidth.

2.2.2 Vibration-rotation bands.

The infra-red spectrum of the sun shows a number of broad absorption bands. The bands have been identified as the vibration bands of water vapour, carbon dioxide and ozone in the Earth's atmosphere. Other constituents such as carbon monoxide, nitrous oxide, methane and hydrogen deuterium oxide have been identified in the spectrum. Nitrogen and oxygen are homonuclear molecules which do not have any vibration spectrum. A molecule with N atoms has 3N degrees of freedom. Translation and rotation account for six degrees of freedom (five in a linear molecule) and the remainder belong to modes of vibration. The energy of vibratory transition is of the order of 0.1 eV, corresponding to a wave-number of about 800 cm^{-1}. The fundamental lines of the vibration spectrum of atmospheric molecules lie in the region 600 to 4000 cm^{-1}. The energy of a rotatory transition is of the order of one thousandth of the energy of a vibrational transition. Consequently, vibrational transitions are accompanied by rotational ones which split one line into a broad band of lines. The bands are called vibration-rotation bands.

2.2.3. Broadening of the Lines.

It is observed that the individual lines in the vibration-rotation bands have finite widths. There are three mechanisms which broaden the lines. Each line has a natural width which depends on the undisturbed life-times of the upper and lower states of the transition. If the life-time is small and, by the uncertainty principle, the uncertainty in the energy of the state is large.

The observed width of a line can never be less than the natural width. The thermal motions of the molecules of a gas lead to Doppler broadening. A molecule travelling towards the source of radiation will absorb photons with a lower frequency than one travelling away from it. The line width depends on the mass of the molecule and the temperature of the gas. Doppler broadening is important in the atmosphere at altitudes greater than a few tens of kilometres. The third source of broadening is the inter-molecular collisions which occur during the absorption process. Two cases must be distinguished, collision with non-absorbing molecule and collision with a molecule of the same species. This latter case is called self-broadening. In the atmosphere, collision broadening is the principle source of broadening. Since the absorbing components constitute less than 0.03% of the atmosphere, self-broadening is not important. Collision broadening is also called Lorentz broadening.

2.2.4. The Lorentz Line profile.

The absorption coefficient $k(\nu)$ expressed as a function of wavelength is called the line profile. It was shown by Lorentz (1906) that the line profile of a collision broadened line is given by

$$k(\nu) = \frac{s}{\pi} \frac{\alpha}{(\nu-\nu_0)^2+\alpha^2}$$

where $s = \int_{-\infty}^{\infty} k(\nu)d\nu$ is the strength or intensity of the line, α is the half width of the line at half maximum and ν_0 is the centre frequency of the line. The strength and central frequency of the

line depends on the particular transition involved and the strength may also depend on temperature. The half-width can be found from kinetic theory. In general it depends on the masses and collision cross-sections of every molecular species present. For the case in which the absorbing gas is diluted by a non-absorbing gas, the half-width is given by $\alpha=\alpha_o\frac{P}{P_o}\sqrt{\frac{To}{T}}$ ... 2.2.1.

where P is the pressure of the mixture, T its temperature and α_o is the half-width at a standard pressure P_o and temperature T_o.

Ladenberg and Reiche (1913) found that the total absorption of a Lorentzian line is given by

$$W(a) = \int_{-\infty}^{\infty}\{1-\exp(-k(\nu)a)\}d\nu$$

$$= 2\pi\alpha x \exp(-x)[J_o(ix)-iJ_1(ix)]$$

where $x = \frac{Sa}{2\pi\alpha}$ and J_o and J_1 are the Bessel functions. The total absorption depends not only on the amount of the absorbing gas but also on the amount of diluting gas and the pressure and temperature of the mixture. The curve of growth for a single line has two asymptotic regions. When x is small, that is, either the amount of absorber is small or the pressure (and hence the half-width) is large, the curve of growth is given approximately by $W(a) = Sa$ ... 2.2.2. This is called the weak line approximation. When x is large, the curve of growth is given by $W(a) = 2\sqrt{Sa\alpha}$ ... 2.2.3. which is the strong line approximation. The physical significance

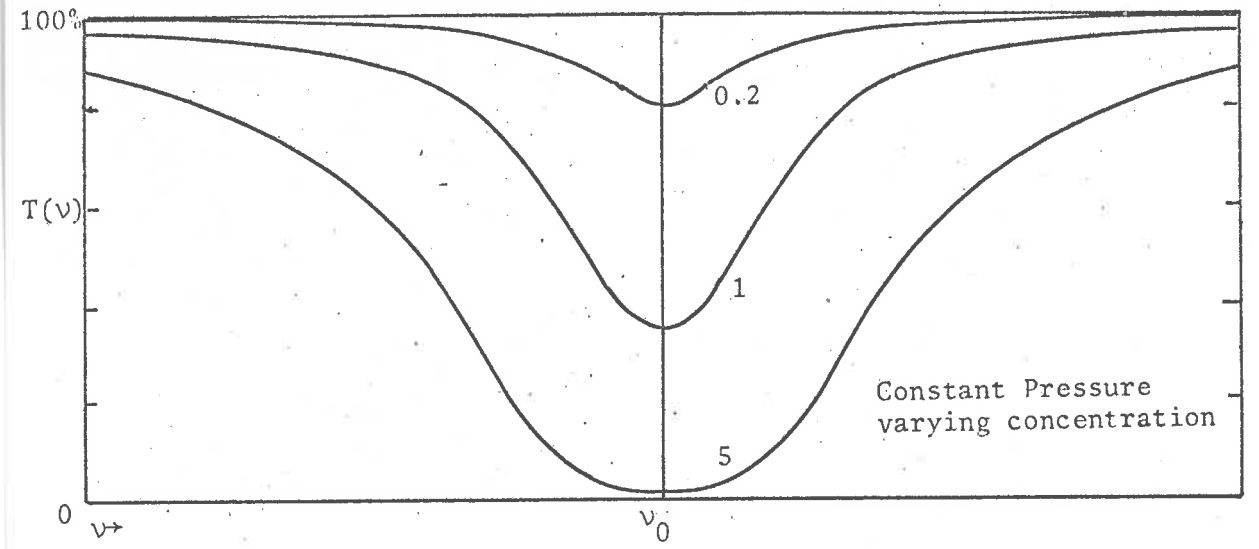

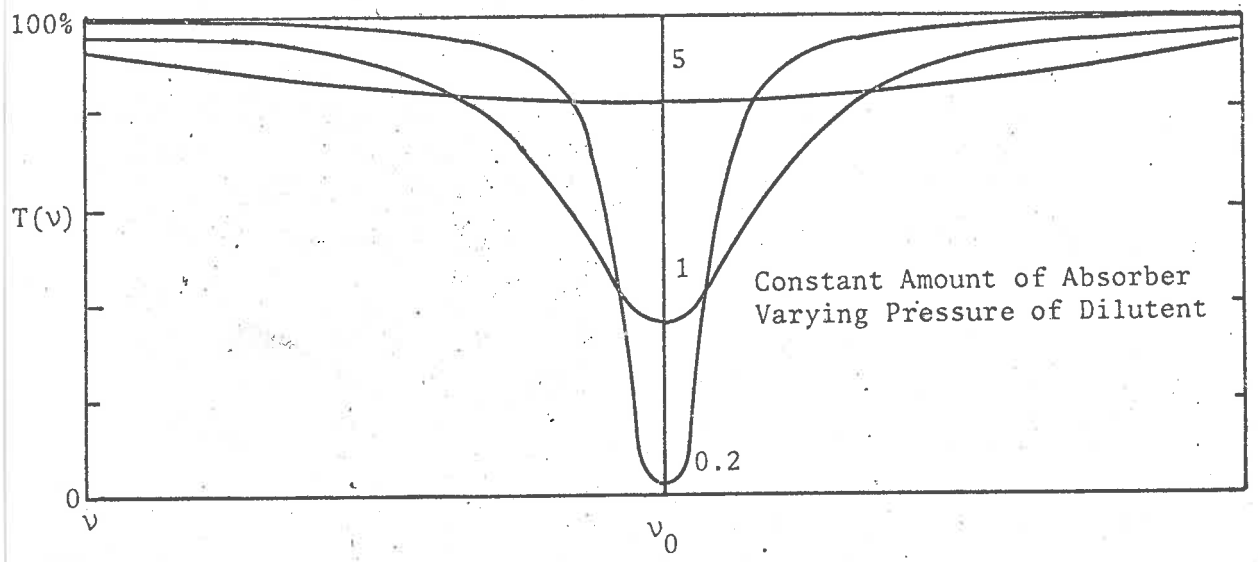

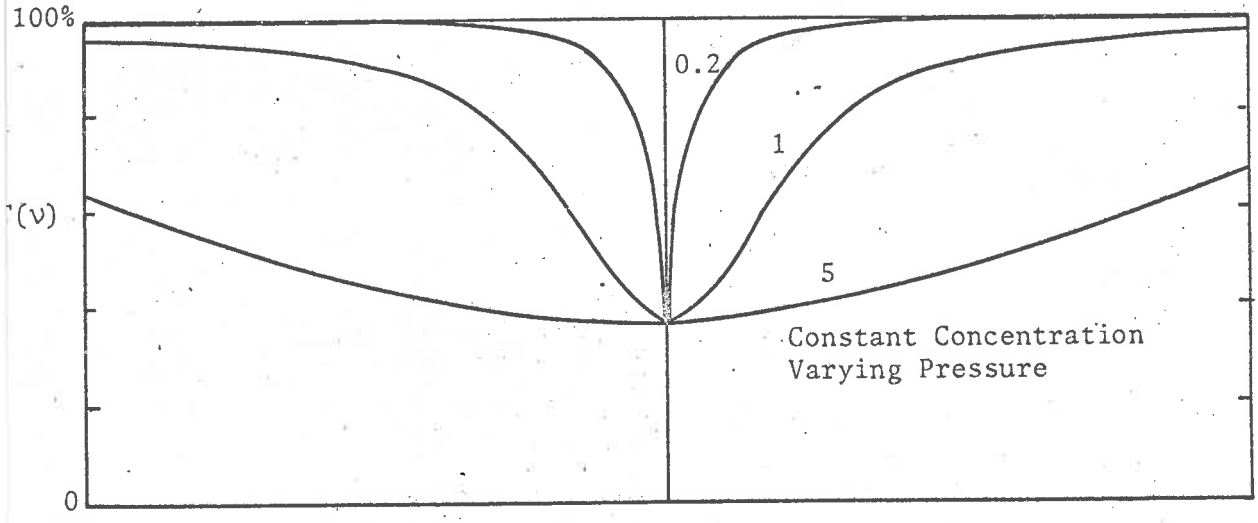

Figure 2.1

Lorentzian Line Profiles.

of these two regions is illustrated in figure 2.1. The transmission of a dilute absorber is shown as a function of frequency. The first case is for constant total pressure and concentration of absorber in the ratio 0.2 to 1.0 to 5.0. When the amount of absorber is large, the transmission near the centre of the line is very small, and any increase in total absorption must take place in the wings of the line. This region of zero transmission is also important when considering overlapping lines. The second case illustrates pressure broadening. The amount of absorber is constant and the pressure of the diluting gas is increased. At low pressure the line is narrow and the total absorption is given by the strong line approximation. As the pressure increases the line becomes wider, the total absorption increases, and at high pressure the total absorption is given by the weak line approximation. In the third case the concentration of the absorber is constant and the transmission for different total pressures is shown. The degree of approximation is the same at all pressures. Thus, if the strong line approximation holds for a particular mixture of gases at some pressure, it holds for all pressures for which collision broadening is the main source of broadening.

2.2.5. Bands of Lorentzian Lines.

If an absorption band consists of a number of Lorentz profile lines which do not overlap, the total absorption is the sum of the absorptions of each line. The curve growth for such a line has the same form as that for a single line. This model of a band corresponds to the case in which the lines are widely spaced and the pressure is

low. At higher pressures the greater widths of the lines will cause them to overlap. If two lines overlap the transmission at a particular frequency is the product of the transmissions of each line. Thus, the overlapping part of a line contributes less to the total absorption than it would if not overlapping. When the absorption is strong, the wing of one line will overlap the central part of another. Since the transmission of the central part is very small, the wing of the other line will contribute very little to the total absorption. If, in a particular mixture of gases, the absorption lines are strong and not overlapping the total absorption will follow the square root law of the strong line approximation of equation 2.2.3. At high pressure the lines will overlap and the total absorption will increase more slowly than the square root law.

2.2.6. The Regular line Model Band.

There are two physically distinct, two-parameter models of absorption bands. The Elsasser Model (Elsasser, 1942) assumes that the band consists of identical, equally spaced lines with the Loretz profile. If the lines have spacing d and strength S then the absorption coefficient is given by $k(\nu) = k'(s) = \frac{S}{d}\frac{\sinh \beta}{\cosh \beta - \cos s}$ where $s = \frac{2\pi\nu}{d}$ and $\beta = \frac{2\pi\alpha}{d}$. The mean absorption is given by

$$\bar{A} = \frac{1}{2\pi}\int_{-\pi}^{\pi}(1-\exp(-k'(s)a))ds$$

There are three asymptotic forms. Firstly, when the half-width of the lines is much greater than the spacing between them, that is $d << \alpha$, then $\sinh \beta \to \cosh \beta \to \infty$ and the mean absorption is $\bar{A} = 1-\exp(-\frac{Sa}{d})$.

The absorption is now independent of pressure and temperature and depends only on the concentration of the absorber. This is Beer's law of absorption. When the absorption is weak and the half-widths are much less than the line spacing, the model gives the same curve of growth as the non-overlapping case. When the absorption of the lines is strong and the half-widths much less than the spacing, $y \to 0$ which gives $\sinh \beta = \beta$ and $\cosh \beta = 1$. The mean absorption is given by $A = \text{erf} \frac{\ell a}{2}$ where $\ell = \frac{2\pi\alpha S}{d^2}$ is called the generalised absorption coefficient. A broad band can be considered as if it were divided into a number of bands, each with its own absorption coefficient. This assumes that the absorption contributed by lines outside the band equal the absorption outside the band due to lines within it. Thus the generalised absorption coefficient can be measured experimentally as a function of frequency and the absorption is given by $\bar{A}(\nu) = \text{erf} \frac{\ell(\nu)\alpha}{2}$. The coefficient can be modified for other temperatures and pressures using equation 2.2.1.

2.2.7. The Random Model Band.

The random model, first proposed by Goody, 1952, of an absorption line assumes that the line spacings are random, and the mean value of the spacing is d, that the line intensities are given by the Poisson d tribution with mean line strength S, and that there is no correlation between position and strength of the lines. The mean absorption of a band is given by

$$\bar{A} = 1 - \exp\left\{\frac{-S_o \alpha a}{d\left(\alpha^2 + \frac{S_o \alpha a}{\pi}\right)^{\frac{1}{2}}}\right\}$$

This model also has three asymptotic forms. Two, for the broad line case and the non-overlapping cases, are the same as for the Elsasser model. The strong line approximation is given by

$$\bar{A} = 1-\exp\left(-\frac{\sqrt{\pi S_o \alpha a}}{d}\right)$$

It is possible to divide a band into a number of narrow bands in the same way as for the Elsasser model and treat each band separately. The mean line strength S can be measured as a function of frequency and the absorption curve is given by

$$\bar{A}(\nu) = 1-\exp\left(\frac{-S_o(\nu)\alpha a}{d(\alpha^2+\frac{S_o \alpha a}{\pi})^{\frac{1}{2}}}\right) \qquad \ldots 2.2.4.$$

Using equations 2.2.1 and 2.2.4 it is possible to calculate the absorption spectra of atmospheric constituents which approximate to those models. Only one spectrum for a standard temperature and pressure is needed. The spectra under other conditions can be found using equation 2.2.4.

2.3. Measurements of the Absorption.

A group at Ohio State University has measured the absorption spectra of many of the minor constituents of the atmosphere. The results of these measurements have been published in two reports of the Air Force Cambridge Research Laboratories. The first report by Howard, Burch and Williams (1957) treated water vapour and carbon dioxide. The second by Burch, Gryvnak, Singleton, France and Williams (1962) treated the weaker bands of carbon dioxide,

nitrous oxide, carbon monoxide and methane. An infra-red beam was passed via a set of mirrors through an absorption cell. The cell was filled with measured amounts of the absorber and some non-absorbing dilutant gas. The dilutant was normally nitrogen. The path length of the beam could be varied to a maximum of about 2000 metres. The amount of absorber a in the beam, the partial pressure of the absorber p_a and the partial pressure of the dilutant p_d were known. The total absorption for each band was measured from the spectra. The Ohio group found that the total absorption could be expressed as a function of amount of absorber in one of the two forms

$$W(a) = c\, a^d\, p_e^k$$

and

$$W(a) = C + D \log a + K \log p_e$$

where $p_e = p_d + Bp_a$ is the effective pressure. The constants c, d, k, C, D, K, and B, were determined empirically. The first form above refers to values of total absorption less than W_c which also determined for each band. The second for, holds for values greater than that amount. B is a measure of the self broadening of the absorber.

2.3.1. Water Vapour.

The theory of water vapour absorption is given by Herzberg, 1945. The water molecule has three atoms and is non-linear. It has three degrees of vibratory freedom. The three modes of vibration are shown in the diagram.

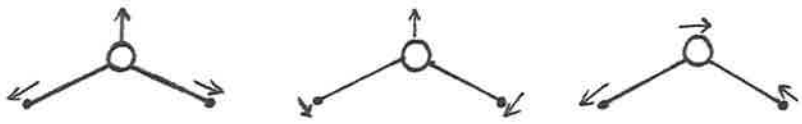

ν_1 ν_2 ν_3

The frequencies of the three modes are ν_1, ν_2 and ν_3 with the corresponding wave numbers 3657.05, 1594.78 and 3755.92 cm^{-1}. The most important bands are the fundamentals and the harmonic $2\nu_2$. The close coincidence between ν_1, ν_3 and $2\nu_2$ produces one broad band of absorption. Other bands are mixtures of both combination and overtones. The three moments of inertia of the water molecule are all different so that the individual lines in the bands show an apparently random and chaotic structure. The random model of the absorption bands fits the water vapour bands very well. In addition to the total absorption measurements, Howard, Burch and Williams determined the values for the constants in equation 2.2.4. They give the following expression for the fractional absorption

$$\bar{A} = 1-\exp\left\{\frac{-1.97a/a_o}{(1+6.56a/a_o)^{\frac{1}{2}}}\right\}$$

Goody points out that to properly include the pressure dependence the expression should be

$$\bar{A} = 1-\exp\left\{\frac{-1.97(p_o/p)(a/a_o)}{(1+6.56(p_o/p)^2(a/a_o))^{\frac{1}{2}}}\right\}$$

Values of a_o are given, and with the above equation it is possible to approximately reproduce the spectrum for any amount of water vapour and any pressure. Figure 2.2 shows $\bar{A}$ as a function of a/a_o.

2.3.2. Carbon Dioxide.

The carbon dioxide molecule has three atoms and is linear. It has four degrees of vibrational freedom and the four modes of vibration are shown in the diagram.

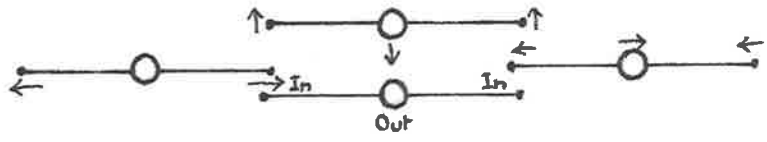

ν_1 ν_2 ν_3

The frequencies of the modes are ν_1, ν_{2a}, ν_{2b} and ν_3. The second and third modes are identical for a molecule at rest, but different when a molecule is rotating.

The first mode of vibration does not have a dipole moment so that there is no absorption at that frequency. The first mode appears only in combination with the other modes. The fundamental vibrations produce the strongest bands in the spectrum. The ν_2 and ν_3 fundamentals have wave numbers of 667.40 and 2349.16 cm^{-1} and overtone bands are more important in carbon dioxide than in water vapour. The band between 500 and 800 cm^{-1} includes fourteen combination bands in addition to the fundamental. Because of the symmetry of the carbon dioxide molecule the individual lines of the absorption bands are regularly spaced and the Elsasser model of the absorption bands fits the observations very well.

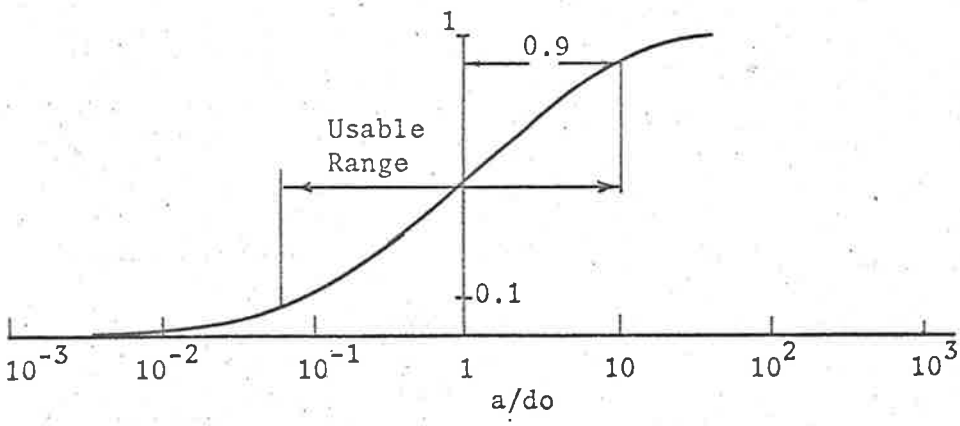

Figure 2.2

Absorption as a function of Concentration for the Random Model.

2.4. Measurement of the amount of absorber.

It is possible to measure the amount of absorber from either the mean absorption at some frequency or from the total absorption over a band. The mean absorption has two drawbacks as a method of measuring the amount of absorber. The measured value of the mean absorption depends on the bandwidth of the measuring instrument. An instrument for measuring the amount of absorber from the mean absorption needs to be calibrated by actual measurement of known amounts of absorber under varying conditions of temperature and pressure. The second drawback is that the mean absorption must lie between zero and one. For small amounts of absorber the atmosphere will appear completely transparent. For large amounts of absorber the radiation will be completely absorbed. The useful range of mean absorption is from about 0.1 to 0.9. From figure 2.2. this range corresponds to two decades of the amount of absorber. In contrast, the measurement of total absorption is independent of the instrument bandwidth and the value measured is not restricted to any range. According to the measurements of Howard, Burch and Williams cited earlier, for small amounts of absorber, the total absorption is proportional to the square root of the amount of absorber. For larger amounts the total absorption is proportional to the logarithm of the amount. The total absorption can be obtained from low resolution spectra.

2.4.1. Overlap of Bands.

The infra-red spectrum of the sun, as measured from the ground, shows a number of absorption bands due to constituents of

the atmosphere. No band can be attributed to one single constituent. Each band observed is the result of the partial overlap of bands of two or more components. To find the total absorption due to one particular component it is necessary to remove the effects of the others. From Lambert's law, the transmission at one frequency due to two components is the product of the transmissions of each component.

$$T_{1,2}(\nu) = T_1(\nu)T_2(\nu)$$

The extension of this to finite bandwidths has been treated theoretically by Kaplan, 1954, and experimentally by Howard, Burch and Williams, 1956. Whenever there is no correlation between the line spacings and strengths of the two components, the mean transmission is given by

$$\bar{T}_{1,2}(\nu) = \bar{T}_1(\nu)\bar{T}_2(\nu) \qquad \ldots 2.4.1.$$

The main absorbers in the atmosphere are water vapour and carbon dioxide. The spectrum of the first can be approximated by a regular array of lines and the second by a random array. The correlation between the two is very small and relation 2.4.1 holds for bandwidths greater than 10 cm^{-1}.

CHAPTER THREE

S P E C T R O M E T R Y

The energy of a beam of light is distributed over a range of frequencies. The relation between the energy per unit bandwidth and the frequency is called the spectrum of light. An instrument which measures the spectrum is called a spectrometer, and the experimental technique is called spectrometry. This chapter reviews three types of spectrometer on a common basis, showing fundamental similarities between instruments normally thought to be different. The discussion of the grating spectrometer given below is similar to that given in many textbooks on optics. The notation is based on to that of Lipson, 'Physical Optics' although the derivation is different. The discussion of the prism spectrometer on the same basis as the grating is original. The refraction of the light at the prism surface is considered to be a diffraction phenomenon so that the action of the prism is derived directly from the wave theory of light rather than via geometrical optics. The treatment of the Michelson interferometer is also original. The Fourier transform treatment given below is chosen because it is the most natural way of treating the spectrometer described in Chapter Four.

3.1. Classification of Spectrometers.

All spectrometers depend for their operation on the principle of super-position. The wave vectors of two beams of light at the same place in empty space, under normal conditions of intensity, will add linearly. Thus, two beams of the same frequency can interfere, and the interference will be constructive or destructive depending on the phase relation between the two beams. In all spectrometers, the beam of light to be analysed is split into two or more beams, a path difference is introduced between the beams and the beams are allowed to interfere. The path difference between the beams results in a fixed phase difference which depends on the frequency of the light. The interference pattern shows maxima and minima whose position depends on the frequency of the light. The intensity of the interference pattern must be measured to find the spectrum. The pattern may be measured by one or more detectors. If a particular spectrometer has more than one detector, it is called a multichannel spectrometer; if it has only one, it is called a single channel spectrometer. The only multichannel spectrometers in general use have a photographic plate as the detector. In the infra-red, detectors are expensive and difficult to make in arrays, so that this chapter treats only single channel spectrometers. Since a spectrometer must measure more than one spectral element it is necessary to alter the interference pattern at the detector. This requires that some part of the spectrometer, usually the detector, is caused to move. The relation between the position of the moving component, the spectrum of the light and the intensity measured

by the detector is called the scanning function. In section 3.3, three spectrometers are considered. They are, an infinite beam spectrometer, the prism; a multibeam spectrometer, the diffraction grating and a two beam spectrometer, the Michelson interferometer. In each case, the scanning function is found.

3.2. The Fourier theory of diffraction.

The optical parts of every spectrometer perform three functions. Firstly, they ensure that the beam to be analysed is parallel, secondly, they split the beam into a number of beams and introduce a path difference for each beam and thirdly, they focus the light so that the beams can interfere. All three of these functions may be performed by one optical component, for example, a concave diffraction grating. In the following, the first component will be omitted and it will be assumed that parallel light enters the spectrometer. The beam splitter and delay components will be represented by a diffraction screen and the focussing device by a lens.

3.2.1. Phase and Configuration Space.

The radiation field of a beam of light can be represented in two different ways. In one representation, called the configuration space representation, the field is specified by the amplitude and relative phase of the field at each point in space. In the phase space representation, the field is considered to be the resultant of infinite plane waves travelling in different directions. It can be shown, (for example Ditchburn, section 6.34, page 195) that the

two representations are related by the Fourier transform. In analysing spectrometers, it is sufficient to consider the one dimensional case. The diagram, figure 3.1 represents a beam of light travelling along the Y axis. The amplitude and relative phase of the beam on the X axis is given by the complex function a(x). This is the resultant of infinite plane waves travelling in a direction perpendicular to the Z axis (which is normal to the plane of the diagram) and inclined at an angle θ to the Y axis. Following the notation of Lipson, the parameter of the phase space representation is $u = 2\pi\sigma \sin\theta$ where σ is the wave-number of the radiation. The quantity $ux = 2\pi x\sigma \sin\theta$ is the difference in phase between points on the axis for a wave travelling in direction θ. The amplitude and relative phase of the waves is given by the complex function $\psi(u)$. The phase and amplitude $dA(x)$ at point a on the x axis due to a small bundle of waves du travelling in direction given by u is given by

$$dA(x) = \psi(u)\exp(-iux)du$$

Integrating over all directions, $A(x) = \int_{\infty}^{\infty} \psi(u)\exp(-iux)du$ which is the Fourier transform of $\psi(u)$. From the Fourier transform theorem it follows that

$$\psi(u) = \frac{1}{2\pi} \int_{\infty}^{\infty} A(x)\exp(iux)dx$$

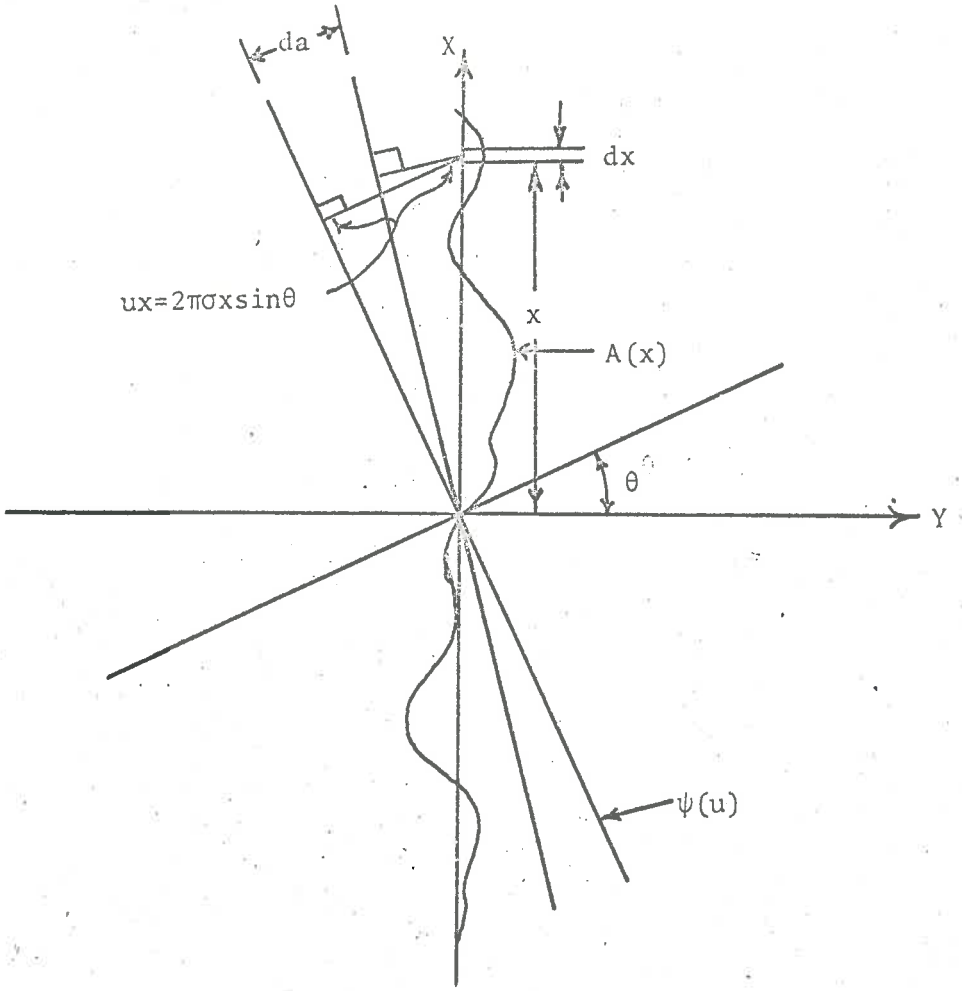

Figure 3.1

Phase and Configuration, Space

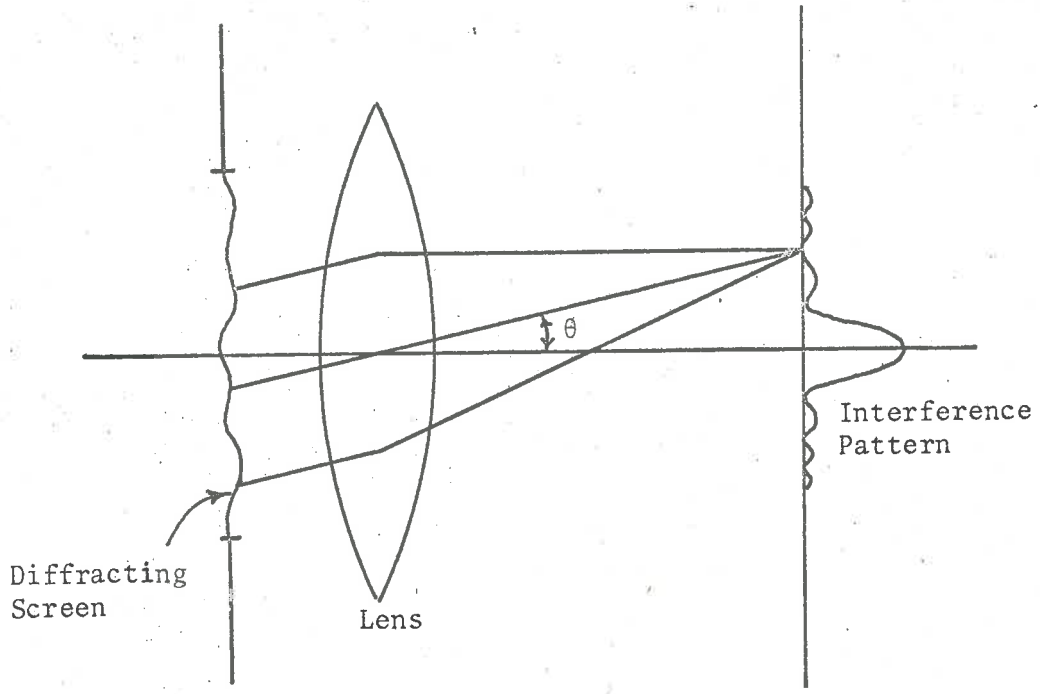

Figure 3.2

Fourier transform Optics

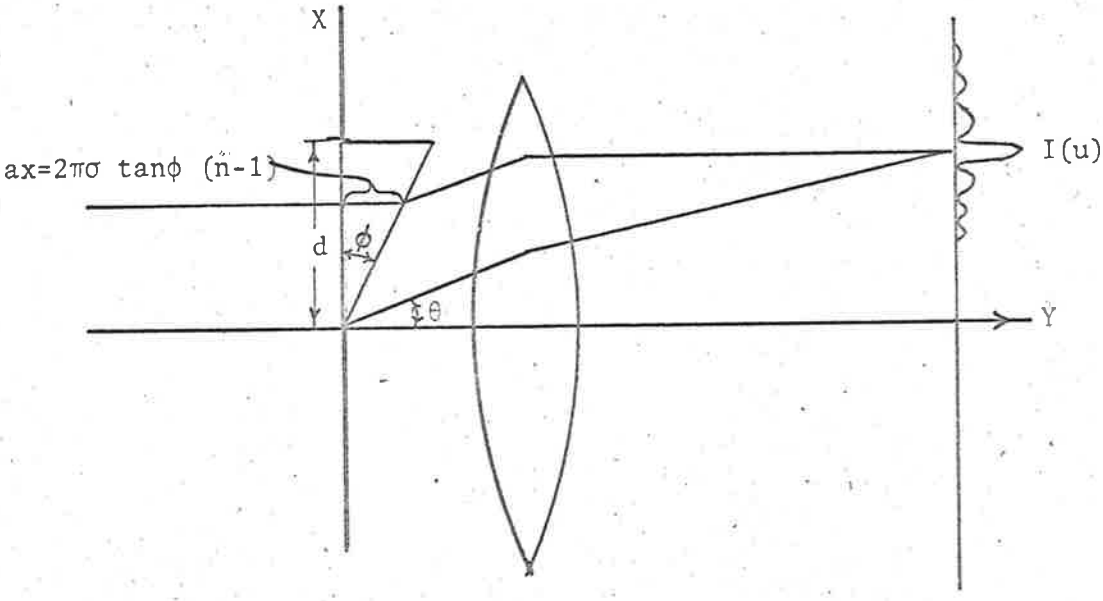

Figure 3.3

Prism as a Diffraction Screen

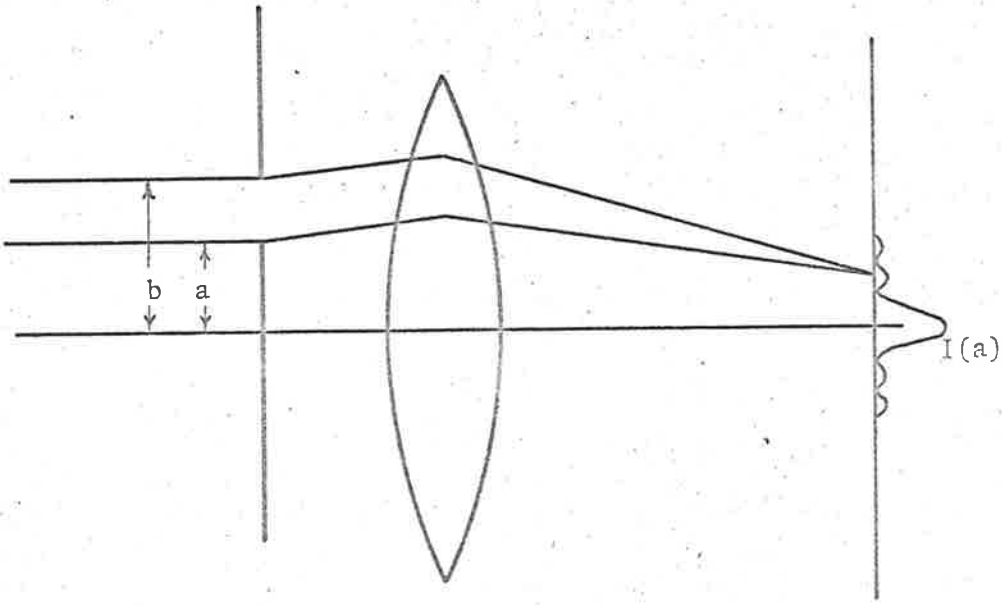

Figure 3.4

Arbitrary Slit as a Diffraction Screen

3.2.2. Space Transformations.

The perfect lens has the property that plane waves travelling in a particular direction are focussed at a particular point in the focal plane of the lens. The amplitude at this point is proportional to the amplitude of the wave and the phase at the point has a fixed relation to that of the wave. The image in the focal plane of the lens is the phase space representation of the radiation field to the left of the lens transformed into configuration space. Since the phase representation is the Fourier transform of the configuration space representation, the image in the focal plane of the lens is the Fourier transform of the configuration space representation of the radiation field to the left of the lens. In treating spectrometers, it will be assumed that the light to be analysed is in the form of an infinite plane wave travelling from left to right along the Y axis, that the beam splittings and phase shifting part of the spectrometer can be represented by a phase screen of finite size in the X direction and infinite extent in the Z direction and that the light from the screen is focussed by a lens larger than the aperture of the screen. Figure 3.2 shows the assumption in diagramatic form.

3.3. Comparison of Spectrometers.

Three different spectrometers will be analysed. The analysis will follow the same course in each case. Firstly, the beam splitting and phase shifting past of the spectrometer will be discussed. This will lead to a function which represents the beam splitter as a diffraction screen. In each case, the diffraction pattern will be

focused by a lens, so that the amplitude of the pattern in the focal plane is the Fourier transform of the function representing the beam splitter. The intensity of the diffraction pattern is given by the square of the absolute value of the amplitude. These calculations are performed for one frequency. The interference pattern for a spectrum is found by integrating the intensity over all frequencies. The scanning function, as defined in paragraph 3.1 is deduced from the integral of the intensity.

3.3.1. The Prism Spectrometer.

In paragraph 3.1, the prism spectrometer was described as an infinite beam spectrometer . The purpose of splitting the light to be analysed into a number of beams is to introduce a phase shift into each beam. In the prism spectrometer, the phase shift is a continuous function of the position at which each element of the incoming beam strikes the prism. Each infinitesimal element of the incoming beam can be considered as one of an infinite number of beams. If the refractive index of a transparent material is n at a particular frequency then a beam which travels a distance δ in the material travels an optical path length $n\delta$. The material introduces a difference of $(n-1)\delta$ between the path in the material and empty space. This corresponds to a phase difference of

$$2\pi(n-1)\delta\sigma$$

where σ is the wave number of the radiation.

A thin prism can be represented as a phase screen whose phase delay increases with distance from X axis. If the apex angle of the prism is ϕ then the delay introduced into the element of the incoming beam

at distance x from the axis is $2\pi(n-1)\tan\phi\, x\sigma$. A prism of width d can then be represented as a phase screen with the function

$$f(x) = \begin{cases} 0<x\ 0 \text{ or } x>d \\ \exp(-i\alpha x) \text{ where } \alpha = 2\pi(n-1)\tan\phi\sigma \end{cases}$$

The amplitude of the interference pattern produced when the light diffracted by such a screen is focussed is given by the Fourier transform of the function f(x) That is,

$$\psi(u,\sigma) = A(\sigma)\int_{-\infty}^{\infty} f(x)\exp(iux)dx$$

$$= A(\sigma)\int_{0}^{d} \exp(i(\alpha+u)x)dx$$

$$= A(\sigma)\left\{\frac{\sin(\alpha+u)d}{\alpha+u}\right.$$

$$\left. -i\left(\frac{\cos(\alpha+u)d}{\alpha+u} + \frac{1}{\alpha+u}\right)\right\}$$

The intensity of the interference pattern is given by

$$I(u,\sigma) = \psi^*\psi$$

$$= A^*A\left(\frac{\sin^2(\alpha+u)d}{(\alpha+u)^2} + \frac{\cos^2(\alpha+u)d}{(\alpha+u)^2}\right.$$

$$\left. + \frac{2\cos(\alpha+u)d}{(\alpha+u)^2} + \frac{1}{(\alpha+u)^2}\right)$$

$$= \frac{4B(\sigma)}{(\alpha+u)}\sin^2\left(\frac{\alpha+u}{2}d\right)$$

The interference pattern is the same as that of a single slit of width d, except that it has been deflected through an angle such that $\alpha = -u$

that is $2\pi(n-1)\tan\phi\sigma = 2\pi\sin\theta\delta$

or $\sin\theta = (n-1)\tan\phi$ which is the same result as obtained by applying Schnell's law and tracing rays through the prism, provided that ϕ is small.

Integrating the intensity over all frequencies gives

$$I(\theta) = \frac{4B(\sigma)}{(\alpha+u)^2} \sin^2\left(\frac{\alpha+u}{2} d\right)d\sigma \qquad \ldots 3.3.1.$$

Since the refractive index n is an increasing function of frequency, in the wave-band for which the spectrometer is designed, the higher frequency components of the light are deflected through larger angles than the lower frequency components. The expression represents the convolution of the spectrum of the light with the diffraction pattern of a single slit. In a single channel prism spectrometer, the moving component which scans spectrum is the detector. It lies in the focal plane of the lens, and scans through a range of values of θ. The scanning function is therefore given by relation 3.3.1. Since the exact form that 3.3.1 takes depends on the dispersion relation of the material of the prism, it is not possible to give it in analystic form. Prism spectrometers are calibrated by measuring the scanning function for spectra which have been determined by some other method. The scanning function for a prism spectrometer is given by the convolution of the spectrum with the diffraction pattern of a single slit, distorted so that the

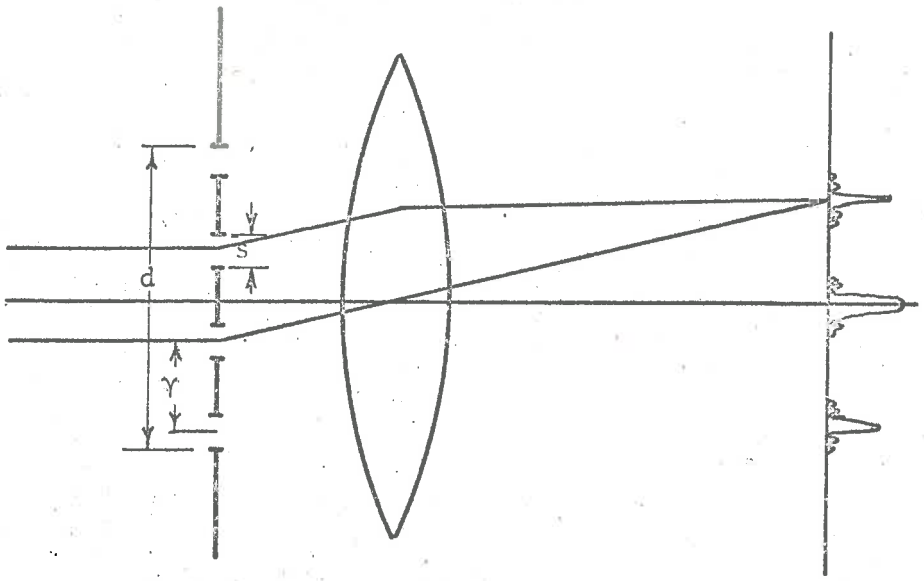

Figure 3.5
Diffraction Grating

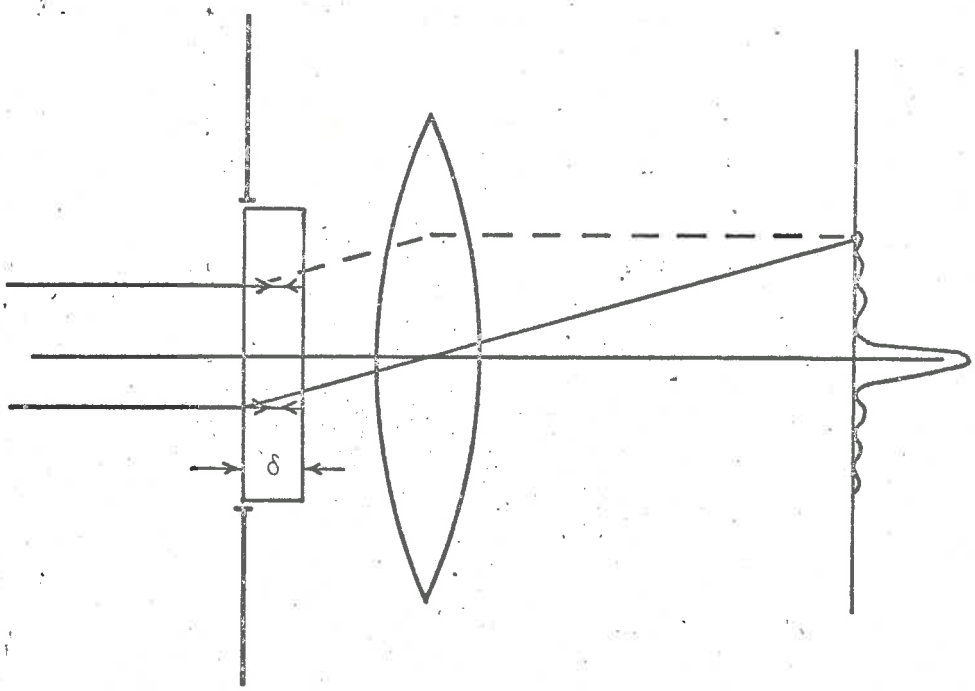

Figure 3.6
Michelson Interferometer as Diffraction Screen

scale is non-linear.

3.3.2. The Diffraction Grating.

The diffraction grating is the only spectrometer normally treated as a diffraction screen. It is usually considered firstly as an infinite grating to allow the use of Fourier series in deriving its most important properties. In this treatment it is considered to be finite to allow the derivation of intermediate results which will be used later on. This treatment also demonstrates the fundamental similarity between diffraction grating and the spectrometer described in Chapter Four.

The diffraction grating is a diffraction screen which consists of many identical elements. Each element diffracts the incoming beam and is considered to be the source of a separate beam. The diffraction grating splits the light to be analysed into as many beams as there are elements in the grating. In the normal grating, each element is a narrow slit which alters the phase or amplitude of the light passing it. In this treatment, the slits will be assumed to pass part of the beam unaltered and to obstruct the rest. In this case the diffraction grating is an amplitude diffraction screen.

The Diffraction Pattern of a single slit.

A single slit can be represented by the function

$$f(x) = \begin{cases} 1 & a<x<b \\ 0 & \text{elsewhere} \end{cases}$$

The diffraction pattern can be represented by the Fourier transform, which is

$$\psi(u,\sigma) = A(\sigma) \int_a^b e^{iux} dx$$

$$= \frac{A(\sigma)}{iu} (e^{ibu} - e^{iau})$$

$$= \frac{A(\sigma)}{iu} (w^b - w^a) \qquad \ldots 3.3.2.$$

where for convenience $w = e^{iu}$

From the properties of the definite integral, the diffraction pattern of a number of slits is the sum of terms having the form 3.3.2.

Consider an array of N slits of width δ at centers γ spaced symmetrically about the origin. The total width of the array is $d = (N-1)\gamma$. The jth slit extends from $j\gamma - \frac{(N-1)\gamma}{2} - \frac{\delta}{2}$ to $j\gamma - \frac{(N-1)\gamma}{2} + \frac{\delta}{2}$

The diffraction pattern of the array is given by

$$\psi(u,\sigma) = \frac{A(\sigma)}{iu} \sum_{j=0}^{N-1} \left[w^{(j\gamma - \frac{(N-1)\gamma}{2} + \frac{\delta}{2})} - w^{(j\gamma - \frac{(N-1)\gamma}{2} - \frac{\delta}{2})} \right]$$

$$= \frac{A(\sigma)}{iu} w^{-\frac{(N-1)\gamma}{2}} \left(w^{\frac{\delta}{2}} - w^{-\frac{\delta}{2}} \right) \sum_{j=0}^{N=1} w^{j\gamma}$$

$$\psi(u,\sigma) = \frac{A(\sigma)}{iu} w^{-\frac{(N-1)\gamma}{2}} \left(w^{\frac{\delta}{2}} - w^{-\frac{\delta}{2}} \right) \frac{w^{N\gamma} - 1}{w^{\gamma} - 1}$$

$$= \frac{A(\sigma)}{iu} \left(w^{\frac{\delta}{2}} - w^{-\frac{\delta}{2}} \right) \frac{w^{\frac{N\gamma}{2}} - w^{-\frac{N\gamma}{2}}}{w^{\frac{\gamma}{2}} - w^{-\frac{\gamma}{2}}}$$

Substituting, $\sin\theta = \frac{1}{2i}(e^{i\theta}-e^{-i\theta})$

$$\psi(u,\sigma) = \frac{2\sin\left(\frac{\delta u}{2}\right)\sin\left(\frac{N\gamma u}{2}\right)}{u\sin\left(\frac{\gamma u}{2}\right)}A(\sigma)$$

The interference pattern observed is given by

$$I(u,\sigma) = A^{*}A\,\frac{4\sin^2\left(\frac{\delta u}{2}\right)\sin^2\left(\frac{N\gamma u}{2}\right)}{u^2\sin^2\left(\frac{\gamma u}{2}\right)} \qquad \ldots\ 3.3.3.$$

When γ_u is small, and since $\delta<\gamma$, δ_u is small

$$I(u,\sigma) = \frac{4B\sin^2\left(\frac{N\gamma u}{2}\right)}{u^2}\cdot\frac{\delta^2}{\gamma^2}$$

which except for the factor $\left(\frac{\delta}{\gamma}\right)^2$ is the same as the interference pattern for a single slit of width. There is a central maximum at $u = 0$ with intensity

$$I(0,\sigma) = N^2\delta^2$$

Since the position of this maximum is independent of σ the central image is white.

The function (3.3.3.) also has maxima when $\frac{\gamma u}{2} = m\pi$ that is, for $\sin\theta = \frac{m\lambda}{\gamma}$ which is the standard expression for the position of maxima in a diffraction grating. To find the nature of these maxima, define $u' = u - \frac{2m\pi}{\gamma}$ so that as $u \to \frac{2m\pi}{\gamma}$, $u'\to 0$

$$I(u,\sigma) = \frac{4B \sin^2 \frac{\delta u}{2}}{u^2} \quad \frac{\sin^2\left(\frac{N\gamma u'}{2} + Nm\pi\right)}{\sin^2\left(\frac{\gamma u'}{2} + m\pi\right)}$$

$$= \frac{4B \sin^2 \frac{\delta u}{2}}{u^2} \quad \frac{\sin^2\left(\frac{N\gamma u'}{2}\right)}{\sin^2\left(\frac{\gamma u'}{2}\right)}$$

As $u' \to 0$

$$I(u,\sigma) \to \left(\frac{4B \sin^2\left(\frac{\delta u}{2}\right)}{u^2}\right) \quad \left(\frac{4 \sin^2\left(\frac{N\gamma u'}{2}\right)}{\gamma^2 u'^2}\right)$$

In the vicinity of these secondary maxima, the interference pattern has the same form as that of a single slit of width $N\gamma$. The intensity at the maximum is given by

$$I(m\pi,\sigma) = \frac{16B \sin^2(m\pi\frac{\delta}{2})}{m^2\pi^2} N^2$$

The factor $\frac{\sin^2\left(\frac{\delta u}{2}\right)}{u^2}$ is the interference pattern of a single slit of width δ, i.e. is the interference pattern of a single element of the grating. The interference pattern of a single element is called the form factor of the grating. If each element consists of a prism, in a transmission grating, or a mirror inclined to the optical axis in a reflection grating, then the form factor is an expression similar to that derived for the prism in paragraph 3.3.1. In this case the intensity of the interference pattern is greatest in the vicinity of some of the secondary maxims rather than in the central maximum as derived from equation (3.3.3). This

is frequently done in practice and the grating is then said to be blazed. If the amplitude at frequency σ is given by $A(\sigma)$

then $$\psi(u,\sigma) = \frac{2A(\sigma) \sin\left(\frac{\delta u}{2}\right) \sin\left(\frac{N\gamma u}{2}\right)}{u \sin\left(\frac{\gamma u}{2}\right)}$$

and $$I(u,\sigma) = \frac{2B(\sigma) \sin^2\left(\frac{\delta u}{2}\right) \sin^2\left(\frac{N\gamma u}{2}\right)}{u^2 \sin^2\left(\frac{\gamma u}{2}\right)}$$

where $$B(\sigma) = A^*(\sigma)\, A(\sigma)$$

Integrating over all frequencies

$$I(\theta) = \int_0^\infty \frac{2B(\sigma) \sin^2 \frac{\delta u}{2} \sin^2\left(\frac{N\gamma u}{2}\right)}{u^2 \sin^2\left(\frac{\gamma u}{2}\right)} d\sigma \qquad \ldots 3.3.4.$$

The usual properties for the grating can be derived from the above equation. As with the prism spectrometer, the detector is moved along the focal plane to scan the spectrum. The scanning function for a particular order is therefore the convolution of the spectrum of the light with the diffraction pattern of a single slit of width $N\gamma$. The convolution is distorted, since the position of a given spectral element depends on its wavelength rather than its frequency. The frequency scale of the diffraction grating spectrometer is determined by its construction rather than the material from which it is made as is the case in the prism spectrometer. Calibration of

the spectrometer is needed only to verify its correct operation and the spectrometer can be used to measure wavelengths in terms of laboratory standards of length. The scanning function as a whole consists of an infinite series of the single order scanning functions as found above. The frequencies present at a particular angle are given by $\sigma = \frac{m}{\gamma \sin \theta}$

Some means must be provided for distinguishing between the various orders. The normal practice is to restrict to range of frequencies to which the detector responds to about one octave. The lowest frequency of the first order coincides with the highest frequency in the second order, so that the two orders do not overlap. When the spectral region of interest is small, grating spectrometers are operated in very high orders. The echelon grating has N about thirty, δ nearly equal to γ and is blazed to operate with m of about 35,000.

3.3.3. The Michelson Interferometer.

The prism and the grating spectrometers are both wave-front-division interferometers. The Michelson interferometer is an amplitude division interferometer. The incoming light is split into two beams of equal amplitude. The beams travel over physically separate paths and the path difference can assume values from zero to large multiples of the wave-length in use. The function representing the beam splitter as a diffraction screen is

$$f(x) = \begin{cases} \frac{1}{2}\left(1+e^{2\pi i \delta \sigma}\right) & -\frac{d}{2} < x < \frac{d}{2} \\ 0 & \text{elsewhere} \end{cases}$$

where $2\pi\delta\sigma = \gamma$ is the phase difference for a path difference of δ.

The diffraction pattern is given by the Fourier transform of this

$$\psi(u,\sigma) = \frac{A(\sigma)}{2} \int_{-d/2}^{d/2} e^{iux} + e^{i(ux+\gamma)} dx$$

$$= A(\sigma) \frac{(1+e^{i\gamma})}{u} \sin\left(\frac{ud}{2}\right)$$

The interference pattern seen in the focal plane is given by

$$I(u,\sigma) = A^{*}A \frac{\sin^2\left(\frac{ud}{2}\right)}{u^2} (1+e^{i\gamma})(1+e^{-i\gamma})$$

$$= B(\sigma) \frac{2\sin^2\left(\frac{ud}{2}\right)}{u^2} (1+\cos\gamma)$$

where $B(\sigma)$ is the energy spectrum of the light. The factor $\frac{2\sin^2\left(\frac{ud}{2}\right)}{u^2}$ is the only part of the expression which depends on u. This is the diffraction pattern of a single slit of width d. Most of the energy is concentrated in the central image around $u = 0$. For reasonable dimensions of spectrometer and detector, the detector will completely cover the central image. Integrating over all angles

$$\int_0^{\infty} I(u,\sigma)\, du = 2B(\sigma)(1+\cos\gamma) \int_0^{\infty} \left(\frac{d^2}{2}\right) \frac{\sin^2\left(\frac{ud}{2}\right)}{\frac{d}{2}\left(\frac{ud}{2}\right)^2} d\left(\frac{ud}{2}\right)$$

$$\text{i.e.} \quad I(\sigma) = 2B(\sigma)(1+\cos\gamma)\left(\frac{d}{2}\right)^2$$

Integrating over all frequencies

$$\int_0^\infty I(\sigma)\, d\sigma = I(\delta)$$

$$= \frac{d^2}{2}\left\{\int_0^\infty B(\sigma)d\sigma + \int_0^\infty B(\sigma)\cos(2\pi\sigma\delta)d\sigma\right\} \qquad \ldots 3.3.5.$$

which is the scanning function.

The first part of the scanning function is the total intensity of the light. If the second part is considered as a function of δ then it is the Fourier cosine transform of the spectrum. In the Michelson interferometer, when used as a spectrometer, the moving component is one of the mirrors. The detector is mounted in the focal plane of the lens and on the optical axis. The scanning function is given by 3.3.5.

The interferometer has one disadvantage compared to the prism and diffraction grating. The latter produce the spectrum of the light in a directly interpretable form. The former requires that the inverse Fourier transform be performed on the measured data before the spectrum can be obtained. This is described in greater detail in a later chapter. The interferometer has two advantages. The first is common with all amplitude division interferometers. In the treatment above, the interferometer was treated as a one dimensional diffraction screen. This assumed that the dimension of the aperture in the Z direction was large compared to that in the Y direction. In practice the two dimensions are equal, and the two dimensional Fourier transform should have been used.

The above treatment can be justified only because the scanning function found does not use the whole of the interference pattern. The energy entering the Michelson interferometer is focussed onto a small spot. The internsity measured is proportional to the area of the aperture. The energy entering a prism or diffraction grating spectrometer is focussed onto a line parallel to the Z direction. The intensity measured at a point in the focal plane is proportional to the width of the aperture. The intensity measured in the interferometer is proportional to the square of the linear dimensions of the beam splitter whereas the intensity measured in the prism or diffraction grating is directly proportional to its dimensions. This is called the Jaquinot advantage. (Jaquinot, 1948) The other advanatge is the Felgett advantage which is described in the next paragraph.

3.3.4. The Felgett Advantage.

The Felgett, or multiplex advantage arises from the properties of both the Fourier transform and certain types of detector. When a number of signals are encoded by means of some orthogonal transformation, such as the Fourier transform, so that information from each signal is present at all points in the domain of measurement, then the signals are said to be multiplexed. When signals are multiplexed the energy which carries the signal is distributed over the whole domain of measurement. In a spectrometer, the signal required is the spectrum of the light which is being analysed. The total intensity of the light is

$$I_T = \int_0^\infty B(\sigma)d\sigma$$

The mean intensity of the light on the detector is given by the mean value of the scanning function. In the case of the grating and prism spectrometers, this is approximately $\bar{I} = \bar{B}(\sigma)$. In the case of the Michelson interferometer, the mean intensity at the detector is

$$I(0) = \frac{1}{2}\int_0^\infty B(\sigma)d\sigma$$

which is half the total intensity. The mean intensity at the detector of the Michelson interferometer is greater than that of the prism or grating spectrometers. This greater intensity is not in itself an advantage. If the precision with which a detector could measure the intensity was constant, then the multiplex advantage would not exist. The precision of a measurement is determined by the moise generated in the detector. If the noise is proportional to the intensity then the precision of measurment is constant. Some detectors, for example, photomultipliers, have this property and so they can not achieve the multiplex advantage. Some detectors, particularly those used in the infra-red generate noise which is constant and independent of the intensity being measured. The noise is thermal noise in the detector element. It is also known as Johnson noise and Nyquist noise. The precision of a measurement in the presence of thermal noise can be increased by integrating the output of the detector. Thermal noise consists of random fluctuations which tend to cancel out.

If the output of a detector consists of a signal due to the light being detected plus Johnson noise, the signal integrates proportionally to the square root of the integrating time. The signal to noise ratio is proportional to the square root of the integrating time.

Suppose that the scanning function is measured at N points and that the integrating time for each measurement is T. The scanning function for the grating spectrometer, in one order is given by

$$I(\theta) = \int_0^\infty \frac{2B(\sigma)\ \sin^2\left(\frac{\delta u}{2}\right)\ \sin^2\left(\frac{N\gamma u'}{2}\right)}{u^2\ \sin^2\left(\frac{\gamma u'}{2}\right)}\ d\sigma$$

or approximately, $I(\theta) = B(\sigma')$ ... 3.3.6.

where $\sigma' = \frac{m}{\gamma \sin \theta}$

The energy of one spectral element is present at the detector for one sampling period. The signal to noise ratio for one spectral element is proportional to $\sqrt{T}$. A similar result can be found for the prism spectrometer. The scanning function for the Michelson interferometer is

$$I(\delta) = \frac{1}{2} I(0) + \int_0^\infty B(\sigma)\cos(2\pi\delta\sigma)d\sigma$$

This does not reduce to a form similar to 3.3.6. Energy from all spectral elements is present at the detector for all the measurements. The mean intensity of any spectral element at the detector is $\frac{1}{2} B(\sigma)$. The integrating time for every element is therefore NT so that the signal to noise ratio is proportional to $\sqrt{NT}$. This gain in signal to noise ratio is the multiplex advantage.

CHAPTER FOUR

THE INTERFEROMETER

This chapter describes an interferometer which is designed to measure spectra of the kind described in chapter two. The interferometer must be capable of measuring spectra over the band of infra-red radiation between 500 cm^{-1} to 5000 cm^{-1}. The spectra will be formed by the absorption of sunlight by the atmosphere, so that no form of double beam spectrometer is acceptable. That is, it must measure the actual spectrum of the light entering it rather than compare the source of light with the light passing through the absorber. It is intended that the interferometer be flown on a balloon, so that it must be light in weight, insensitive to environmental conditions and automatic in operation. The interferometer described here is a Fourier transform spectrometer satisfying these conditions.

4.1.1. Figure 4.1 shows the basic parts of the interferometer using the conventions of chapter three. The diffraction screen

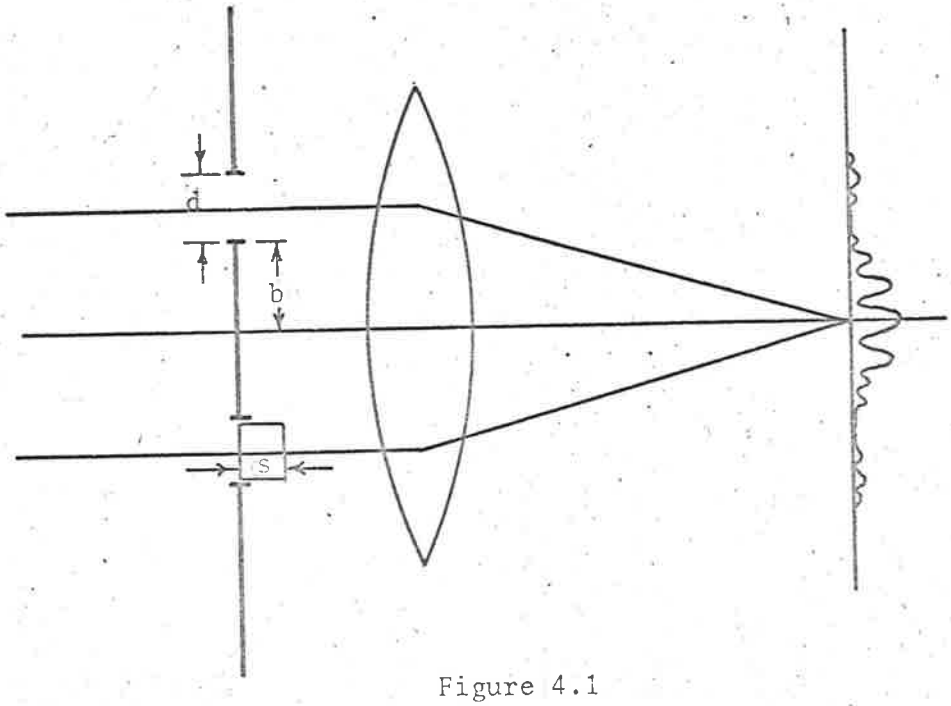

Figure 4.1

Theory of the Interferometer

has two slits, each of width d. The separation of the slits is 2b. The diffraction screen acts as the beam splitter, so that this is a wave-front division interferometer. A system of mirrors, to be described in section 4.2 introduces a time delay into the beam passing through one of the slits. This corresponds to a path difference of δ between the beams through the two slits. The phase delay for this path difference is $\gamma = 2\pi\sigma\delta$. The function representing the diffraction screen is

$$f(x) = \begin{cases} 1 & b < x < b + d \\ e^{i\gamma} & -(b+d) < x < -b \\ 0 & \text{elsewhere} \end{cases}$$

The diffraction pattern is given by the Fourier transform of this

$$\psi(u,\sigma) = A(\sigma) \int_{-\infty}^{\infty} f(x)\, e^{iux}\, dx$$

$$= \frac{4}{u} A(\sigma)\, e^{i\gamma} \sin\frac{du}{2} \cos\frac{1}{2}(2bu + du + \gamma)$$

The intensity of the interference pattern is given by

$$I(u,\sigma) = \psi^*(u,\sigma)\, \psi(u,\sigma)$$

$$= \frac{16}{u^2} A^*(\sigma)A(\sigma) \sin^2\frac{du}{2} \cos^2\frac{1}{2}(2bu + du + \gamma)$$

In the interferometer constructed, b was 0.1 mm, d was 0.4 mm. Figure 4.2 shows a graph of the intensity function given above for these values of b and d for a wavelength of two microns, and phase

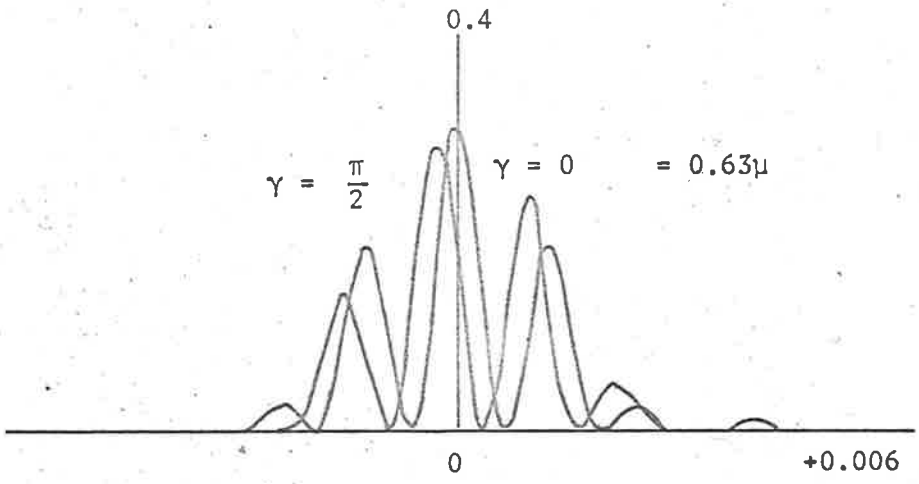

Figure 4.3

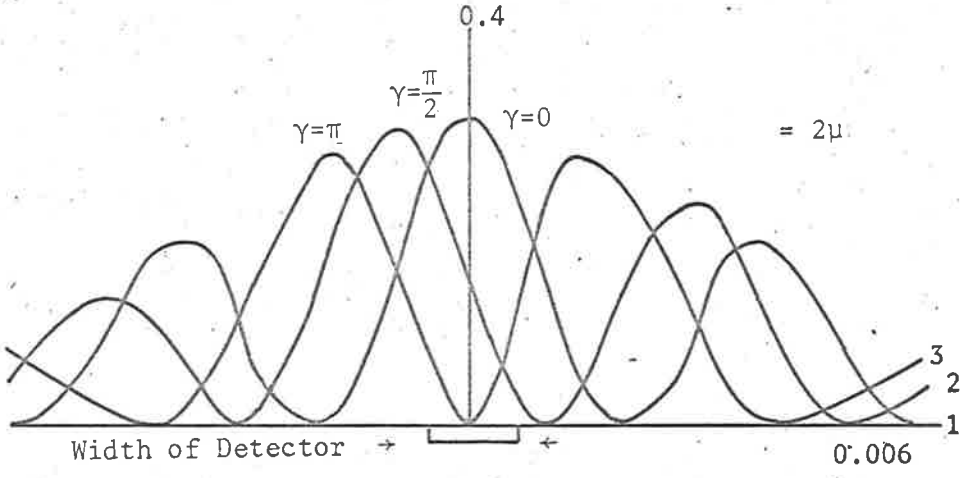

Figure 4.2

Interference Pattern of Interferometer

delays of zero, $\frac{\pi}{2}$ and π. These delays correspond to path differences of zero, half a micron and one micron. Figure 4.3 shows the intensity of the interference pattern for the same values of b and d for a wave-length of 0.63 microns the wave-length produced by the laser for testing.

The intensity at the centre of the interference pattern is given by

$$I(u,\sigma) = \psi^*(u,\sigma)\ \psi(u,\sigma)$$

$$= \frac{16}{u^2} A^*(\sigma)A(\sigma)\ \sin^2\frac{du}{2}\ \cos^2\frac{\gamma}{2}$$

$$= \psi d^2 B(\sigma)\ \cos^2\frac{\gamma}{2}$$

where $B = A^*A$

is the spectrum of the incident radiation.

Integrating over all frequencies

$$I(\delta) = 2d^2 \left(\int_0^\infty B(\sigma)d\sigma + \int_0^\infty B(\sigma)\ \cos\ 2\pi\sigma\delta\ d\sigma \right) \qquad \ldots\ 4.1.1.$$

The first term of this expression is the mean intensity of the radiation and the second term is the Fourier cosine transform of its spectrum. The form of the expression is the same as that found for the Michelson interferometer.

4.1.2. Band width and resolution.

The expression 4.1.1 above is the scanning function of the interferometer. The path difference δ is varied from zero to some maximum and the intensity at the centre of the pattern is measured at the various values of δ. Suppose that δ is varied in equal steps,

that the measurement is made at the end of each step and that there are N steps. Suppose further that there is only one frequency present in the spectrum. The scanning function reduces to an expression of the form $I(\delta) = C \cos 2\pi\sigma\delta$.

To measure C and σ at least two measurements of I must be made. Since I is a periodic function, the measurements must be made at different points on the cycle. If the two measurements are made without reference to any other information about the period, the actual period may be any integral multiple of the period found from the measurements. If it can be guaranteed that the two measurements were made in the same cycle of the function, then the period is known exactly. The period of the function is given by

$$T = \frac{1}{\sigma\delta}$$

so that the step size must be less than $d\delta$ where $d\delta = \frac{1}{2\sigma} = \frac{\lambda}{2}$ = half the wavelength. (The step size may not equal $\frac{\lambda}{2}$ otherwise the measurements may, by chance, coincide with the zeroes of the function. This will give the period of the function provided it is known that C is non-zero. It will give no information about C). The problem of distinguishing between functions with integral multiple periods is called aliasing. It occurs whenever a function containing periodic components is measured at discrete intervals. Aliasing can only be avoided by ensuring that the interval between measurements is less than the period of the highest frequency component in the function. Rearranging equation shows that the highest wave-number measurable by the interferometer is a function of the step size and is given by $\sigma = \frac{1}{2d\delta}$.

The theory given above cannot predict any lower frequency of operation of the interferometer. It is assumed that the Fourier transform representation of diffraction is valid for all frequencies. In fact, that representation is valid only for wavelengths which are short compared to the width of the slits. The slits in the interferometer as constructed are about 0.4 mm so that the lower frequency limit occurs for wavelengths of the order of 0.1 mm, or in wave-numbers, 100 cm^{-1}.

The resolution can be estimated by considering a spectrum consisting of two frequencies, $\sigma + \frac{d\sigma}{2}$ and $\sigma - \frac{d\sigma}{2}$ where $d\sigma$ is small. The scanning function then becomes

$$I(\delta) = C_1 \cos 2\pi(\sigma + \tfrac{d\sigma}{2})\delta + C_2 \cos 2\pi(\sigma - \tfrac{d\sigma}{2})\delta$$

that is

$$I(\delta) = (C_1 + C_2) \cos(2\pi\sigma\delta) \cos(2\tfrac{d\sigma}{2}\delta)$$

$$+ (C_2 - C_1) \sin(2\pi\sigma\delta) \sin(2\pi\tfrac{d\sigma}{2}\delta)$$

For small path differences, the coefficient of $\cos 2\pi\sigma\delta$ is approximately constant, and the coefficient of $\sin(2\pi\sigma\delta)$ is approximately zero. Measurements near zero path difference give the sum of the intensities of the two components. To find the difference, it is necessary to make a measurement at a path difference sufficiently large as to make the coefficient of $\cos(2\pi\sigma\delta)$ zero. That is,

$\cos(2\pi \frac{d\sigma}{2} \delta) = 0$

therefore $d\sigma = \frac{1}{2\delta}$

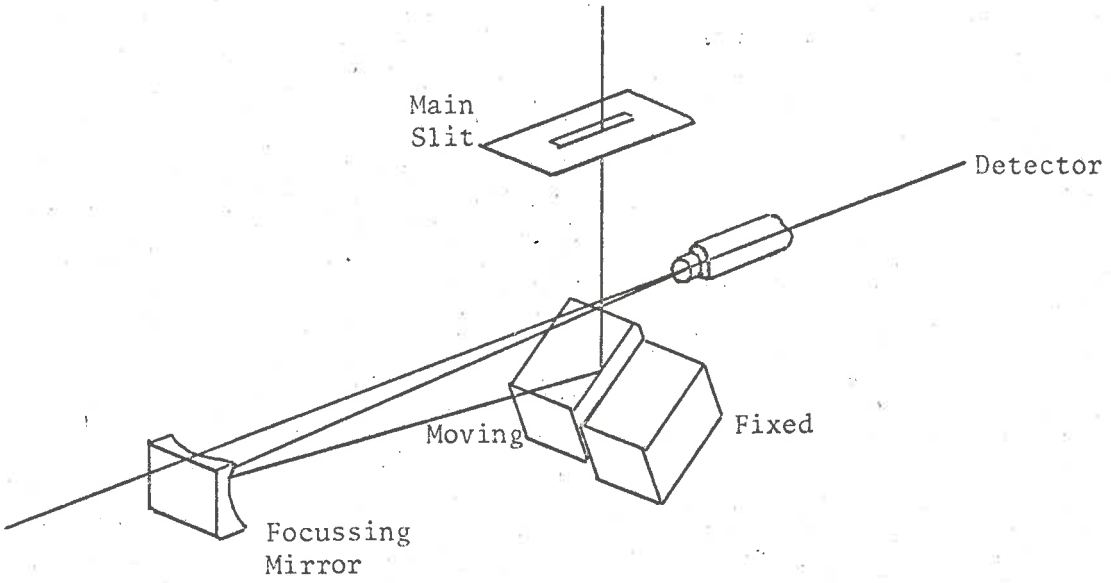

Figure 4.4

Mirror Arrangements

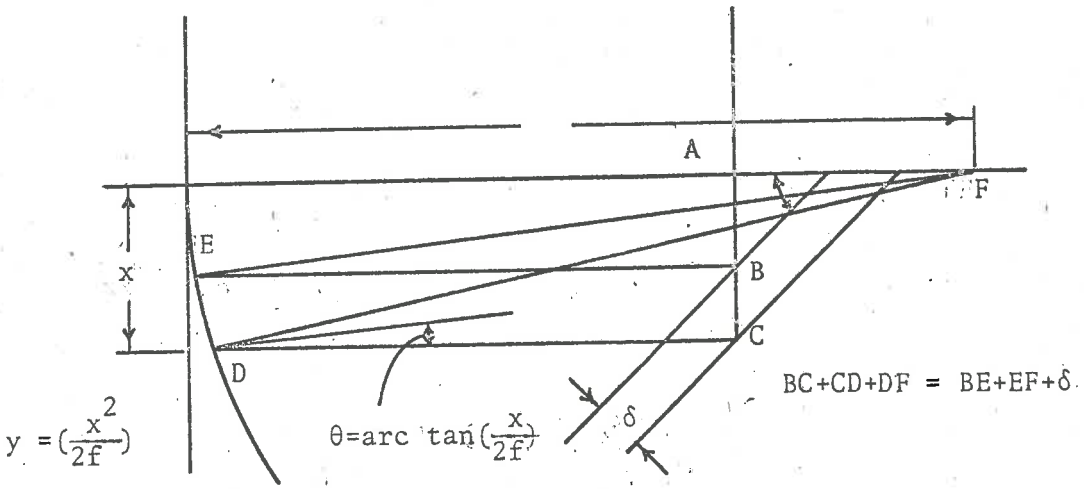

Figure 4.5

Ray tracing through the interferometer

PLATE ONE

The optical components of the interferometer

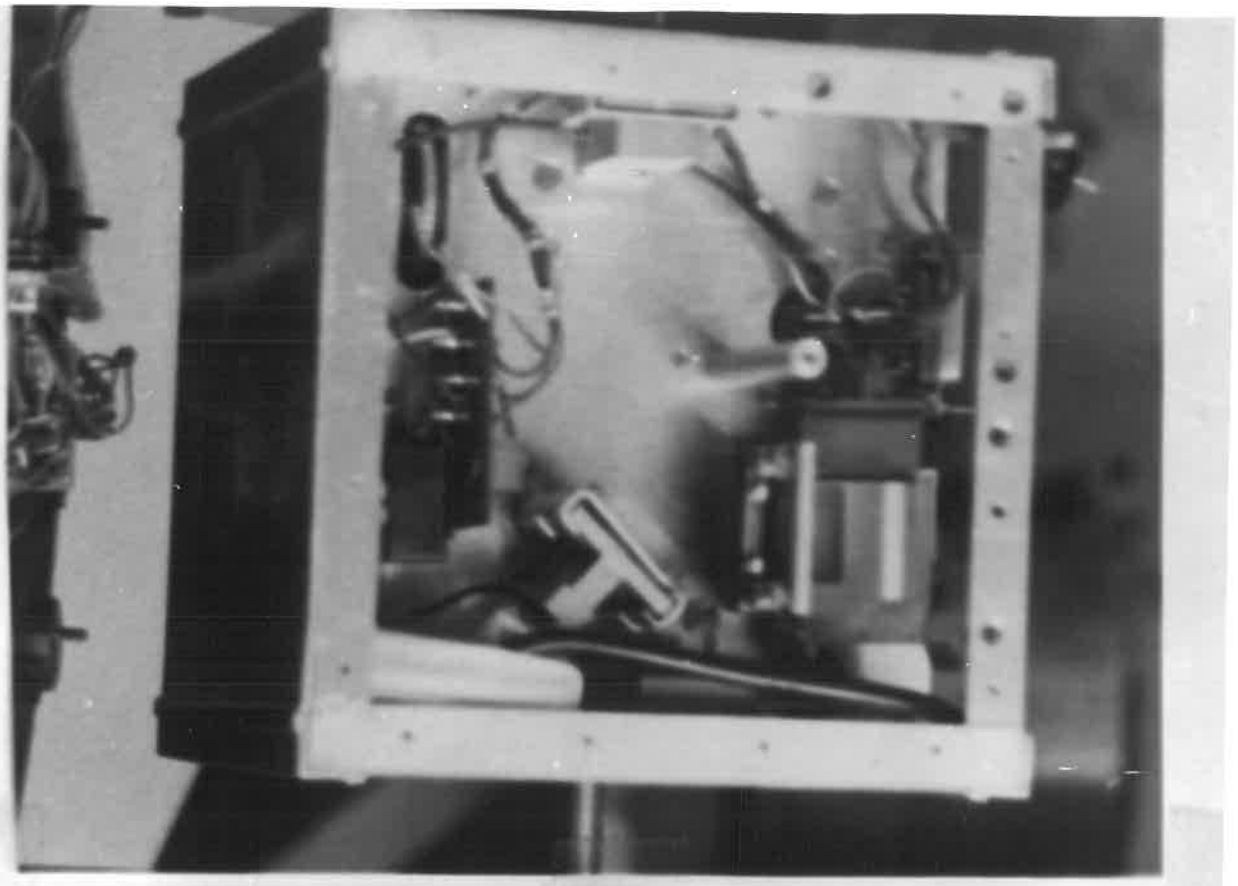

The coefficient of $\sin(2\pi\sigma\delta)$ is then $C_2 - C_1$.

Therefore, to resolve two components separated by $d\sigma$ the path difference must vary from zero to a maximum value given by

$$\delta_{max} = \frac{1}{2d\sigma}$$

4.2. The Optical Path.

The interferometer described in the last section requires a diffracting screen with two slits, a means of inserting a path difference into the beam from one of the slits and a means for focussing the beams. Figure 4.4 illustrates the way this is achieved. The principal components of the interferometer are, (1) a wide slit, (2) a pair of plane mirrors one of which is fixed and the other capable of moving and (3) a parabolic mirror for focussing the beams. Mirrors are used in preference to lenses because they have no chromatic aberration and, having an aluminium reflecting surface, negligible absorption over the infra-red wave-lengths. The wave-band over which the interferometer can operate is not limited by the optical materials used in its construction.

The location of the components and the light path can best be described in terms of coordinate geometry. Suppose that the light entering the interferometer is travelling in the -Z direction. The plane ZOX is called the fundamental plane of the interferometer. This plane corresponds to the optical axis of the theory in the preceding section. The centre of the slits, the axis of the focussing mirror and the detector all lie in this plane.

Light enters the interferometer travelling in the -Z direction through a slit which lies in a plane parallel to the XOY plane. This is called the main slit. The edges of this slit correspond to the outer edges of the two slits of the theory. The width of the main slit is 2(b+d). In the interferometer constructed, the main slit was one millimeter wide. The length of the slit was about twenty millimeters. The light then falls on one of two mirrors. These mirrors are mounted so that their normals lie in the fundamental plane and make an angle of 135 degrees with the X direction. Each mirror therefore reflects the light falling on it through an angle of ninety degrees so that it travels in the -X direction. The mirrors lie on either side of the fundamental plane, so that the plane is between them, and the edges of the mirrors are parallel to that plane. The edges of the mirrors nearest to the plane define the inner edges of the two slits of the theory. In the actual interferometer they are both about 0.1 mm from the plane, so that the value of b is 0.1 mm and, from the width of the main slit, d is 0.4 mm. The mirrors are twenty millimeters long and ten wide. The length of the mirrors as projected in the XOY plane and the YOZ plane is about fourteen millimeters. Ignoring diffraction effects for the moment, the beams leaving the mirrors are parallel and each is fourteen millimeters in the Z dimension, 0.4 mm in the Y dimension, 0.2 mm apart and travelling in the -X direction.

The two beams fall onto a parabolic mirror whose axis lies in the fundamental plane and is parallel to the X direction. The parabolic mirror focusses the two beams onto the detector. The focussing mirror is twenty millimeters square and has a focal length of ten centimeters. The pole of the paraboloid is at the centre of the top side of the mirror. The distance from any point in the plane of the main slit to one of the plane mirrors and hence to the detector is a constant. The distance depends on the position of the plane mirror. When the mirrors lie in the same plane, the distance is the same for both mirrors, but when the planes of the mirror surfaces are distance δ apart, the path lengths from the main slit to the detector differ by δ. Figure 4.5 shows the geometrical construction of the two paths from the slit to the detector. One of the plane mirrors is fixed in position. The other can be moved in such a way that its surface is always parallel to that of the fixed mirror and the distance between the two surfaces can be varied. In this way, the mirrors split the incoming light into two beams and introduce a path difference between the two beams. The focussing mirror forms the interference pattern at the detector which measures the intensity of the centre of the pattern. The moving mirror is the component which moves to provide the scanning function.

4.3. The Mechanical Construction.

The interferometer was built on a single aluminium plate. All the optical components are mounted on one side of this plate. The mechanical components are mounted on the other. The plate was

PLATE TWO

The screw and lever system

The interferometer set up for alignment

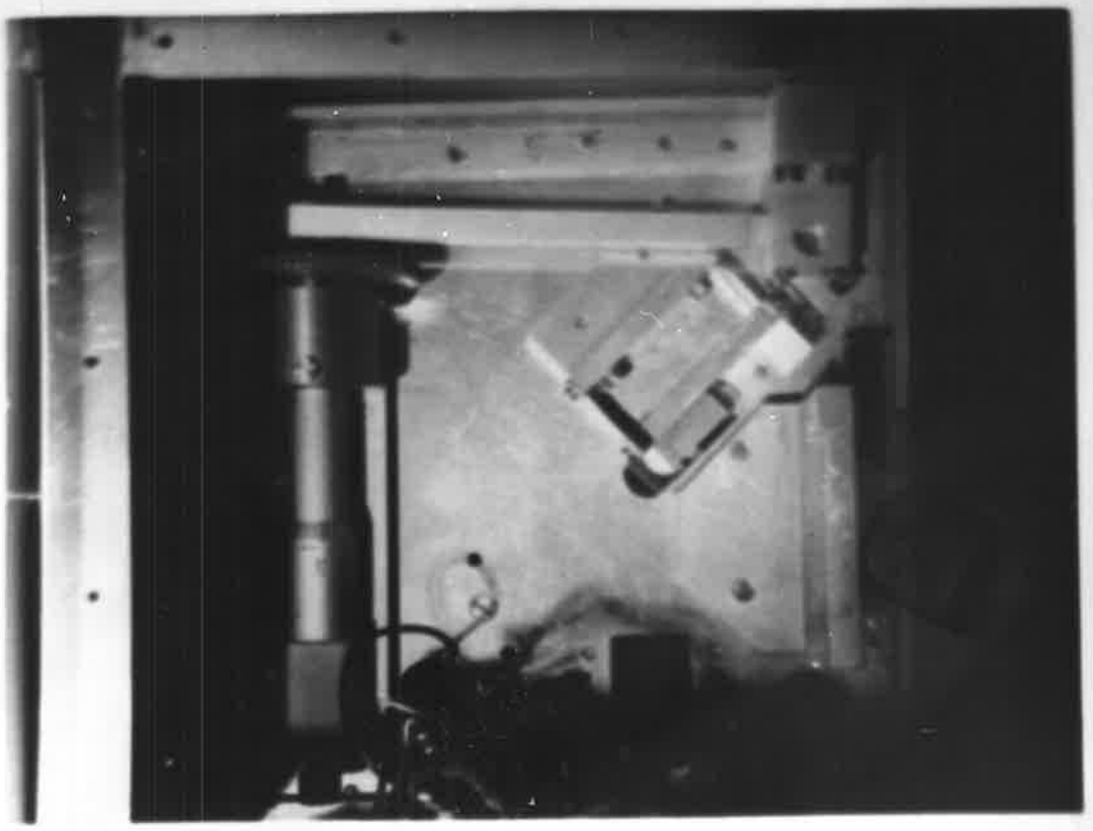

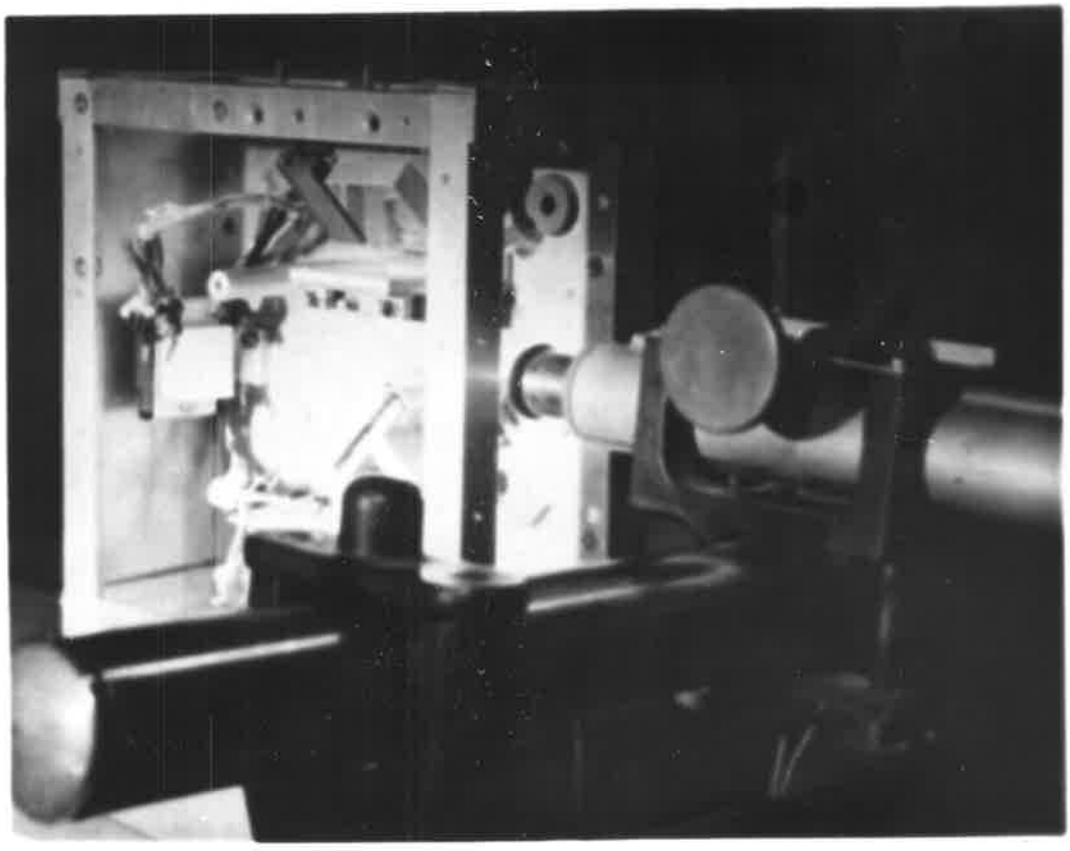

mounted inside a box of aluminium angle. The box was covered with thin aluminium sheet. The interferometer was constructed so that it could operate without the covers, so that all adjustments can be made with all the optical components in place. The only adjustment which cannot be made in situ is the width of the main slit. Mounted on the box was the gnomon of the sun pointer. The box was fitted with an axle so that it could be mounted on a two axis attitude stabiliser. An electronic control drives motors on the stabiliser so that the gnomon always points at the sun. The pointing accuracy was about one degree.

The main requirements of the mechanical part of the interferometer are, firstly, some means of moving one mirror, so that it always remains parallel to another, fixed mirror; secondly, that the mirror be moved in equal steps of the order of one micron in length; thirdly, that all the mirrors be mounted securely, but without strains and be provided with three point adjustment so that their relative positions can be set up exactly; and fourthly, that the main slits be provided with adjustments so that its width and direction can each be altered without affecting the other. Auxilliary to the interferometer is a chopper mirror which provides sky cancellation. This mirror must oscillate between two positions, but the vibration must not affect any of the optical adjustments.

4.3.1. The Mirror Carriage.

The moving mirror is required to move in a direction normal to its surface, but to remain always parallel to the fixed mirror. The mirror mounting is fixed to a carriage which is fixed to the

base plate by two flat springs. These springs are of the same length and parallel to each other. They permit the carriage to move back and forth in a direction normal to the mirror surface, but act like a parallel rule and force the carriage to remain parallel to its original direction. The springs are quite flexible in this direction, but, because of their width are very stiff in the direction perpendicular to the base plate. This holds the distance between the fixed and moving mirrors constant.

4.3.2. The Mirror Drive Chain.

The mirror is driven by an electric motor through a drive chain. The purpose of the drive chain is to reduce the motion of the motor so that one revolution of the motor moved the mirror a very small distance. The drive chain consists of a worm gear, a screw and a lever. Normally such devices are used to gain a mechanical advantage. Here they are used for the effect of their velocity ratio.

The worm gear is attached to the axle of the electric motor. A semicircular piece of brass shim is fixed to the hub of the worm to interrupt the light path between a small light bulb and a photocell. This is provided so that the electronics controlling the interferometer can count the number of rotations. The worm meshes with a sixty-four tooth pinion. One rotation of the motor turns the pinion one sixty-fourth of a revolution. The pinion is attached to the screw, which is constructed from a micrometer screwgauge. This was the most accurate form of screw available at the time. The micrometer screw has a pitch of 0.025 inches, or

about 0.635 mm. One rotation of the motor moves the screw through 0.015625 of the pitch or about 9.82 microns.

The motion of the screw is further reduced by a lever. This lever has two arms at 135 degrees to each other. One arm is ten centimeters long and the other is one centimeter. At the junction of the arms is a fulcrum. The fulcrum is a form of pivot constructed out of flat spring. Two pieces of spring lie in the same plane parallel to each other. The third spring is perpendicular to the other two and lies between them. One end of each spring is attached to the lever and the other end is attached to the baseplate. The width of the springs provides the stiffness which holds the lever at a fixed distance from the baseplate, similar to the springs which hold the mirror carriage. Whereas the springs which hold the carriage are parallel and permit the carriage only parallel motion, the springs which hold the lever are at right angles to each other and permit the lever to rotate about the line of intersection of the springs. They do not permit any other motion. Since the motion of the pivot involves only the elastic forces of the springs, there is no friction, stiction or backlash in the pivot. In addition, there is complete freedom from wear. The pivot is virtually a perfect fulcrum. The pivot as described above was designed and under construction when it was discovered that there was an assembly based on the same principle available commercially under the trade name 'Flexipivot'. Since this was smaller and more accurately made, a commercial unit was used in the interferometer.

At each end of the lever is a small screw. Each screw is made of hardened steel and has a rounded end. These two screws were adjusted so that the angle between the line from the end of one screw to the centre of the pivot and the line from the other screw to the pivot is as close 135 degrees as possible. It is these screws and the centre of the pivot which define the actual lever. The screw on the long arm of the lever rests on the anvil of the micrometer screw. The screw at the other end of the lever bears on a projection of the moving mirror carriage. The lever arms are 10 cm and 1 cm long respectively so that the motion of the carriage is one tenth of the motion of the micrometer. The total velocity ratio from the motor to the mirror carriage is such that one rotation of the motor moves the carriage through 0.982 microns. From the theory given above, the shortest wave-length that can be handles when the step length corresponds to one rotation of the motor, is about 2.0 microns. Initially, it was proposed to use a differential screw to drive the mirror, but it was not possible to construct such a screw sufficiently accurately with the facilities available. The method used above was developed to take advanatge of the available micrometer screws as a standard of length. Subsequent to the construction of the interferometer, a differential screw has become commercially available. This screw is capable of motion of the order of 0.5 microns without using a lever.

4.3.3. Sky Cancellation.

The sun's radiation is similar to that of a black body at a temperature of about 6,000 K. Its radiation is mainly in the optical region of the spectrum, with a maximum around 0.5 microns. The Earth absorbs this radiation, which warms the Earth so that it is emitting thermal radiation at the same rate as it is received from the sun. The temperature of the Earth is about 300 K. If it radiated like a black body, its spectrum would have a maximum around ten microns.

Since the flux per unit area emitted by the Earth must equal the flux per unit area received from the sun, it can be said that in the infra-red, the Earth is brighter than the sun. The atmosphere, which is heated both by its own absorption of the sun's light and by contact with the Earth, also emits thermal radiation. The atmosphere, as discussed in chapter two, strongly absorbs radiation in several bands in the wavelength region from two to twenty microns. It follows from Kirchoff's law of radiation, that the atmosphere should also be a stronger emitter in those bands. A detector open to the sky and sensitive to radiation longer than about five microns will receive much more radiation from the sky than from the sun. The interferometer is designed so that only light from a small part of the sky, an area about that of the sun's disk is focussed on the detector at any one time, so that when the interferometer is receiving light from the sun, the proportion of light radiated by the atmosphere between the sun and the detector is as small as possible.

To reduce the effect of the sky radiation even further, the interferometer is fitted with a chopper which alters the direction from which it receives radiation. In one position of the chopper, the interferometer receives light from the sun and from the sky in the same direction. In the other position it receives light from the sky about five degrees from the sun. If the sky radiation is the same from both directions, then the difference in the amount of radiation in the two positions is the radiation of the sun alone. This technique is called sky cancellation.

The chopper consists of a plane mirror of about 2.5 cm square. It is mounted on a pivot about which it is allowed to rotate through an angle of about two and a half degrees. A tongue of steel is attached to the mirror mount and travels between two stops. Each stop is made of a flexible magnetic material. When the tongue hits one of these stops, the flexibility prevents a hard bounce and the magnetism holds the tongue in place. The pivot about which the mirror turns is parallel to the main slit of the interferometer. In one position, the mirror reflects light through about ninety degrees. In this position, light from the sun will form the interference pattern on the detector. In the other position, the mirror refelects light through about eighty-five degrees. The interference pattern of the sun's light is moved five degrees perpendicular to its long axis. The interference pattern at the detector is that due to the sky about five degrees from the sun. The detector amplifier measures the difference in the two signals. The power for the oscillation of the mirror is provided by an electric motor which makes one

rotation in about 0.1 seconds.

An eccentric peg on the axle of the motor turns in a square hole attached to the mirror mount. When the peg contacts the side of the hole, it moves the mirror sharply from one position to the other. In this way, the time that the mirror is moving is about one fifth of the time for which it is at rest. For forty per cent of the time, the interferometer is focussed on the sun, for an equal time it is focussed on the sky and for about twenty per cent of the time it is moving between the two. It makes a lot of clattering while running, but a check with a stroboscopic lamp showed that the mirror moves smoothly between its two positions with no sign of bounce.

4.3.4. The Mirror Mountings.

The fixed mirror, the moving mirror and the focussing mirror must all be mounted so that they are not strained, they can be adjusted easily and they do not change their relative positions as the interferometer moves. The mirror mounting is illustrated in figure 4.6. The fixed part of the mounting is fixed to the base plate, or in the case of the moving mirror, to the carriage. Curved around the fixed part is a thin aluminium plate. Three 10 BA screws pass through large holes in the plate, through threaded holes in the fixed part to bear on the flange of the plate. A phosphor bronze leaf spring between the plate and the fixed part holds the two apart. The screws push the plate and fixed part together. This forms a three point kinematic mount. In practice, the leaf springs were not

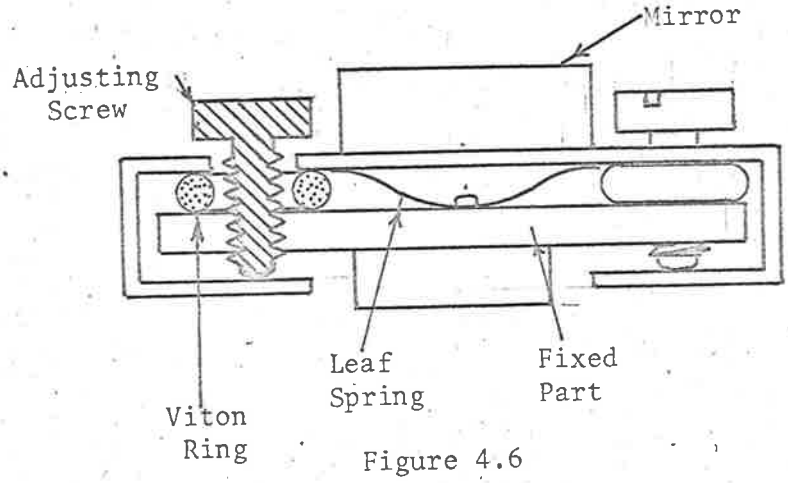

Figure 4.6

Section through Mirror Mounting

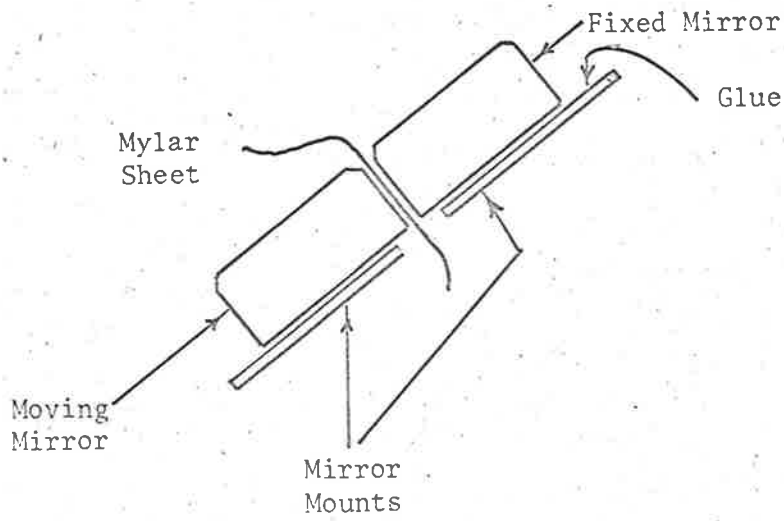

Figure 4.7

Setting the gap between the mirrors

sufficient to hold the mount in position against vibration and it was found necessary to insert thin rings of Viton, a synthetic rubber, around the screws to supplement the spring's force. This proved very successful.

The mirrors are all thick compared to their length, so that they can support fairly large strains without a great deal of distortion. Nevertheless, it was desirable that the supporting forces should be as small as possible, provided that they were sufficient to hold the mirrors in place at all angles and against vibration. A simple three point holder in which the supporting forces are supplied by some resilient material such as cork, is the normal solution to this. It was felt that unless the forces on the cork were very large, after a few hours of vibration the cork would have compressed sufficiently for the mirrors to rattle. A number of different mounting methods were considered. The one chosen was the simplest and proved to be most effective. The mirrors were glued directly to the aluminium plates with Tarzan's Grip. The supporting forces are spread over the whole of the back of the mirror, so that at any point they are small. The glue has a small amount of flexibility which will tend to distribute any concentrations of force. The bond between the glass of the mirrors and the glue and between the aluminium and the glue is weak, so that if any strains developed sufficiently to distort the mirrors, the stresses involved would break the bond with the glue and the strain would be relieved. To check that glue made a

satisfactory mount one of the chopper mirrors was glued to a large plate of the same thickness as the plates of the mountings. The plate was bent with the aid of rubber bands and the mirror checked for distortion. In checking, the mirror was placed horizontally and an optical flat placed on it. If the mirror was distorted Newton's rings would have been seen. They were not seen when the mirror mount was bent, but they were seen when the optical flat was pressed down with a pencil. They were also seen when a small piece of grit was lodged between the flat and the mirror. It was assumed, therefore, that a glued amount was sufficiently strong to hold the mirror in position and yet be strain free. The use of glue to mount the mirrors provided a very convenient way of ensuring that the edges of the fixed and moving mirrors were parallel. The moving mirror was glued to its plate with an over hang on the side next to the fixed mirror. When the glue had dried, the interferometer was set up so that the angle between the side of the moving mirror and the mounting plate for the fixed mirror formed a valley, as shown in figure 4.7. A piece of this mylar, which does not bond to the glue at all, was placed on the side of the moving mirror and the fixed mirror glued into place on its mount so that it was resting in the valley. When the glue was set the fixed mirror mount was dismantled, the mylar removed and the mount reassembled. The edges of the mirror were parallel and separated by the thickness of the mylar. As stated above, it is the edges of the mirrors which define the inside edges of the two

slits of the theory. The distance between the edges is not the thickness of the mylar. This distance is determined by the chamfer on the edges of the mirrors. Each chamfer is about 0.1 mm wide, and this is the distance b of the theory.

4.3.5. The Slits.

There are two slit assemblies in the interferometer. The main slit is the one which defines the outer edges of the two slits of the theory. The other slit performs no optical function, but serves to reduce the amount of light entering the interferometer off the optical axis.

The jaws of the main slit are made from a razor blade edge. Each jaw is spot-welded to a thin piece of steel which has slot-holes at the ends. Screws passing through the slot-holes hold the jaws onto a brass plate. This plate, as shown in figure 4.8 is bent up at the sides and through the flanges are two 10 BA screws. These screws bear on a flange on the jaws so that the jaws can each be adjusted. Each jaw can be moved independently, so that they can be set parallel at any distance apart. The plate holding the jaws has a pair of slot holes and is mounted on a similar plate which is also provided with adjusting screws. In this way the jaws of the slit can be adjusted and locked in position outside the interferometer.

When the slit is assembles in the interferometer it is possible to adjust its position without disturbing the relative positions of the jaws. The other slit is mounted in the plane of

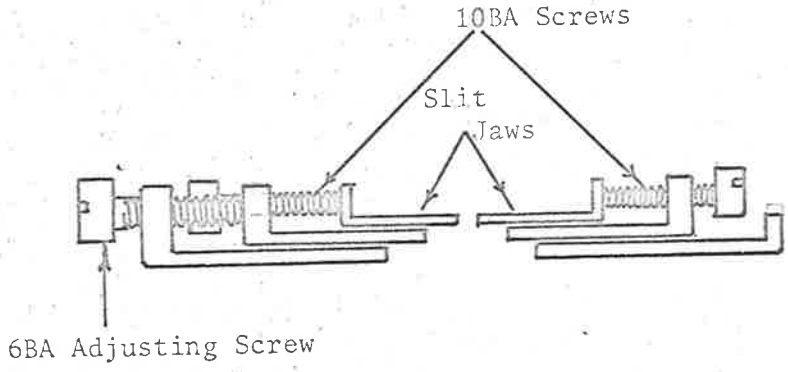

Figure 4.8

Section through slit Assembly

the skin of the interferometer box. It is parallel to the main slit and two or three times as wide. Light passing through this slit normal to the plane of the slit is reflected through ninety degrees by the chopper mirror and passes through the main slit. Other light passing through the slit does not go through the main slit but is scattered away from the detector. This slit consists of two phosphor bronze jaws screws through slot hóles to a brass plate. These jaws can easily be adjusted, and since their separation is not critical, there is no need for adjusting screws.

4.4. Aligning the interferometer.

The optics of the interferometer were aligned using a low power laser with a wavelength of about 0.63 microns. The alignment was performed in four stages. In the first stage, the three millimeter diameter beam of the laser was used as a ray tracer to depict the optical paths through the instrument. In the last two stages, the beam of the laser was widened by a telescope so that the light covered the whole of the entrance slit.

4.4.1. Preliminary Adjustment.

The entrance and main slits of the interferometer and the detector were removed and the mirrors set to approximately the positions described in section 4.2. The laser was set up on an optical bench to produce an approximately horizontal beam. The chopper mirror was put into the position in which it reflected

light through ninety degrees. When the interferometer was placed in the beam, the position of the beam on the mirror could be seen by the scattering from the dust particles on the surface. The interferometer was manoeuvred into a position where the beam was reflected from the centre of the chopper mirror, to the centre of the line between the fixed and moving mirrors to the centre of the focussing mirror. These three lines define the -Y, -Z and -X directions respectively. The X and Y directions were approximately horizontal and Z was vertical. The main slit was adjusted and measured under a travelling microscope. The jaws were set at exactly one millimeter apart and strictly parallel. The microscope was calibrated for distances of ten microns and capable of resolution of the order of one micron, so that the separation and parallelism of the jaws was accurate to better than one per cent. The main slit was returned to its mounting bracket, which, being horizontal, could support the slit assembly in place without screws. By carefully removing the slit assembly from its bracket, adjusting the position, but not the width, of the slit and returning it, it was possible to set the slit so that the vertical beam could pass through the centre of the slit from the chopper mirror to the gap between the fixed and moving mirrors. The entrance slit was similarly adjusted so that light could pass through the entrance slit to the chopper mirror. All this was done without moving the interferometer. The interferometer was then moved and the two slits screwed into place. This completed the preliminary adjustment.

At this stage it is possible to send a beam through the entrance slit to the centre of the focussing mirror via the centre of the other slit and mirrors.

4.4.2. Second Stage Adjustment.

For the second stage of the adjustment, a telescope was used to widen the laser beam. The telescope was focussed for infinity and put in the path of the beam, so that the beam went into the eyepiece. The beam from the objective was a uniform parallel beam, forty millimeters in diameter. The interferometer was positioned in the beam until the beam could be seen on the focussing mirror. The interferometer was in approximately the same position as in stage one. The entrance slit was sufficiently wide to illuminate the whole of the main slit. The light passing through the main slit formed a line at a small angle to the gap between the fixed and moving mirros, but lying across the gap. The main slit was carefully adjusted so that the light from the slit appeared to illuminate both sides of the gap equally. The image at the focussing mirror was a little faint, but was made much easier to see when a piece of paper was put in front of the mirror. The image seen on the paper showed two lines. The moving mirror was adjusted by means of its mounting screws until the line it cast on the paper was as near as possible to the centre of the focussing mirror. The other mirror was then adjusted so that the line it cast was close to, but not touching the line cast by the moving mirror. The appearance of the image at this stage was of a rectangular patch of light with a thin dark line

across it at a very small angle. The main slit was then adjusted so that the parts on either side of the dark line appeared to be the same in shape and area. The appearance at this stage was of a thin rectangle of light with a dark line down the exact centre. Using the piece of paper, the beam from the focussing mirror was traced and the focal point found. The focussing mirror was adjusted so that the focal point lay in the fundamental plane, that is, the beam from the focussing mirror passed over the gap between the fixed and moving mirrors. The focussing mirror was adjusted so that the focussed beam was seen at the top end of the gap between the mirrors. One screw of the mirror was then turned until the focussed point was no longer seen. This is the end of stage two of the adjustment. At this point, the centre lines of the main slit and the gap between the fixed and moving mirrors are in the same plane, which is the fundamental plane of the interferometer.

4.4.3. The Final Stage of Adjustment.

The interferometer remained in the same position as in stage two. The beam coming from the telescope travelled horizontally in the -Y direction, passed through the entrance slit, was reflected through ninety degrees by the chopper mirror and passed through the main slit travelling in the -Z direction. The beam from the main slit was split into two by the fixed and moving mirrors and reflected into the -X direction. The beams fell on the focussing

mirror which reflected them into cones of rays converging on the X axis. The light passed through the focal point and diverged until they fell on the wall about two meters from the focal point. the image seen on the wall was a pair of rectangles with a narrow vertical gap between them. By making small alterations to the positions of the fixed and moving mirrors, it was verified that the image seen was that of the main slit reflected by the two plane mirrors. A travelling microscope with neither the eyepiece nor objective was placed near the interferometer so that the beam as traced by a piece of paper travelled centrally down the tube. The objective was replaced and the microscope racked in until the centre of the objective was close to the focal point of the focussing mirror. The microscope was moved from side to side on its travelling carriage until an image was seen projected on the wall. This image was the diffraction pattern of a single slit. Moving the fixed mirror slightly identified the image as that due to the moving mirror. The microscope was moved so that the image was in the centre of the area occupied by the rectangular images previously seen. There were then two images of single slit diffraction patterns projected on the wall. The pattern is shown in the top half of Plate 2. Adjusting the screws of the fixed mirror brought the second pattern into coincidence with the first. The appearance of the patterns as they go into coincidence is startling. The broad central maximum of the single slit pattern breaks into five well-defined maxima, with strongly contrasting minima. The interference pattern is shown in

PLATE THREE

Two single slit patterns

The double slit pattern

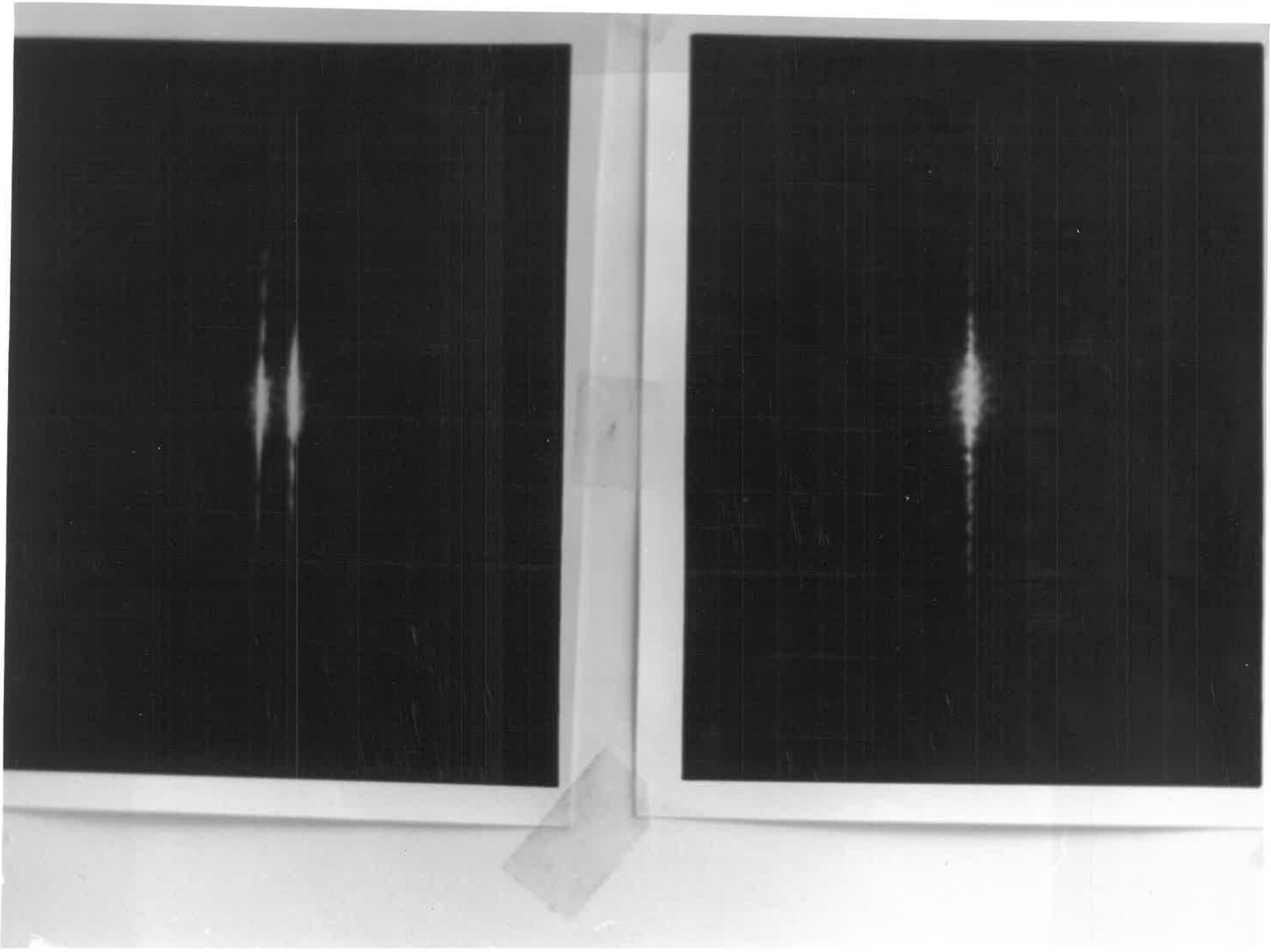

the bottom part of Plate 2. The minima of the original patterns are far less marked. This completes the adjustments which can be carried out in the dark room. At this stage the fixed and moving mirrors were parallel to each other and the adjustment was fixed by a drop of glue on the adjusting screws. Further tests were carried out in the dark room, but these will be described in section 4.5.

4.4.4. Adjustments made in Sunlight.

The interferometer was reassembled, with the detector as near as possible to the focal point of the focussing mirror. The interferometer was mounted on the pointing mechanism which was set up in the best possible position where as few as possible reflections would affect the pointing accuracy. When the pointer was as closely locked onto the sun as possible, the focussing mirror was adjusted so that a strong signal was measured by the detector. The position of maximum signal was found, and it was assumed that this was near the centre of the interference pattern. An interference filter, with a broad pass band centred on 3.64 microns was placed in front of the detector. The moving mirror was scanned back and forth until a series of maxima in the output from the detector amplifier were found. The central maximumum was assumed to correspond to a path difference of zero.

4.5. Testing the Interferometer.

The first tests of the interferometer were performed in the dark room. Measurement of the single slit interference patterns showed that the width of the slits were about 0.4 mm. These

measurements were performed as follows. The direction of travel of the microscope was parallel to the long axis of the interference pattern. The position of a minimum in the projected image of the interference pattern was marked and the reading on the microscope scale noted. The microscope was racked along until the next minimum coincided with the mark. The difference between the new microscope reading and the old gave the distance between minima in the focal plane of the focussing mirror. The position of the main slit had to be altered slightly so that the widths of the central maxima of each single slit pattern were the same. Measurements of the double slit pattern showed that the width of the gap between the mirrors was 0.2 mm. The pattern consisted of a long horizontal spindle whose brightness, and to some extent, width followed the pattern given in section 4.1.1. The interferometer adjustments were varied to test the effect on the diffraction pattern. When the main slit was moved out of position, but remaining parallel to the original position, the single slit plattern varied in the distance between minima, as mentioned above. The double slit pattern under the same conditions did not change in dimensions, but the contrast between the maxima and minima was reduced. The ultimate pattern resulting from this maladjustment was the pattern of a single slit one millimeter wide. Twisting the main slit so that its centre line no longer lay in the fundamental plane resulted in the double slit pattern tilting away from the vertical. This was particularly easy to see when the pattern was out of focus. Under these conditions the image was a

broad horizontal band crossed by vertical black bands. If the main slit was turned through a very small angle, the black bands would turn through a large angle. This provided a very sensitive method of checking whether the main slit had moved.

The motion of the moving mirror was checked to see whether it was in fact parallel. The interference pattern was observed as the motor drove the micrometer screw from one end of its travel to the other. No difference in the appearance or size of the interference pattern was noted. The envelope of the pattern remained steady where it was projected on the wall, and the minima of the double slit pattern marched steadily across from one side to the other. It was concluded that the fixed and moving mirrors remain parallel to each other over the whole range of motion of the mirror carriage, It was also concluded that the motion of the mirror does not disturb any of the other optical components.

The mirror mounts were tested for resistance to vibration by running the chopper motor for several hours and observing the interference pattern. It was found that the chopper did vibrate the interferometer as a whole, so that it had to be held in place while the test was performed. With the interferometer securely clamped by its frame the interference pattern remained steady on the wall and its appearance did not change after several hours. The double slit fringes did not move.

The above tests were repeated several times as alterations to the interferometer necessitated re-alignment. The linearity of the movement of the mirror was checked using a linear transducer. This

is a differential transformer in which a movable magnetic core provides the coupling between the windings. A built in oscillator provides the input to the transformer and a phase sensitive detector measures the amount of unbalance of the signal. The output of the transducer is a voltage which is proportional to the displacement of the core from its central position. The core of the transducer was connected to the mirror carriage and the body to the base plate. The mirror drive motor was permitted to drive the mirror from one end of its travel to the other, and the output of the transducer measured with the telemetry unit. The accuracy of the measurement was about two microns. It was found that the step length varied slightly at the ends of the travel, but near the zero path difference position, variation was not measurable.

4.5.2. Testing in Sunlight.

The tests carried out in sunlight were in general less satisfactory than those carried out in the dark room. The main difficulty was that the pointing control tended to lock onto the dust halo around the sun rather than the sun itself. Testing under different sky conditions, both in Adelaide and Mildura showed that the pointing accuracy improved with clearer skies. The best conditions were obtained immediately after a shower of rain. Since most of the dust and haze in the atmosphere lies in the turbulent region below about 4,000 feet, it was assumed that at altitudes greater than this, the sun would present a sufficiently hard-edged appearance for the pointer to lock onto. It was not possible to

perform a fully comprehensive test at ground level. The tests described below were mainly incident on the final stage of adjustment described in the last section. The short period of observing time which was available precluded the use of the chopper and required that the motor driving the moving mirror be run at full speed. Once the position of zero path difference had been established, the motor was run at its design speed, so that the mirror moved at about 0.6 microns per second. In most tests the output of the detector was measured with a millivoltmeter. In a few tests the output of the detector drove the Y axis of an XY chart recorder and the output of the linear transducer drove the X axis.

Once it was established that the detector was at the centre of the interference pattern, the variation of the intensity as the mirror moved was measured with several interference filters in front of the detector. With no filter at all the interferogram showed a broad maximum around the zero path difference, with shallow minima on either side. With a broad band filter passing wavelengths from about 2.8 microns (3600 cm^{-1}) to about 25 microns (400 cm^{-1}) the interferogram was similar, but the minima were a little more pronounced. A filter passing 3.0 microns to 4.3 microns (3,300 to 2,350 cm^{-1}) showed three maxima. A similar filter passing 4.3 to 5.7 microns (2,300 to 1,750 cm^{-1}) showed a similar interferogram with the minima further apart. A narrow band filter centered on about 2.7 microns (3,700 cm^{-1}) appeared to show a cosine curve as predicted by theory, but the amplitude was so small and the noise on the signal so large that it was not possible to be sure. The general appearance of these interferograms is illustrated in figure 4.7.

4.6. Comparison with other Instruments.

The interferometer described here has a number of advantages over other spectrometers and one substantial disadvantage.

Firstly, this interferometer possesses the multiplex advantage. This is common to all Fourier transform spectrometers, in particular the Michelson interferometer. This is only an advantage when the detector used is the principal source of noise, and the noise is independent of the signal strength, as discussed at the end of chapter three. In the interferometer constructed, the detector is a thermistor at the ambient temperature, so that these conditions are satisfied and the multiplex advantage exists. The interferometer does not have the other advantage of the Michelson interferometer, the Jaquinot advantage. This advantage is common to all amplitude division interferometers, but the interferometer described here is a wave-front division instrument.

Secondly, this interferometer is constructed without any refracting components. Few optical materials transmit light over more than one octave without absorbing light in one or more parts of the spectrum. This is the principal advantage of the prism spectrometer. In broad band infra-red spectrometers for laboratory use, the width of the collimator slit is altered as the spectrum is scanned so that the total energy reaching the detector is constant. This means that the resolution of the instrument varies over its operating wave-band. Further, in laboratory instruments

it is possible to have a beam direct from the light source and another through the absorbing medium whose spectrum is to be measured. Comparison of the two beams gives the absorption spectrum of the sample, irrespective of the absorption in the prism. This is not possible when the sun is the light source and the sample is the whole of the Earth's atmosphere. The Michelson interferometer also suffers from frequency sensitive components. The beam splitter is either a semi-reflecting film on a transparent substrate or it is a self-supporting film. In the first case, one of the beams must traverse the transparent substrate three times. Since all optical materials are to some extent dispersive, the beam splitter introduces a phase difference between the beams separate from that introduced by the path difference between the two mirrors. This phase difference is frequency dependent, so that for a given position of the mirrors the effective path difference is different for each frequency. To overcome this a slab of glass of the same thickness as the beams splitter substrate is inserted in the path of the other beam, so that that beam must also traverse three thicknesses of optical material. As with the prism spectrometer, this optical material will limit the band-width of the instrument. When the beam splitter is a thin film, interference takes place in the film, and the beam splitter acts like a poor quality Fabry Perot interferometer. A practical self-supporting film must be at least a few microns in thickness. This is the same order of magnitude as the wave-length

of the radiation to be measured. The light transmitted through the beam splitter shows a channelled spectrum which, for spectrometry purposes is as bad as absorption in the optical path. In Michelson interferometers designed for operation in the far infra-red, the thickness of the beam splitter is much less than the wave-length, so that these instruments are very successful in this application. The diffraction grating shares with the interferometer described here the property that it is possible to build a spectrometer without refracting components. However, as pointed out in the discussion in chapter three, the diffraction grating spectrometer is limited to about one octave, unless there is some means of separating the orders. Such means normally involve refracting and absorbing components.

The main disadvantage of the interferometer is that there is no fixed standard for determining the wavelength. The calibration of a prism spectrometer depends on the chemical composition of the prism. The calibration does not change appreciably with environmental conditions such as temperature or pressure. Similarly, the calibration of a diffraction grating depends on the accuracy of the ruling engine during manufacture. This interferometer, as well as the Michelson interferometer, in effect carries its ruling engine with it. The calibration depends on the accuracy of the micrometer screw. For the purpose of this experiment this is not a great disadvantage, but for high resolution work it would be necessary to have some stable strength standard, such as a monochromatic light source to monitor the position of the moving mirror.

CHAPTER FIVE

THE TELEMETRY UNIT

The interferometer described in Chapter four is designed to measure the sun's spectrum at various altitudes in order to calculate water vapour and carbon dioxide content of the atmosphere. It is intended to be flown on a balloon to altitudes greater than twenty miles for periods of several hours. It is necessary that automatic controls be provided to operate the interferometer, point it at the sun, measure the output of the detector, record the measurements and monitor the operation of the whole experiment. This chapter describes the electronic units which perform these tasks. The telemetry unit is described first. It was decided that the results would be recorded on the ground from data transmitted by radio from the balloon, rather than record the data on some medium on the balloon. Radio transmission was preferred because the techniques were known and the equipment was available and reliable. Direct recording instruments suitable for the experiment did not exist and it is believed that such an instrument would have taken many years of development.

Nevertheless, the telemetry unit described in this chapter was designed so that if such a recorder became available it could have been accommodated without difficulty.

5.1. Requirements of the Telemetry.

To provide a basis for the design of the telemetry unit, a computer simulation of the experiment was performed. The University of Adelaide's Cirrus Computer was used for the simulation. This had a cathode ray screen and facilities for interactive computing so that the effect of the experiments described here could be quickly seen. An artificial spectrum, consisting of a rectangular band, a broad triangular band and a narrow triangular band to approximate a line, was assumed. The Fourier transform of this spectrum was found analytically and an interferogram, such as would be generated by the interferometer, calculated for about 260 path differences. Two hundred and fifty six points from the interferogram were taken, 'mangled' in various ways to simulate different forms of telemetry and the result applied to the Fast Fourier Transform subroutine to recover the spectrum. The computer then displayed the original spectrum and the one calculated from the interferogram on the cathode ray screen, so that the two could be compared. In the first set of experiments the values of the interferogram were truncated to different precisions. It was found that ten or more bits precision produced a spectrum which was, except for a few points, indistinguishable from the original. For fewer bit

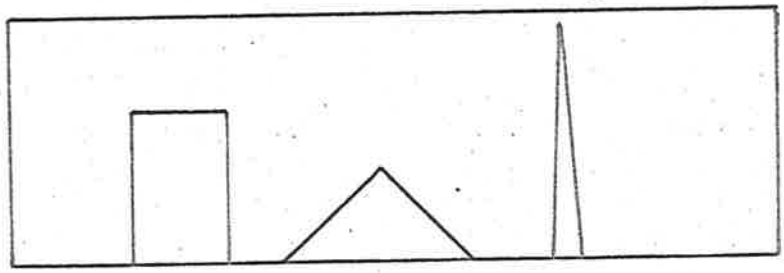

Original Spectrum

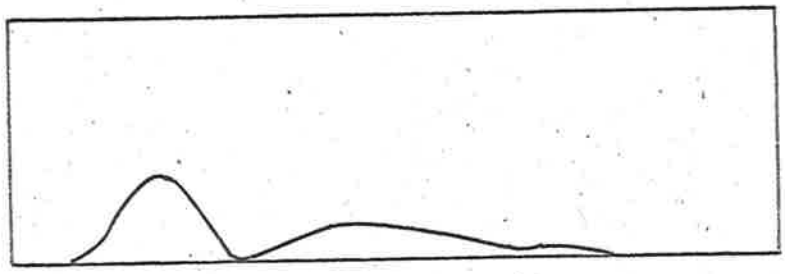

Low Precision Data

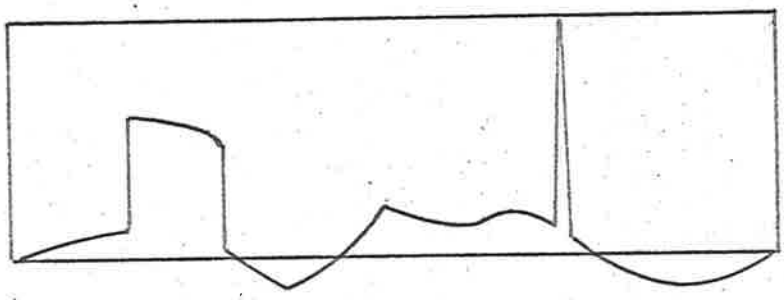

Single Bit Error

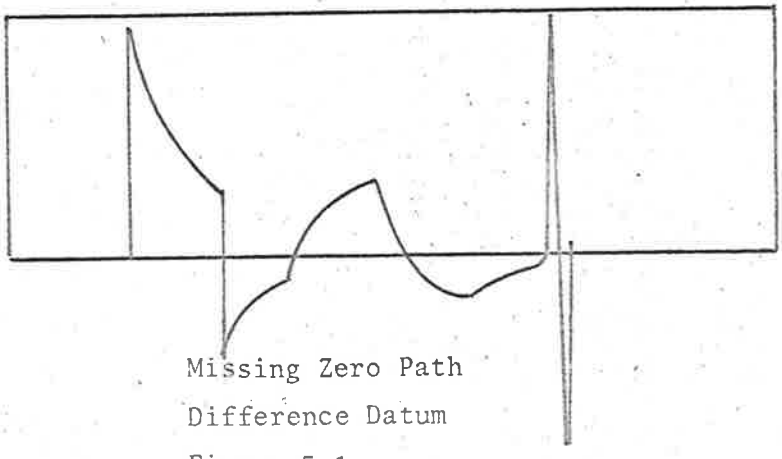

Missing Zero Path

Difference Datum

Figure 5.1

Simulated Telemetry Errors

precision, the accuracy of the spectrum was less. At five bit precision the rectangular and broad triangular bands both looked like Gaussian bands, and the narrow triangular band had vanished. It was concluded that the measurements of the infrared flux should be made to an accuracy better than ten bits. This simulation was repeated, for a different purpose, on a different computer and using a different program. The repeat showed that a five bit precision could give a spectrum which was similar to that found using twelve bits. The reason for the discrepancy is not knwon. It may be a programming fault or the effect of a shorter machine word, but since the original computer has been dismantled, it is not possible to verify this.

In the second set of experiments, the interferogram was truncated to twelve bits of precision and single bits of the data were inverted to simulate the effects of transmission noise. The bits to be inverted were chosen either by the programmer or by the computer as determined by a pseudorandom number generator. A single bit in error in the whole interferogram added a sine curve to the calculated spectrum. The amplitude of the added curve depended on the bit position within the data word. A single bit error in a low order bit produced no observable difference in the spectrum. A single bit error in a high order bit produced a sine curve whose amplitude was several times that of the original spectrum. The number of cycles of the sine curve shown in the spectrum depends on the word in which

the error occurred. If the error was in a data word corresponding to a small path difference, the sine curve was long and easily recognisable as such. For long path differences there were a large number of cycles of the sine curve within the spectrum displayed, so that the sine curve looked like a collection of random points, and the original spectrum was chopped up so as to be unrecognisable. Experiments with randomly chosen errors showed that recognisable spectra could usually be recovered, but that multiple errors usually obscured the spectrum. When the values of the interferogram were printed out it was easy to see which words were in error and they could usually be corrected. It was decided that for convenience in recovering the spectra, the error rate of the telemetry system should be less than one bit per interferogram, that is, the error rate should be less than one bit in 3,000. The overall error rate achieved by the telemetry unit in an actual flight was about one bit in 5,000 during the balloon's ascent.

In the third set of experiments with the simulator the data was again truncated to twelve bits. One or more words of the interferogram were omitted and the rest moved to fill the gap, with extra words being inserted at the end. This corresponded to the case in which a datum has been missed, and the data following has been attributed to path lengths different from those at which the data was measured. The effect depended upon the position of the datum omitted. If the datum corresponded to a large path difference, small spikes appeared on

the spectrum, which was otherwise unchanged. If the datum corresponding to zero path difference was omitted 'differentiation' similar to that in electronic circuits containing a high pass filter was seen. In general, the omission of a point in the interferogram produced a spectrum which bore little resemblance to the original spectrum, but without prior knowledge of the original spectrum it was not possible to recognise that the result was wrong. Nor was it possible to recognise which point had been omitted by inspection of the interferogram. It was therefore deemed essential that the omission of a data point be recognised and the identity of the point omitted be known. This was achieved by grouping the data into records of a fixed format and numbering the records serially before transmission. The original spectrum and three of the mangled ones are shown in figure 5.1.

5.2. Overall Design.

Figure 5.2 is a block diagram of the whole telemetry unit. The telemetry unit measures analogue voltages, converts them to digital form, encodes them and transmits them to a ground stattion. The separate separate parts of the unit are as follows:-

HPADC. This is a high precision analogue to digital converter. It measures the input voltage which must lie in the range 0 to 10 volts, and its output is a twelve bit number proportional to that voltage. It performs one conversion every 0.8 seconds, although the conversion time is about 0.4 seconds.

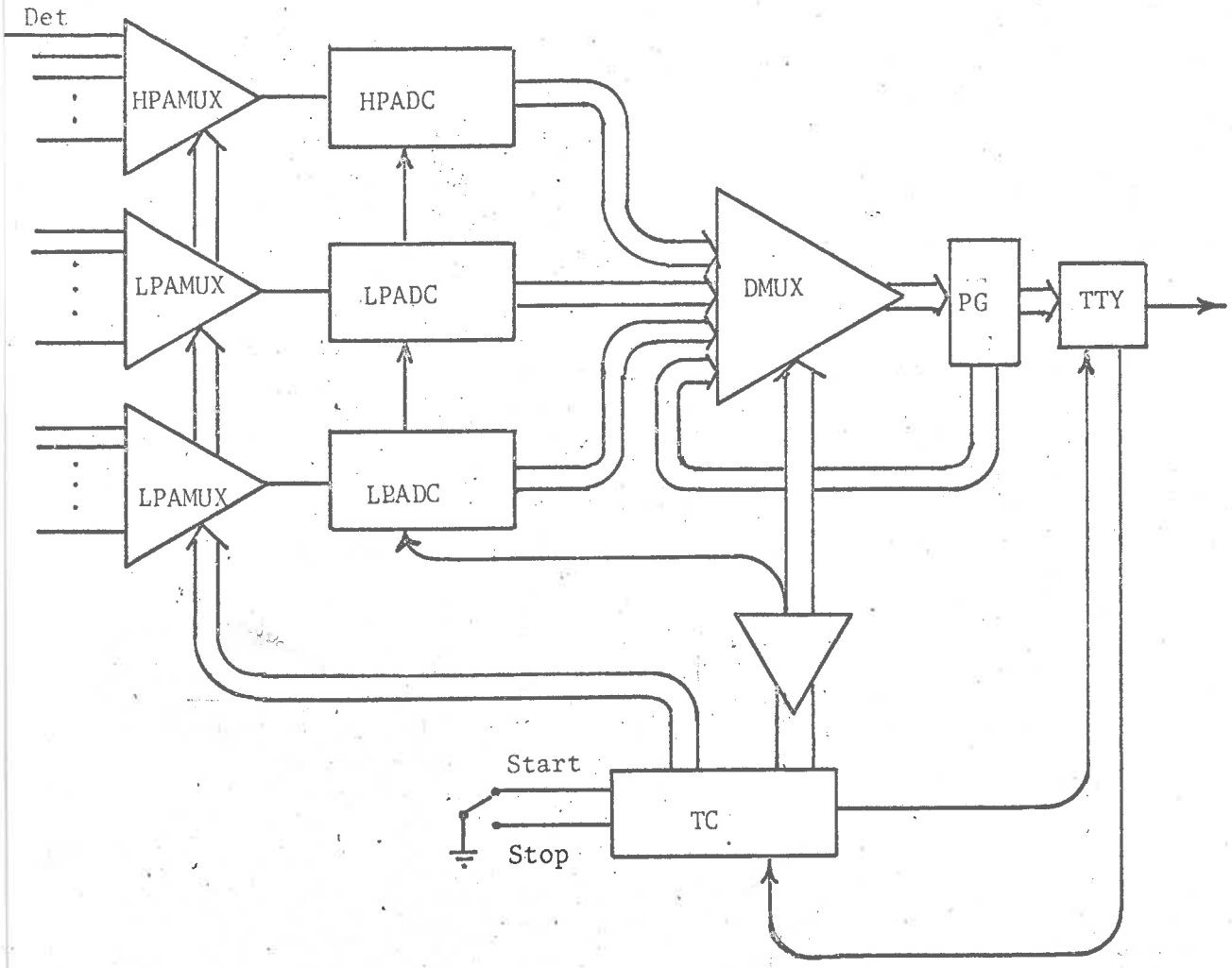

Figure 5.2

Block diagram of Telemetry

HPAMUX. This is a high precision analogue multiplexer. It connects one of its eight inputs to the HPADC every 0.8 seconds. The multiplexer is constructed of reed relays which have a very small 'on' resistance, about 0.1 ohms, a very high 'off' resistance, about 10^8 ohms and no voltage offset. The first input, marked Det, is connected to the HPADC once every 1.6 seconds. The other seven are selected in order in the alternate periods. The whole cycle takes 12.8 seconds, in which time the Det input has been read eight times and the other seven once each. (One of the other inputs is actually read twice, but the result of the second conversion is never transmitted.)

LPADC. These are two low precision analogue to digital converters, which, although basically identical to the HPADC, are restricted to six bits in the output. The conversion time is about 6.3 milliseconds, but they make only one conversion in 0.8 seconds in synchronism with the HPADC.

LPAMUX. These are a pair of low precision analogue multiplexers. They connect one out of their fifteen inputs to the corresponding LPADC once every 0.8 seconds. They are constructed of diodes, so that there is considerable offset and non-linearity in the resulting measurements.

DMUX. The digital multiplexer transmits digital data from its forty-eight inputs to the parity generation circuit. The transmission is performed in eight frames, each frame consisting of six bits in parallel. One frame is transmitted every 0.1 seconds.

The eight frames constitute one word of information. The word contains the results of the HPADC measurement, one measurement from each LPADC and twenty-four bits of digital data from elsewhere.

PG. The Parity Generator receives the six bits of each frame from the DMUX and generates a seventh bit such that the total number of bits in each frame is odd. This provides an error checking capability since, if a frame is received in which the total number of bits is even, then it is knwon that at least one error has occurred in transmission. The PG also generates a longitudinal parity check. Each of the six inputs to the PG is applied to the trigger input of a flip-flop. After seven frames of a word have been received from the DMUX each flip-flop will contain a zero if the total number of ones in that bit position was even and one if the total number of ones was odd. The output of these flip-flops provides the eighth frame of the word. In one word, the total number of bits in any one bit position is even so that the flip-flops are all reset to zero when their outputs are transmitted via the DMUX back to their inputs. The output of the PG can be written down as eight rows each of seven columns. Each row corresponds to one frame of data. The total number of ones in any row should be odd and the total number of ones in any column should be even. If a single error occurrs in the transmission of one word, then there will be

exactly one row with an even number of ones and exactly one column with an odd number of ones. The row and column identify the bit in error and the error can be corrected by complementing that bit. For example, in any actual flight the following word was received:-

```
0 1 1 1 0 0 0
1 1 1 1 0 1 0
0 1 1 1 0 1 1
0 0 1 1 1 0 1 *
0 0 0 1 1 0 1
0 0 1 0 1 1 0
1 1 1 1 1 0 0
0 1 0 0 0 1 1
  *
```

The fourth row contains an even number of ones and the second column contains an odd number. If the bit at the intersection of the row and column is changed from a zero to a one, the correct relation is restored. In this way it is possible to correct single errors in the transmission of data. This scheme provides the correction of all single errors, the detection of all double errors, the detection of all triple errors, although a few of these may counterfeit single errors and be corrected as such, and the detection of most quadruple errors. If the probability of a single error in one word is p and the errors occur independently of each other, then the probability of four errors

occurring is p^4. There are $\binom{56}{4} = \frac{56!}{52!\,4!}$ ways in which quadruple errors can occur. Of these there are only 56 x 6 x 7 ways in which the errors will not be detected. The probability of an undetected quadruple error is therefore $0.0064p^4$. Actual measurements show that p is about 0.002. The probability of an undetected error in one word is of the order of 10^{-13}. In practice errors do not occur independently, but even so, the above scheme does provide confidence in the integrity of the data.

TTY. This section accepts the data, seven bits at a time, from the PG and encodes them serially for transmission as a single bit stream. The system of encoding is identical to that used in the teletype telegraph machine, and the unit does have an output which can drive a teletype machine directly, although this is not used in flight. When idle, the unit transmits a series of ones. To transmit a frame, it transmits a single zero pulse, called a start pulse. It then transmits the seven bits of data and an eighth bit which is always one and serves no function whatsoever. The frame is completed by two ones, which are interpreted as the stop pulse. The TTY unit transmits one frame in 0.1 seconds. It transmits fifteen words, of eight frames each, successively in twelve seconds. It then idles for 0.8 seconds. This is to permit accurate synchronisation of the transmitted data with the transcribing teletype machine on the ground. It also provides a convenient signal to the operator as

to when to stop and start the tape when changing reels or performing other tasks. The TTY unit also provides the basic timing pulse of the telemetry unit. This pulse, denoted by T_c occurs at 0.1 second intervals. It is high for a period of 0.073 seconds, during the transmission of the start pulse, and the seven data bits, and low for 0.027 seconds approximately.

TC. The timing and control unit counts the T_c pulses in a seven bit counter. The first three bits of the counter are used to derive the frame Pulses T_0 to T_7. These pulses have the same shape as T_c, but occur at 0.8 seconds intervals, in cyclic order. The fourth bit of the TC counter controls the HPAMUX. When this bit is zero, the interferometer detector is connected to the HPADC. When it is one of the last three bits of the counter control the HPAMUX so that one of the other seven inputs is connected to the HPADC. The overall sequence of events is as follows. During time T_c a start pulse, six data bits D_0 to D_5 and a parity bit P are transmitted. This is called one frame. The data in each frame is selected by one of the timing pulses T_0 to T_7. In frames 0 to 2, digital data is transmitted. Frame 3 contains the odd numbered bits of the LPADC's and frame 4 the even bits. The odd and even bits of the HPADC are transmitted in frames 5 and 6 respectively. The longitudinal parity bits are transmitted in frame 7. This sequence of eight frames is called one word. The words are numbered from 0 to 15 depending on the contents of the last four bits of the TC counter. At the

end of T_7, the AMUX's are stepped on to another input and at time T_0 the ADC's start the conversion. The LPADC's measure a different input in each word. The HPADC measures the interferometer detector output during even numbered words and seven other voltages during the odd numbered words. A sequence of fifteen words is called one record. At the end of each record the TTY unit is set to idle, that is, it emits a continuous one signal during which the teletype does not punch any tape. This idle period allows the operator to stop and start the transcription of data to paper tape in such a way that punching can begin at the beginning of a record.

5.3. Circuit Description.

The circuits which implement the system described in the last paragraph were constructed on double-sided printed circuit boards. The arrangement of the boards does not correspond to the arrangements described in the last paragraph. There are two reasons for this.Firstly, in some cases it was impossible to put one unit on one board. For example, the DMUX requires fifty-eight connections, but the maximum number allowed by the connectors available was fourty-four. Secondly, by distributing several units over several boards it was possible to make the boards identical. This meant that construction was easier, maintenance was easier and fewer spare parts had to be carried. Where identical units on identical boards were required to do different jobs, extra connections were

provided so that the circuit operations could be altered by altering the wiring between the boards.

5.3.1. The one bit Digital Multiplex.

The DMUX unit is distributed over six printed circuit boards. Each board handles all the functions associated with one bit position in the data frame. The board contains two bits of the HPADC counter, two bits of one of the LPADC counters, one bit of the DMUX, a parity propagate stage, one bit of the longitudinal parity assumulator, one bit of the TC counter and two gates associated with the TC unit. Figure 5.3 is a logic diagram for one board. Each part is marked to show to which logical unit it belongs and in which integrated circuit package it is. The ADC stages are both two-bit ripple carry counters. The HPADC stage has clear inputs. The DMUX unit samples its eight inputs under the control of eight timing pulses T_i. The output of the DMUX stage toggles the longitudinal parity accumulator. The 7473 flip-flop is a master-slave type so that the output does not change until the end of the toggle pulse. At time T_7 its output is returned to the toggle input. If at that time its output was one, then at the end of that time it is triggered into the zero state. If it is in the zero state at time T_7 it remains in that state. In this way, it is always reset to zero after time T_7 and the total number of ones produced since the last T_7 will be even.

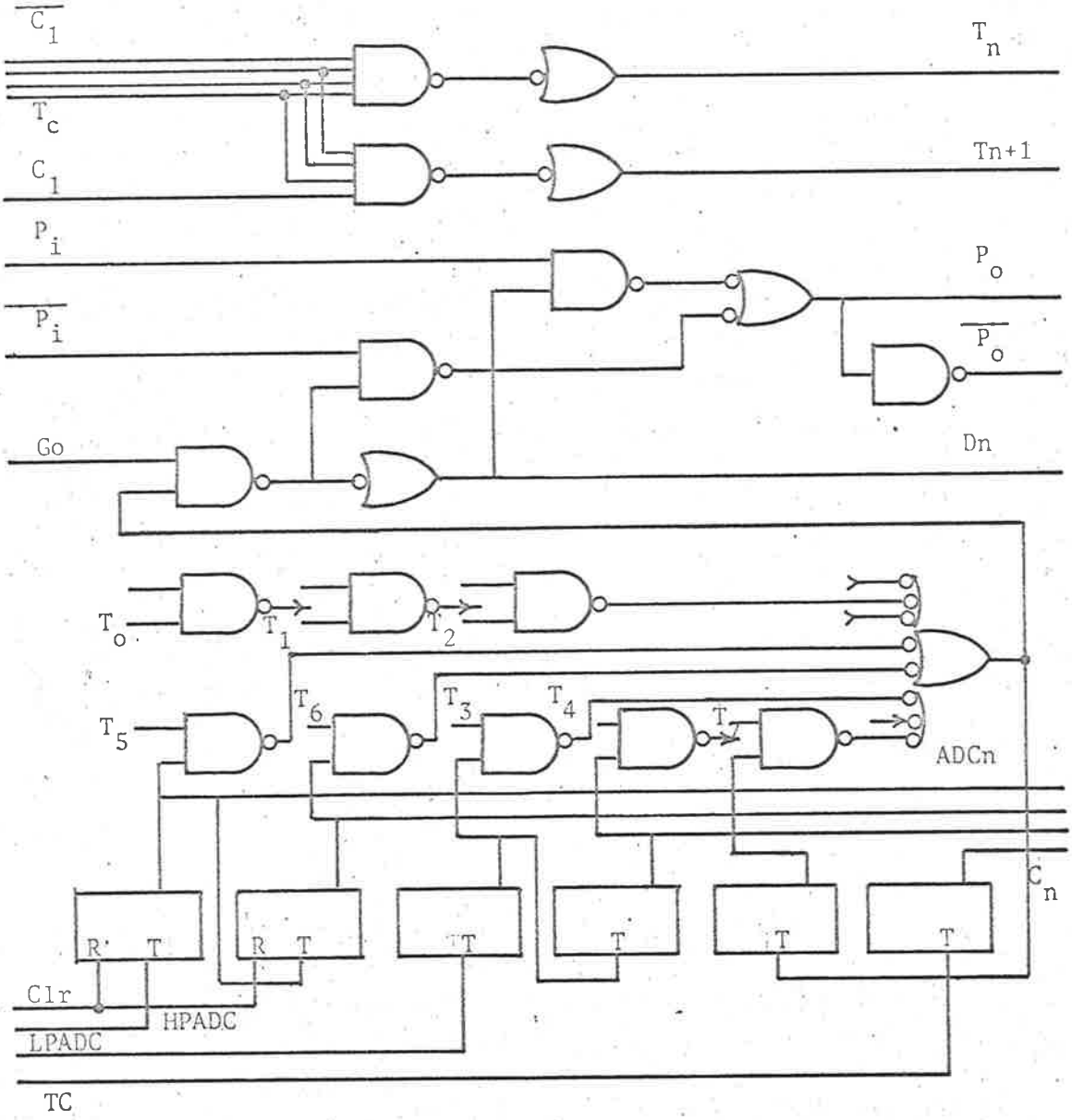

Figure 5.3
One bit of Digital Multiplex.

The output of the DMUX unit, gated by the GO signal, is applied to the parity propagate unit. This unit accepts the parity from the previous stage, performs the exclusive -or operation with the data signal and passes the result onto the next stage. If there are an even number of ones on the previous stages, the parity signal received will be zero. If the data bit from this stage is one, then the parity output will be one indicating that there are an odd number of ones to the next stage. Both true and complemented outputs from the parity stage are necessary for propagation, so that at the last stage even or odd parity can be chosen at will.

The TC counter stage is one stage of a ripple carry counter. The TC gates on this board perform the And function. Three inputs are common to both gates. The fourth input is separate. On four of the boards the four input gates generate the timing pulses T_0 to T_7. Two of the common inputs come from either the true or complement outputs of the second and third bits of the TC counter. The separate inputs come from the true and complement outputs of the first bit of the counter. The two gates on one board, therefore, generate an even numbered timing pulse and the successive odd numbered pulse. The remaining input to the gates is connected to the T_C pulse. This ensures that the multiplexer gates are enabled during the whole time that the TTY unit is transmitting the

data and also provides a 27 msec interval between the end of one timing pulse and the beginning of the next. On one board the common inputs to the TC gates are the true outputs of the last three bits of the TC counter. The separate inputs are the true and complement outputs from the fourth bit of the counter. One of the gates is high during the last word of the record. This signal which is the complement of the GO signal disables the TTY unit, so that the last word is not transmitted and a continuous logical one is output. This provides the inter-record gap referred to above. The other output is high during the penultimate word of the record. This signal is transmitted as data and gives a punched indication of the end of a record, which is necessary since the inter-record gap produces no indication on the punched tape.

5.3.2. The Analogue to Digital Converters.

The analogue to digital converters have three parts. Firstly, a section which generates pulses and counts them to define a fixed time interval, secondly, a section which accepts pulses from the first section and emits some of them. The number of pulses emitted in the fixed time interval is proportional to the voltage being measured. The third section counts the pulses emitted. Each ADC board contains an input amplifier, a dual slope integrator and associated timing circuits and four stages of main timing counter. The circuit diagram figure 5.4 shows one board. The dual slope integrator operates as follows. When the flip-flop F1 is in one state current from the input

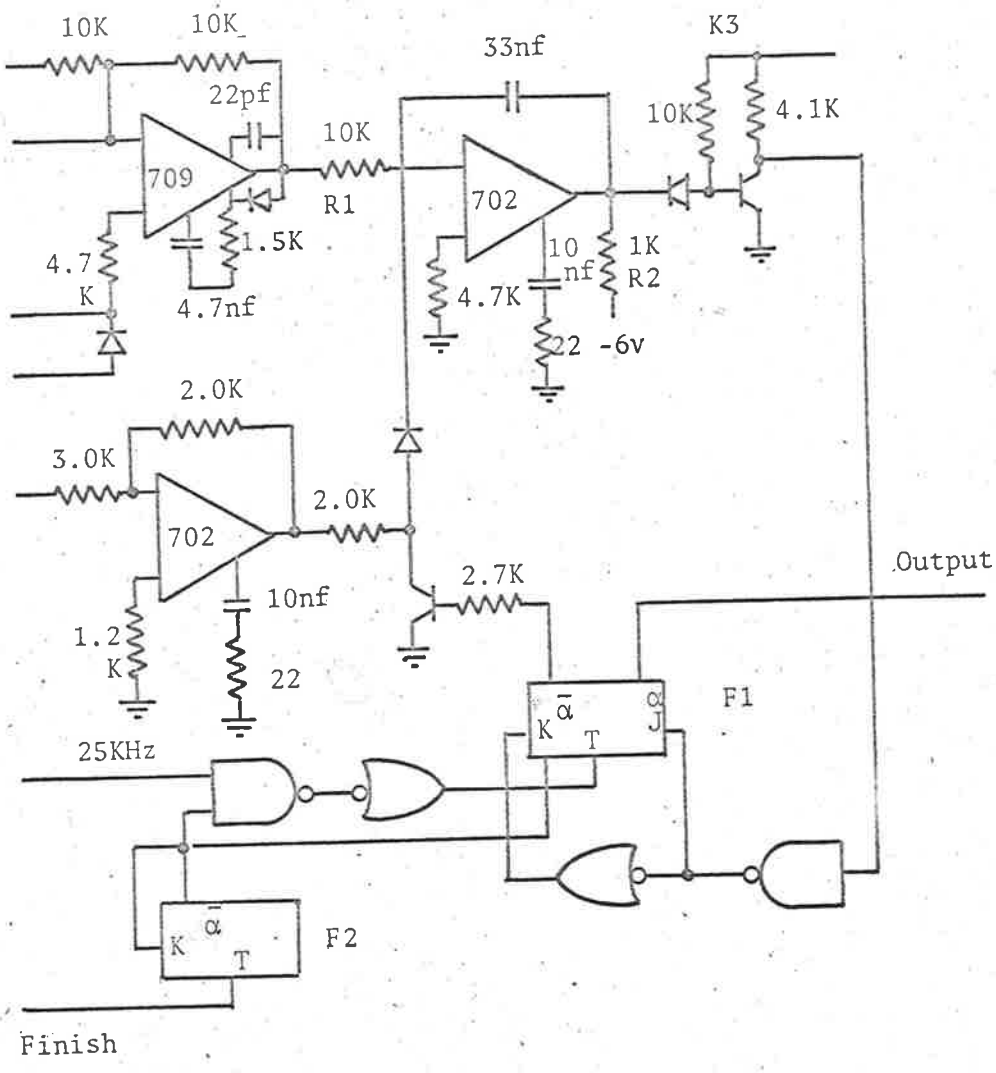

Figure 5.4

Analogue to Digital Converter.

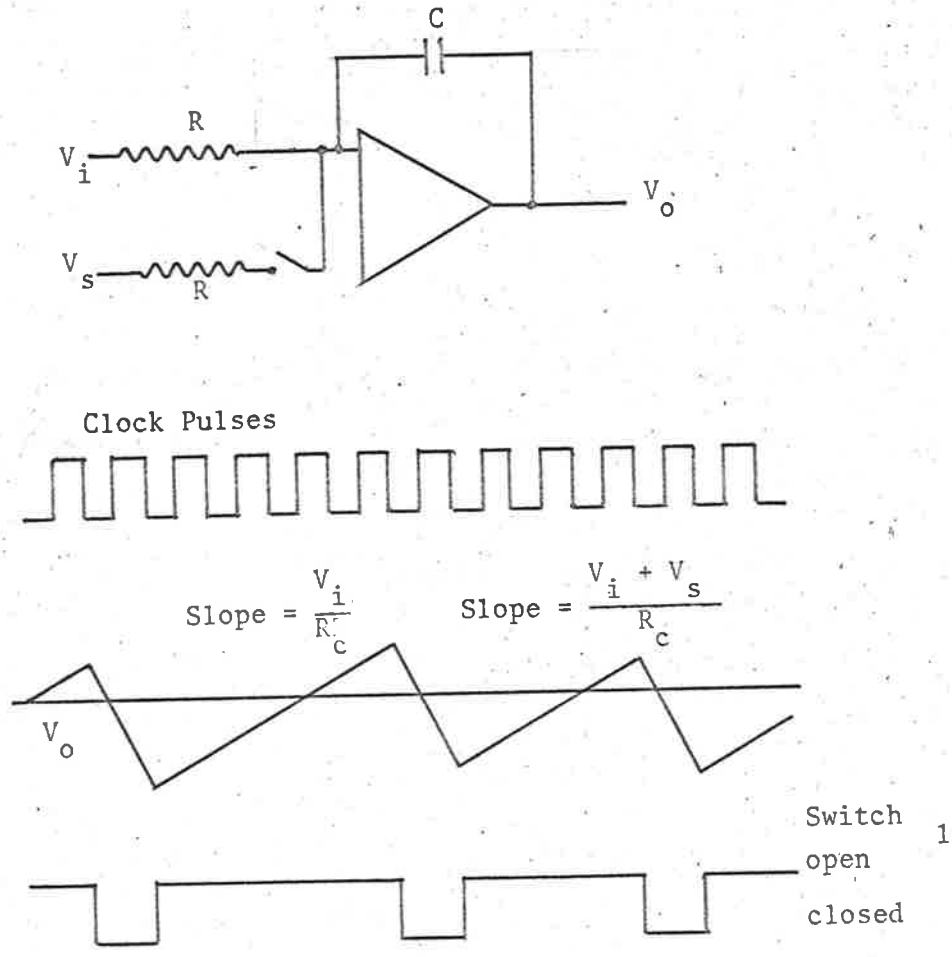

Figure 5.5

Operation of Analogue to Digital Converters

amplifier through resistor R1 is integrated and the output of the integrator is a voltage which increases with time. When the flip-flop is in the other state, current from the constant current source is integrated and the voltage from the integrator decreases with time. The current source is switched in and out by the transistor and diode gate. The polarity of the integrator output is tested by the resistor and diode network R2, D1 and R3. The input to the flip-flop is one when the output of the integrator is positive. While the ADC is performing a conversion pulses enter the clock input of the flip-flop. If the output of the integrator changes sign the state of the flip-flop changes at the end of the next clock pulse. The sequence of events is illustrated in figure 5.5. The slope of the ascending part of the integrator output is proportional to the input voltage. The slope of the descending portion is determined by the constant current generator and is such that the integrator output will always go negative within one clock pulse, and the output of the unit would be pulses at half the clock rate. Figure 5.5 represents a simplified version of the integrator. When the switch is open the output of the integrator is given by $V(t) = V_i\frac{t}{RC}$. When it is closed the output is $V(t)=(V_i+V_s)\frac{t}{RC}$. Suppose that the interval between clock pulses is T and that over a period of N pulses the integrator output was negative N times. If the voltage at the beginning of the period was zero

then the voltage at the end will be

$$V = V_i \frac{(N-n)T}{RC} + (V_i+V_s) \frac{nT}{RC}$$

Since the negative going part of the waveform always brings the output negative, and the positive going part eventually reaches a positive voltage, the output at the end will also be near zero. This gives approximately $\frac{n}{N} = \frac{V_i}{V_s}$.

The number of pulses emitted by this circuit is proportional to the input voltage. The conversion is started by a pulse which clears flip-flop F2. Clock pulses are permitted to pass to the flip-flop F1 until a single pulse is received by F2, which is set and remains set. The low precision ADC's receive a pulse after 128 clock pulses. This allows up to sixty-four output pulses (128 clock periods, with the output alternately one and zero). For the high precision ADC, N is 8192, allowing up to 4096 output pulses.

The input amplifier is a simple operational amplifier. The summing point is made available for the LPAMUX input, to allow for changes of gain and offset between different readings. For the high precision ADC it is necessary that the gain be constant, and the input is taken through a stable metal film resistor. There are two inputs provided to the non-inverting input of the amplifier. One or both of these is connected to earth. The input via the diode is intended for use with the LPAMUX to offset the diode in the input switch. The other is for the HPADC.

5.3.3. The High Precision Analogue Multiplexer.

This unit consists of two boards. Each board contains four reed relays operated by a four input gate, as shown in figure 5.6A. The four gates on each board are connected as shown in figure 5.6B. One of the gates has all its inputs taken to the connector, the other three have some inputs in common. On one board the independent gate is connected to the complement output of the fourth bit of the TC counter. This relay is closed during the even numbered words of a record. It connects the detector amplifier to the HPADC, so that the detector reading is transmitted during the even numbered words of the record. The other three gates receive inputs from the last three bits of the TC counter, so that they operate, on one board, during words one, three and five and on the other board, during words nine, eleven and thirteen. The independent gate on the other board operates during words seven and fifteen.

5.3.4. The Low Precision Analogue Multiplexers.

The basic switch is shown in figure 5.7. The diode D1 is connected to the summing point of the ADC input amplifier. Because the amplifier is connected in operational feedback this point is a virtual ground. When the transistor T1 is conducting, both sides of the diode are near ground potential, the voltage drop across it is small and its impedance is very large. When the transistor is not conducting, current can flow from the input network to the amplifier and the voltage drop across the diode

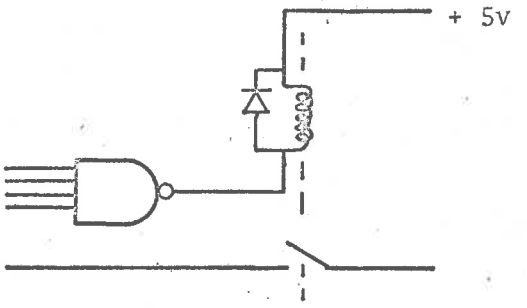

One Reed Relay Gate.

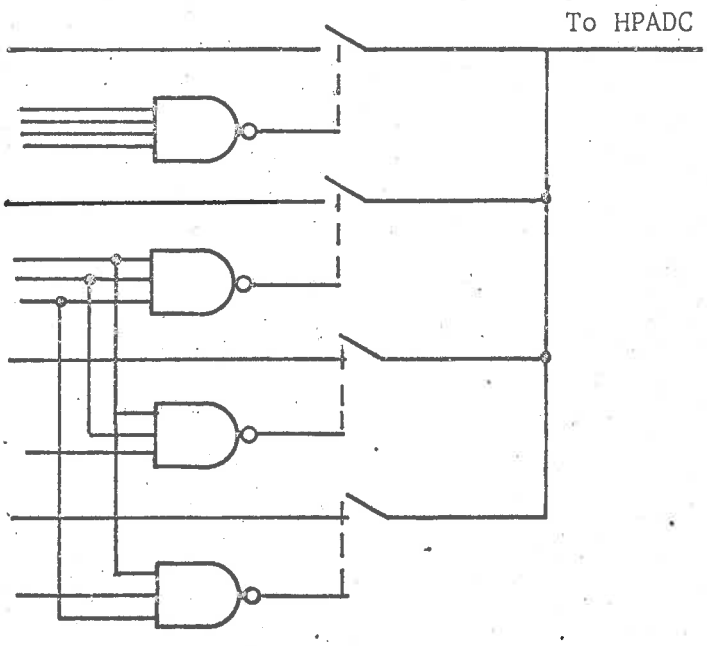

Figure 5.6

High Precision Analogue Multiplex Board.

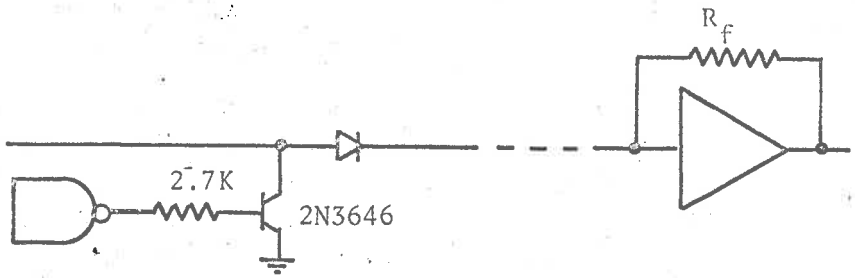

One switch.

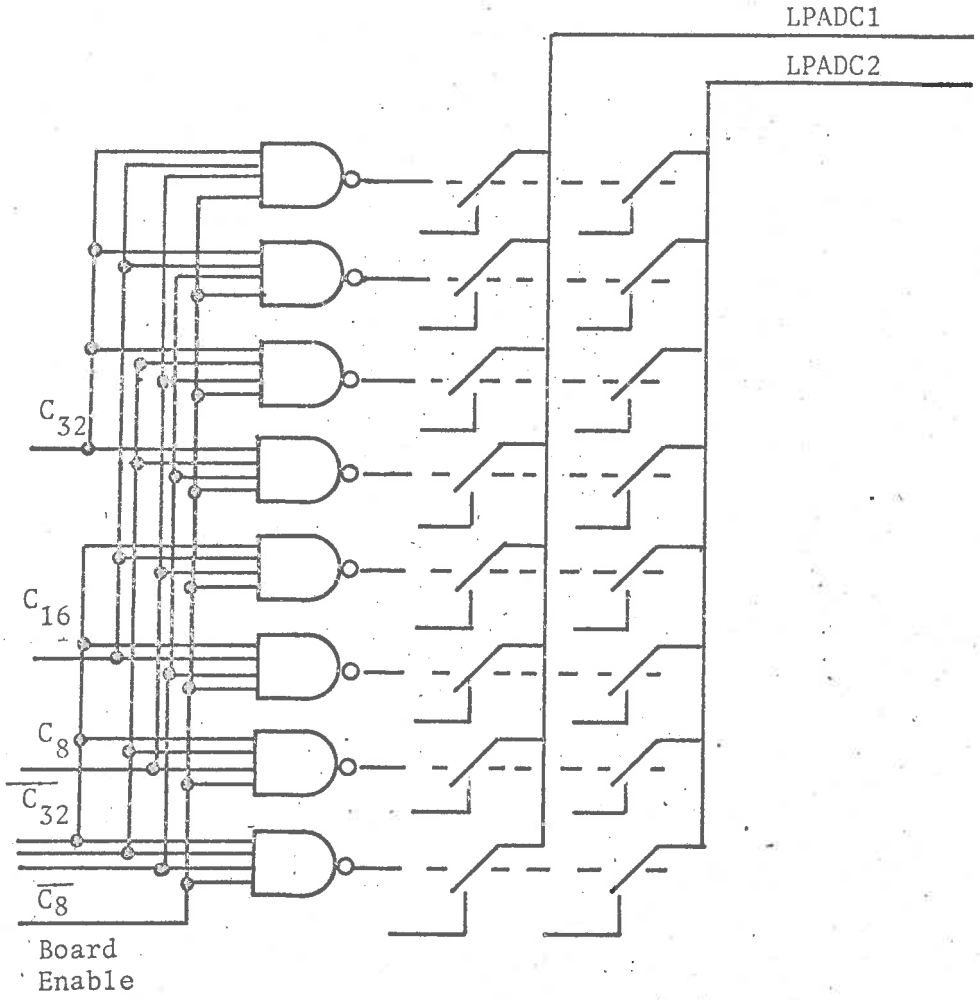

Figure 5.7

Low Precision Analogue Multiplexer

depends on the magnitude of that current. The voltage output by the amplifier is given by $V_o = I_{in}R_f$ which also depends on the input current, so that for data reduction purposes it was convenient to measure the voltage drop across the diode as a function of the number output by the ADC. Several diodes were measured and it was found that their characteristics in this respect were similar. For the data reduction program it was assumed that all the diodes had the same characteristic. Each switch has one or two resistors supplying the input current. One is connected to the voltage to be measured and determines the gain of the ADC amplifier. The other is connected to a standard supply voltage and provides a current to offset the current to be measured. This enables a high gain to be used for a measurement which is not expected to vary over a large range so that greater accuracy of measurment is possible. For example, the voltage of the battery which supplies the five volt regulator is expected to vary between seven volts and five volts. Resistor R1 was chosen as 2.7K and the offset resistor R2 was chosen as 6.8K. The ADC gives an output of zero for a five volt input and sixty-three for a seven volt input.

Each analogue switch is controlled by a four input NAND gate. Each gate operates two switches. The switches and their gates are built up on two boards, with sixteen switches to each board. Each board provides half the LPAMUX for both LPADC's. The gain and offset resistors are mounted on two other boards, one board for LPADC.

5.3.5. The Teletype Unit.

The TTY unit accepts one frame of data as seven bits in parallel and produces a serial bit stream. A 110 Hz multivibrator drives a divide by eleven counter. When the counter contains zero none of the four input gates is enabled, so that the output of the eight input gate is zero. As the counter progresses through values 1 to 7, the four input gates are enabled in turn and the data D_0 to D_5 and P appear at the output of the eight input gate. When the counter is in states 8, 9 and 10, the fourth bit is set and the output of the eight input gate is one. This produces the waveform shown.

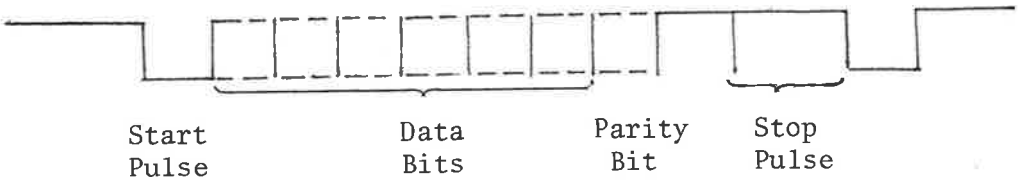

Extra gates ensure that the output is one when no data is to be sent. The TTY unit contains a driver amplifier suitable for operating a teletype machine directly. This was used while testing on the ground. In flight the output of this amplifier drove a voltage controlled oscillator.

The telemetry unit was designed to accommodate any output unit. For some devices a serialliser, such as the teletype unit, is necessary. A high speed paper tape punch could accept the seven bits in parallel. Similarly, the seven bits could be accepted in parallel by an incremental digital tape recorder, and the tape produced would be directly readable by a normal seven

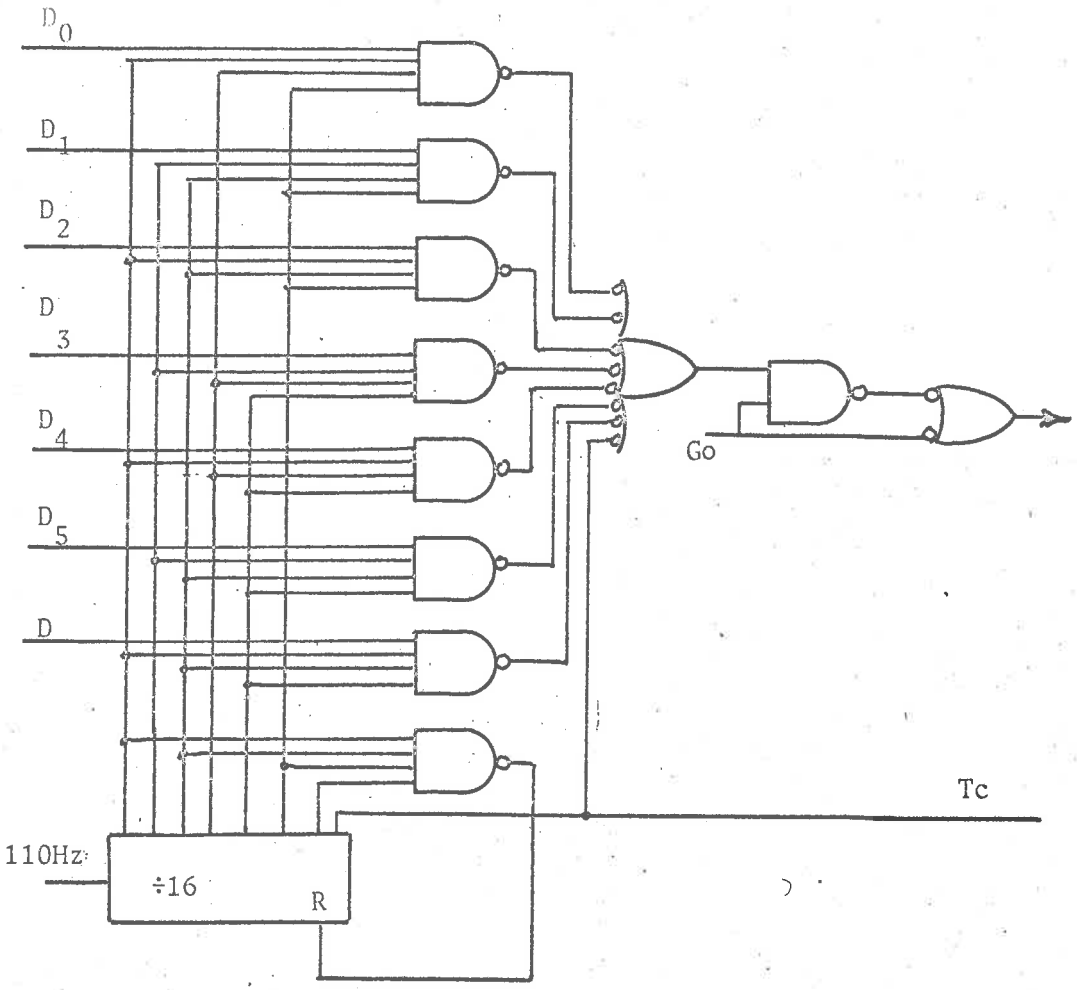

(a) Encoder

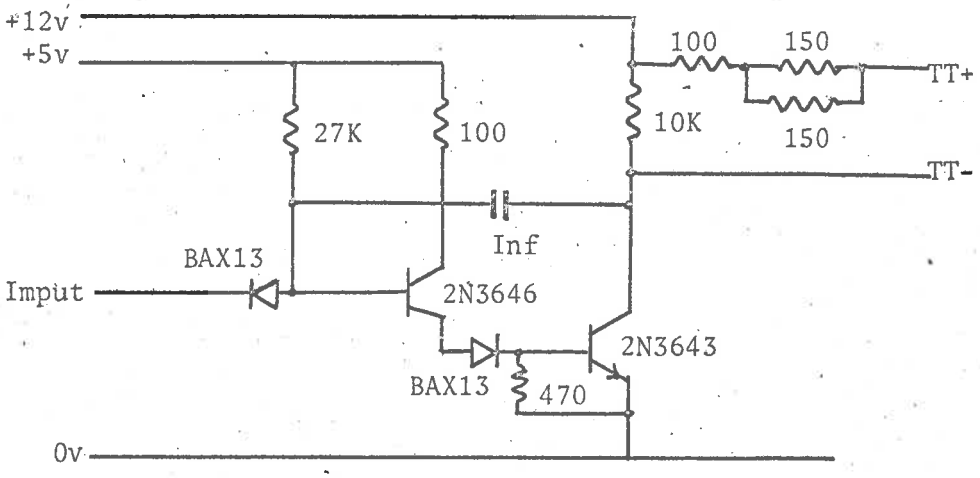

(b) Teletype Driver

Figure 5.8

track computer tape unit. It is possible that such a recorder could become available in the future.

5.3.6. The Controller.

The control board contains two circuits. One of these controls the overall operation of the telemetry unit, the other provides a serial sixteen bit clock which numbers each record which is transmitted.

A momentary ground on one of the inputs to gates G1 or G2 will set them into one or the other of two states. At time T_7 this state is copied into flip-flop F1. The other flip-flop F2 is the fourth bit of the TC counter. When F1 is in the RUN state, that is, its output is zero, the gate G3 has a one output and the timing pulse T_7 complements F2.

F2 will continue counting while either the RUN signal of F1 or the GO signal, generated in complement form, as mentioned above, on one of the DMUX boards, is one. If the unit is set to stop, then it will run until the TC counter reaches the last word of the record. It will then stop with the last four bits of the counter set at one. The first three bits of the counter will continue running. A momentary ground on the start input will reset gates G1 and G2. The immediately following time pulse T_7 will set F1 into the RUN state and the next T_7 will trigger F2. The change of F2 will ripple through the TC counter, resetting it to zero, and the GO signal will appear. In this way it is ensured that output will always commence at the beginning of the

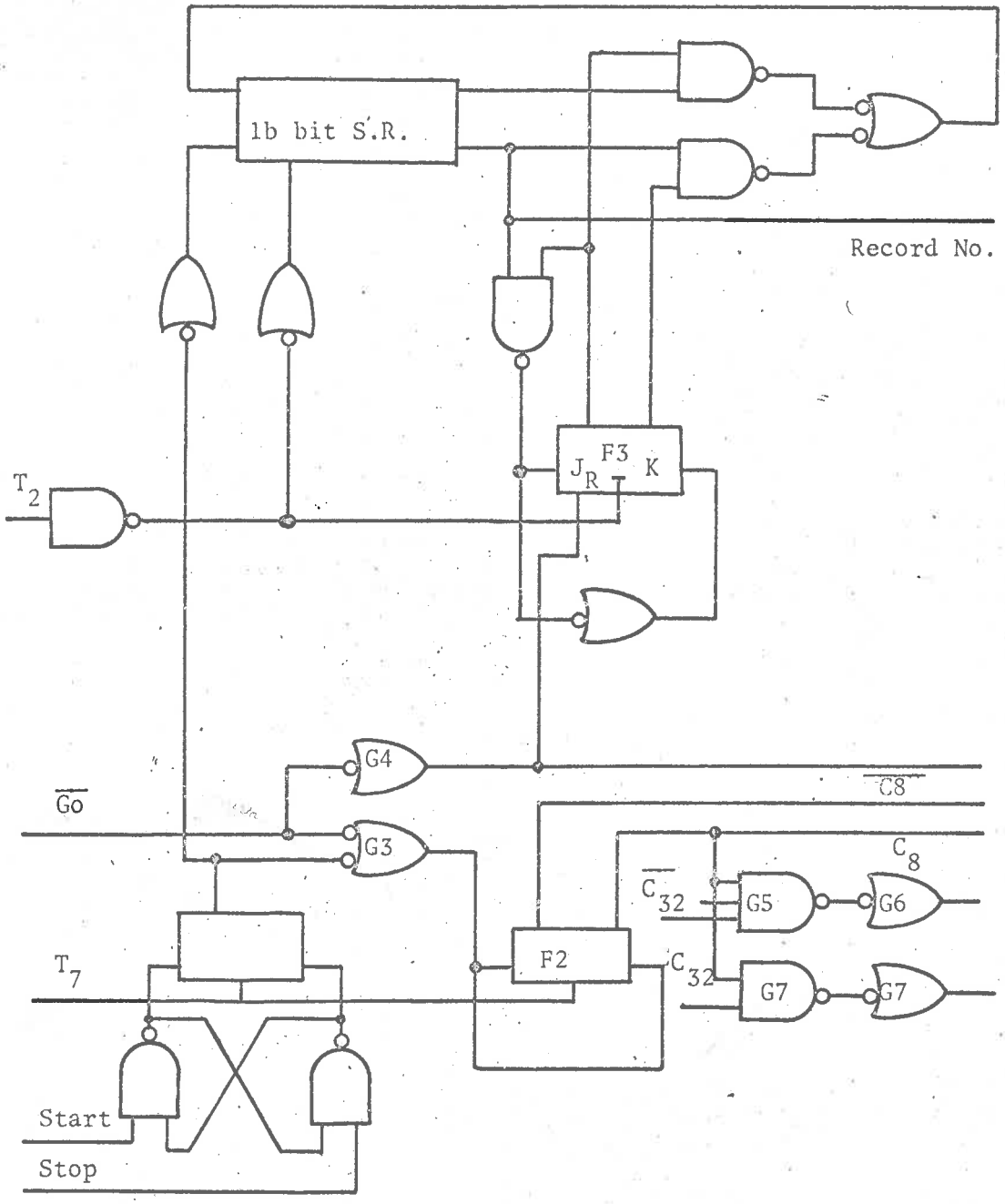

Figure 5.9
Controller Board

5.9

record and that it will continue until the end of a record. F2 controls the HPAMUX. When it is in the zero state, the detector is connected to the HPADC. When it is in the one state, it enables the signals from the last bit of the TC counter to the HPAMUX via the four gates G5-8 so that one of the other inputs can be converted.

The top section of the control board circuit contains the sixteen bit clock. At the beginning of a record the flip-flop F3 is set into the zer state and, via the gates G9-11, inverts the output of the sixteen bit register. At the end of each clock pulse, T_2, F3 is set to the same state as the output of the register. When F3 is in the one state, the gate G12 prevents any further change of F3. The overall effect is that the output of the register is inverted up to and including the first zero bit. Subsequent bits are copied without change. The result is returned to the shift register. This has the effect of incrementing the contents of the shift register by one for each record. The output of the shift register is connected to one of the digital inputs of the DMUX so that one bit of the clock is included in each word of the record. The input of the shift register is gated by the run signal, so that when the telemetry unit is turned off the clock is reset to zero.

5.3.7. The Pointer Control.

The pointer control is shown in Figure nine. The three photocells A, B and C are mounted at the base of a 25 cm long gnomon. The gnomon is mounted on a interferometer which in turn

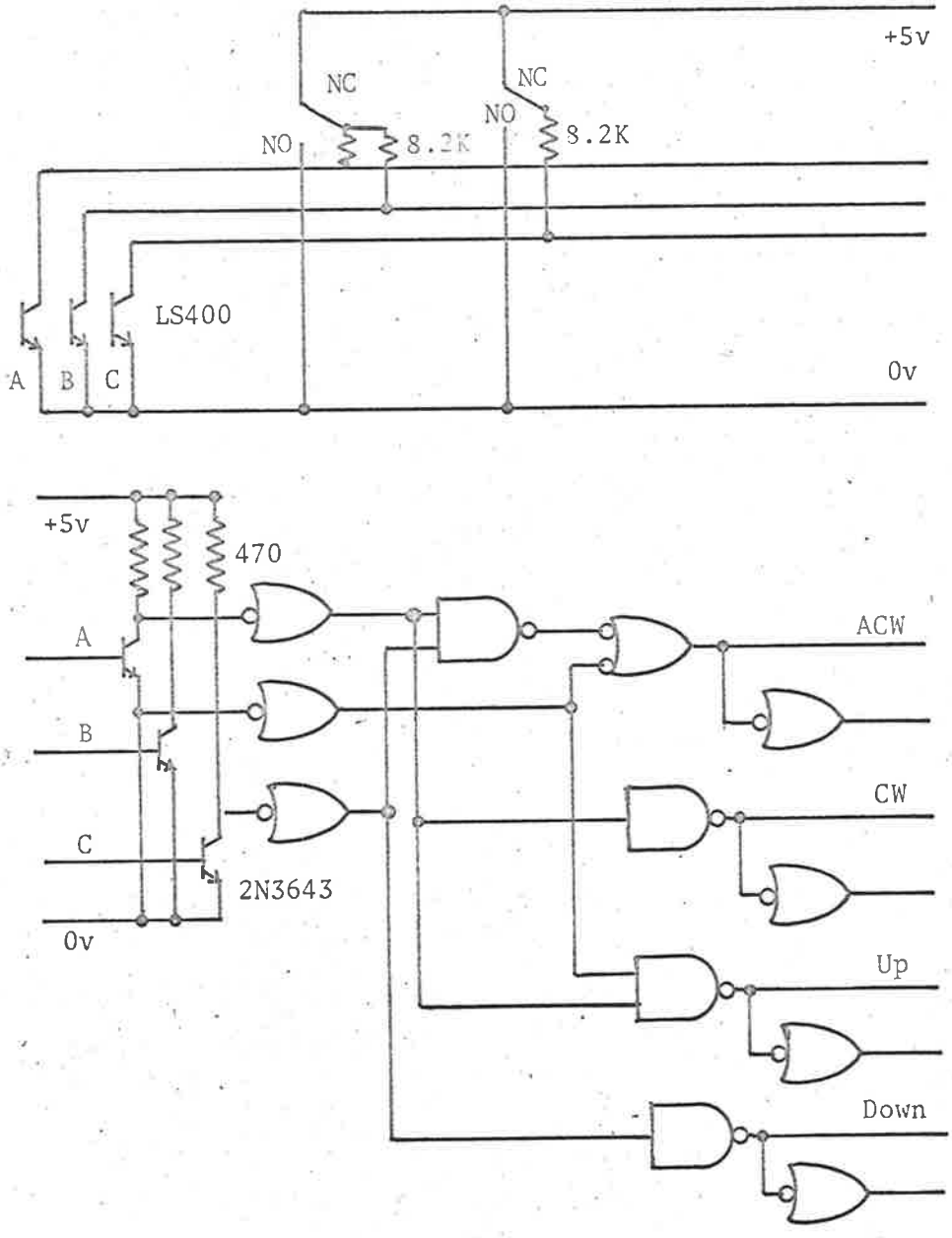

Figure 5.10

Pointer Controller

is mounted on a sun pointer, the mechanical details of which are given in Harwood (1966). The interferometer can be moved in altitude and azimuth by two motors. When none of the photocells are illuminated by the sun, the turntable is rotated anticlockwise until one or more cells are in sunlight. The logic then moves the turntable towards the illuminated photocell until all three are in sunlight. It then stops. The photocells have a sensitive area less than two millimeters in diameter so that the pointing accuracy is about half a degree, but the sun has a diameter of about half a degree, so that the overall accuracy is about one degree. Each motor control consists of four transistors in a push-pull configuration, as shown in the lower part of the figure. This enables the motor to be run from a single source of power. The logic is arranged so that whenever the motor is stationary both sides of the motor are connected to the power supply or the earth. This gives a measure of dynamic braking which, although not great, did prevent a small amount of jitter as it locked onto the sun.

5.3.8. The Detector Amplifier.

The infra-red detector is a thermistor manufactured by Barnes Engineering. It consists of a thin film of the oxides of nickel, 0.1 mm square and 10 microns thick. Two such thermistors are deposited on a sapphire substrate. One thermistor is exposed to incident radiation, the other is shielded. When the exposed thermistor absorbs the radiation its temperature is raised, which alters its resistance. The detector is thus a thermal

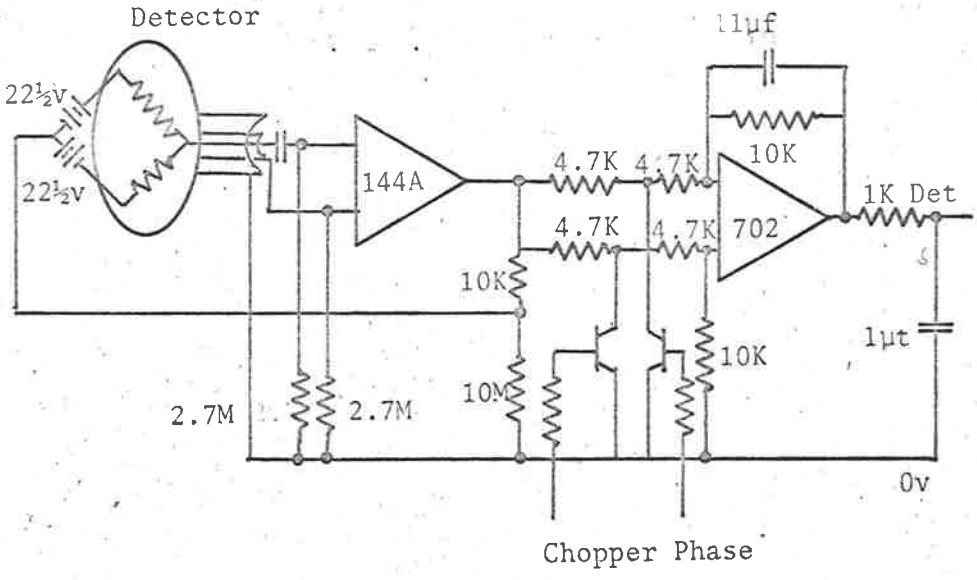

Figure 5.11

Infa-red Detector A mplifier and Phase Detector.

5.11

detector and has the characteristics common to all thermal detectors, viz., wide bandwidth (in this case from 0.65 to 35 microns), long response time (about five milliseconds) and low detectivity (D* = 7850 volts/watt/H_z). (A discussion on infra-red detectors may be found in Potter and Eisenman, 1962). The resistance of the detector is about 2.7 megohms. The two thermistors are connected in a bridge circuit with batteries as the other two arms. The thermistors have similar resistance and the same temperature coefficient, so that the voltage across the bridge is approximately zero. The thermistors are on the same substrate and are exposed to the same ambient temperature, so that changes in the ambient temperature make very little difference to the voltage across the bridge. The difference voltage is measured by a high impedance, low noise amplifier shown in Figure 5.11. The 144A amplifier is a FET input operational amplifier manufactured by Analogic. It has an input impednace of 10^{11} ohms and a noise figure of 10^{-6} volts/Hz in the waveband in use.

The infra-red beam is interrupted by the chopper mirror. The resultant AC signal is converted to DC in the phase sensitive detector. The phase signal is derived from a photocell mounted inside the interferometer in sucha position that sunlight passing through the slit falls on it. The signal from the photocell is amplified in the same way as that used in the interferometer control.

5.3.9. The Interferometer Control.

The interferometer control unit operates the scanning motor of the interferometer. It counts the number of rotations that the drive motor makes and periodically reverses the motion. A 'grain-o-wheat' light bulb is mounted in the interferometer close to the worm gear on the motor. Its light falls on a photocell and the beam is interrupted by a semicircular shield fixed to the worm gear. The signal from the photocell is amplified and the output of the amplifier is squared to give a standard digital pulse. These pulses are counted in a nine bit ripple counter and the output of the last stage operates a bidirectional amplifier similar to that used on the pointer control. The current driving the motor can be controlled by a set of potentiometers. The current was adjusted so that the motor made one rotation in more than 1.6 seconds in each direction. Another motor control was designed. This control stepped the motor in each direction on a signal from the telemetry unit. It did not prove successful because it relied on dynamic braking to slow the motor at the end of each step, and the amount of dynamic braking possible was not sufficient to prevent the motor oscillation.

5.3.10. Power Supplies.

The power supplies are derived from five batteries. Two batteries, of fourteen size C alkaline cells, provide plus and minus twenty-one volts which are regulated to give plus and minus twelve volts. One battery, of eight alkaline cells provides

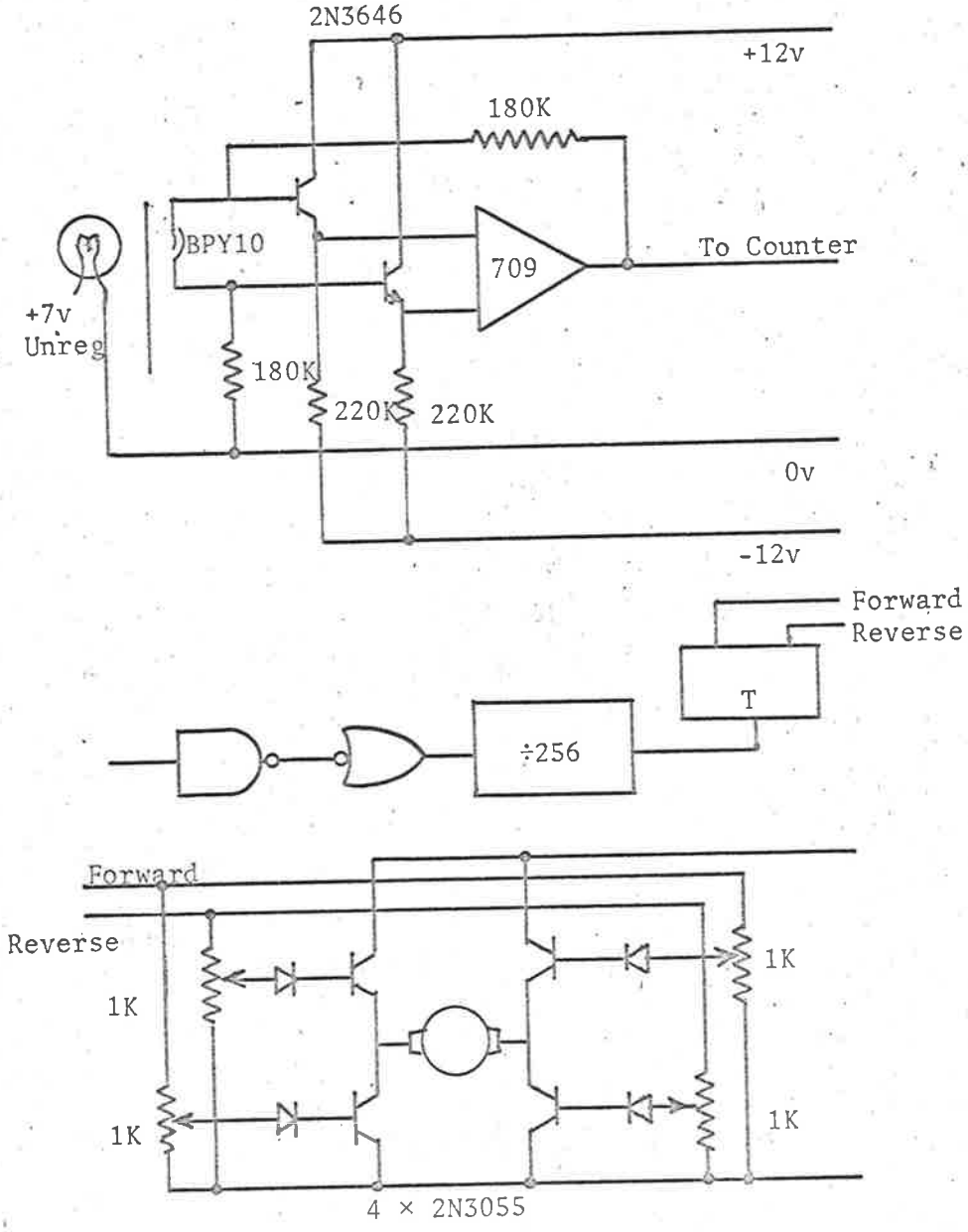

Figure 5.12

Interferometer control

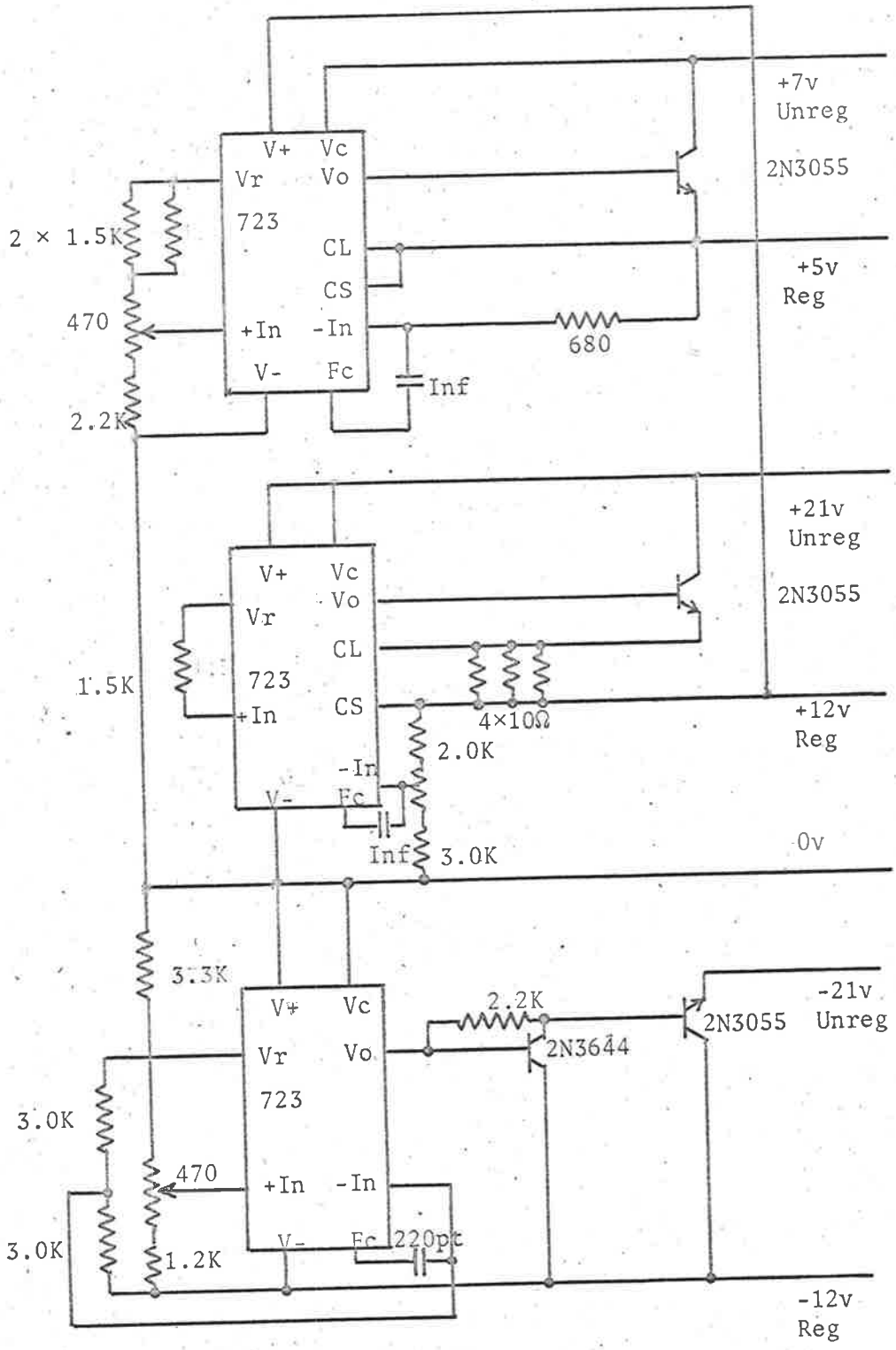

Figure 5.13

Power Supplies

twelve volts unregulated for the transmitter. A battery of five, ten amp-hour nickel cadmium cells provides about seven volts which is regulated to give the five volt supply for the digital circuitry. A similar battery provides seven volts unregulated which powers the motors of the interferometer and sun pointer. The voltage regulators are based on the Fairchild 723 integrated circuit. The circuits are given in figure 5.13. The twelve volt regulators operate for all input voltages from twenty-one to fifteen. This allows the use of cells of a much smaller capacity, and hence weight, than would be necessary if the current was taken directly from batteries. At the end of a flight the alkaline cells are very heavily discharged, but because of the regulators there is no alteration in the operation of the telemetry unit. The twelve volt regulators are standard circuits. The five volt regulator is unusual in that the reference voltage supply obtains its own current from the plus twelve volts line. This has two consequences. Firstly, the five volt line will be turned off simultaneously with the twelve volt line. Secondly, the regulator operates when the seven volt battery potential has fallen to 5.6 volts.

There are two other voltage regulators, which are used to provide calibration voltages. One has an output of about 8.68 volts and the other about 4.70 volts. Two inputs to each ADC measure these voltages which provide a means of in flight calibration.

5.3. The Telemetry Format.

The tables below show what data is transmitted by the telemetry unit and where it appears in the record. The first table describes one word of data and the second described the complete record.

Frame Number	Bit Number	Value
0	1	Indicates that the telemetry unit has been turned off manually and will stop at the end of this record.
0	2	Indicates that this is the last word in a record.
	3	One bit of the record number. The lowest significant bit is transmitted in the first word of the record and the highest significance bit in the last.
	4	Indicates that power supplies to the pointer control and the interferometer control have been turned on by the altitude switch.
	5 & 6	Not used.

Frame Number	Bit Number	Value
1	1 - 3	Indicate which of the pointer photo-cells are illuminated.
	4 - 6	Not used.
2	1 - 3	The lower order three bits of the interferometer control counter.
	4	The direction that the interferometer motor is turning.
	5 & 6	Not used.
3	1 - 3	Bit 1, 3 and 5 of the LPADC number one.
	4 - 6	Bit 1, 3 and 5 of the LPADC number two.
4	1 - 3	Bit 0, 2 and 4 of the LPADC number one.
	4 - 6	Bit 0, 2 and 4 of the LPADC number two.
5	1 - 6	The odd bits of the HPADC.
6	1 - 6	The even bits of the HPADC.
7	1 - 6	Longitudinal parity bits.

TABLE ONE

Word Number	HPADC	LPADC1	LPADC2
0	Detector	0 volts	-21 volt battery
1	0 volts	4.8 volt Cal	Pointer photo-cell A
2	Detector	8.7 volt Cal	Pointer photo-cell B
3	4.8 volt cali-bration	-12 supply	Pointer photo-cell C
4	Detector	12 volt supply	7 volt battery motors
5	8.8 volt cali-bration	5 volt supply	7 volt battery logic
6	Detector	+21 volt battery	Not used
7	Not used	Transmitter Battery	Not used
8	Detector	Not used	0 volt
9	Not used	Not used	4.8 volt Cal
10	Detector	Not used	8.8 volt Cal
11	Not used	Not used	-12 volt supply
12	Detector	Not used	Not used
13	Linear Trans-ducer	One side of interfero-meter motor	Not used
14	Detector	Other side of motor.	Not used

TABLE TWO

CHAPTER SIX

DATA PROCESSING

The telemetry unit described in the preceding chapter performs the experiment, measures the results and converts the data obtained into machine readable form. This chapter describes the means by which the data is transmitted from the balloon to the ground and converted into a human readable form. The first part of the chapter describes the data link between the balloon and the ground. The telemetry unit can be used without this link, for testing purposes, since the function of the data link is to reproduce, on the ground, the digital wave-form which is produced by the telemetry unit. The second part of the chapter describes a suite of computer programs which accept the data produced by the telemetry unit and decodes it into a convenient form.

6.1. The Data Link.

The data link is that part of the telemetry equipment which accepts the digital bit stream from the telemetry unit on the balloon and produces the same bit stream on the ground, usually

at a later date. The data link was standard equipment used by the University of Adelaide for many previous experiments. The most important characteristic of the data link is the amount of noise it inserts into the signal. The data link is the only source of adventitious noise in the experiment. Noise appears in the infra-red detector as an unavoidable consequence of its physical nature. Noise which appears in the data link has nothing whatever to do with the experiment. The use of digital telemtry and the error correcting codes are designed to reduce this noise as much as possible.

The digital bit stream from the telemetry unit modulated a voltage controlled oscillator (VCO). For a digital zero bit, the output frequency of the VCO was about 6.9 KHz. For a digital one bit, the output frequency was about 7.7 KHz. These lie within the international standard Band 11.

The output of the VCO frequency modulated a radio transmitter. The transmitter radiated one watt of power at a frequency of 71.5 MHz. The maximum deviation of the modulation was about 30 KHz. The whole telemetry system can be described, in the usual notation, as PCM/FM/FM. The original data is converted into a pulse code, which frequency modulates a carrier, which, in turn frequency modulates another carrier.

The transmitted signal was received by a Nems-Clarke telemetry receiver. The output of the receiver is usually called the video signal because it usually contains frequencies from

a few tens of hertz to a few tens of kilohertz. For this experiment, the video signal contained the frequencies produced by the VCO. The data was recorded on an Ampex instrumentation recorder. This recorder could record signals either directly, in which case they had to be in the range 50 Hz to 15 KHz, or else in the FM mode in which case the signals had to lie in the range 0 to 500 Hz. The video signal from the receiver was recorded on one channel in the direct mode. The video signal was also connected to a discriminator and demodulator. An active filter selected frequency components in the video signal which lay within the bounds of Band 11. A VCO operating on band 11 was synchronised with the selected signal via a phase locked loop. The voltage required to synchronise the oscillator was directly proportional to the voltage which modulated the VCO at the transmitter, so that this voltage reproduced the original bit stream. This voltage was recorded in the FM mode on another channel of the recorder.

The FM recording was considered to be the prime source of the data. The direct recording of the video signal was purely for insurance in the event of a breakdown of some part of the system.

The discriminator was capable of reproducing analogue voltages. Noise in the transmission path introduced spurious voltages into the signal. A clean digital signal was derived from the signal

using a comparator. Voltages above a threshold were taken to be digital ones and voltages below that limit taken to be zeroes. The overall system was so successful that on one occasion, the signal was inaudible through receiver noise which included a television commercial and yet few errors were introduced into the data. Those errors which did occur were corrected by the error correcting code, so that even under these conditions, the overall error rate was zero.

6.2. The Punching Convention.

The paper tape was punched on a Teletype ASR 33 machine. It attempted to print all characters which it received. As the input data was in pure binary, the characters printed could not be interpreted in terms of original data. Some characters did not print at all, and since the carriage return was an odd parity character and occurred frequently and the line feed was even parity, and should not appear at all, the characters which were printed were rapidly obliterated by overprinting. The punch could be turned on or off while the teletype was printing. The exact representation of the frame received was punched in one row of the tape. The rows and columns of the tape correspond exactly to the rows and columns of the telemetry record described in section 5.1.1. The first six columns with the sprocket hole between the third and fourth columns, contain the data transmitted. The seventh column contains the frame parity bit and the eighth column is always punched while valid

data is being recorded. The teletype can be switched so that it may receive data from a line, or may copy data from the keyboard to the punch. When the teletype is switched to local, the signals on the line are ignored. The teletype is fitted with an "answer back" mechanism which can be activated by the "Here is" key. One depression of this key will cause the punching of twenty null characters. A null character has no holes punched, except the sprocket hole.

The magnetic tape was played back to reproduce the digital bit stream recorded during the flight through an amplifier whose circuit is given in figure 5.8. When the teletype is connected to the amplifier and switched to the line, the digital bit stream is copied to the printing mechanism. The inter-record pauses which occur every 12.8 seconds are easily recognised because the printing stops for 0.8 seconds. The punching convention uses these gaps to ensure that the first frame of a record can be recognised. For ease of handling, the paper tape must be punched in several sections. Each section begins with a leader. This is a length at least two feet, of tape punched with nulls while the teletype was switched to local. The punch was turned off, the teletype switched to line and the magnetic tape started. When the first inter-record gap was heard, the punch was started. This ensured that the first frame punched was the first frame of a record. During the course of the punching occasional faults occurred. These were generally caused by

a single bit error during the inter-record gap. A space pulse after a stop pulse is always interpreted as a start, which causes an extra character to be inserted. Faults of this nature can be detected by the computer programs, but when they were known to occur, it was thought better to resynchronise the data on the tape. To do this, the punch was turned off, the teletype switched to local and the magnetic tape stopped. A group of nulls was punched. Ten nulls is sufficient, but usually one hit of the "Here is" key was used. The magnetic tape was rewound a short distance and restarted. The teletype was switched back to the line and the punch turned on at the first inter-record gap. When sufficient punched tape had been accumulated for one section, the punching was stopped and a trailer of two or three feet of nulls punched. The tapes were then copied into a standard computer record by program PTCONV.

6.3. The Computer Programs.

Two computer programs are described in this section. The first converts the paper tape produced by the teletype into a standard form acceptable to the computer operating system. Once in this form, the data can be held on the computer's disc storage, recorded on magnetic tape, punched onto cards or otherwise stored. The second program decodes and prints the data to give a complete description of the course of the experiment. The structure of the programs and sunbroutines is as follows. PTCONV calls PTREAD which is a system program.

PTREAD calls ASCIBCD which performs editing functions and calls GETCHR and PUTCHR.

RECORDS calls NEWREC to read in the data, INFRAME, TWOROW, and BYTPAR to decode it, and CULP and CALIB to convert the data to measured values.

NEWREC calls NEWINP to read the data, RECNO, and MATCHBT to check that the data is correctly stored and GETBYT and PUTBYT to rearrange it if it is not.

6.3.1. PTCONV.

The program PTCONV reads the punched paper tape, performs a small amount of editing and writes the data as SCOPE records, suitable for magnetic tape. All paper tape input must be performed using the routine PTREAD, which is supplied in the operating system of the computer. PTREAD is in many ways unsatisfactory for reading the telemetry data and much of the complication of the PTCONV program arises from this. Firstly, PTREAD will read only seven bits from the tape. It is impossible to distinguish for certain between leader tape, in which only the sprocket hole is punched, and a genuine data frame with seven zero bits, in which column eight of the tape is punched. The distinction between the two is made by assuming that ten or more successive zero frames are leader frames. Since ten zero frames in the data implies a substantial fault in the telemetry unit, it is perhaps not important that misinterpretation can occur, but

it is annoying that the only way to check for such misinterpretation is by visual inspection of the paper tape. Secondly, it is impossible to read a tape without performing a code conversion. It is possible to replace the standard conversion routine with another of the same name (ASCIBCD) but the read routine always assumes that the standard routine is used and calculates the number of characters read on that basis. The non-standard routine must be written in Compass in order to access the register containing the number of characters read. Thirdly, PTREAD can detect the end of a tape, but when multiple tapes are to be treated as one file, it requires operator intervention to recognise the end of the file. When more than one tape is to be converted, it is desirable that the user supervise the loading of tapes since it sometimes returns an end of file indication without the operator's intervention. This results in the loss of large amounts of data.

PTCONV reads a block of data from the paper tape using PTREAD. PTREAD calls subroutine ACSIBCD which performs the editing functions. The data is copied from the input buffer into an output buffer. When the output buffer is filled, it is written as a single binary record of 512 words. The last word of the last binary record contains -2. The core of the program is ASCIBCD. This routine accepts the characters, stored by PTREAD five to the word and replaces them eight to the word.

The top four bits of the word are always zero. The other fifty-six bits contain eight, seven bit frames read from the tape. If ten or more successive characters are zero, they are replaced by a single word containing the number -1. Since no genuine data can produce a negative word, this provides a flag to indicate a break in the data. The data recommences in the next word with the first non-zero frame. Since, by the punching convention, the first frame after a section of leader tape is the first frame of a telemetry record, the lower order fifty-six bits of each computer word contains one telemetry word and each fifteen words contains a complete telemetry record.

6.3.2. Printing the Data.

The program RECORDS reads the file created by PTCONV and prints the voltages measured by the telemetry unit. The functions which the program performs include allocating frames to their correct positions in the word and record, performing the error detection and correction, decoding the records, applying the conversion factors to give the results in volts and correcting those factors as dictated by the telemetry self-calibration action. Most of these functions are carried out by subroutines which are described in the following sections.

The data produced by PTCONV is in the form of binary records of 512 words each. RECORDS expects data cards containing, in the first field, the number of a binary record. The telemetry data is skipped until that record is found and read. The second

field of the data card contains the number of the word within that record from which searching may start. The next field is the number of telemetry record which it is desired to print out. The fourth field contains the record number of the first telemetry record expected.

The subroutine NEWREC, which handles the telemetry records will make special checks if this is not the number of the first record found. The last three fields of the input data card contain the hour, minute and second at which the telemetry unit was started.

The output of RECORDS contains the data from three telemetry records on each page. At the top of the page is given the number of the binary record and the number of the word within that record at which the search for the first record begins. The next line gives the contents of that word and the next three words as they appear on the input tape. The first line of each telemetry record printout contains, firstly, its telemetry record number; secondly, the binary record number and the word number at which this record can be found; thirdly, the time at which this record was transmitted and finally, the conversion constants for the ADC's. The next fifteen lines contain the data of each word of the record. The first field of each line contains the data word as it exists in one computer word. When synchronisation of the data has been carried out correctly by PTCONV, the first four words of the first record on the page are the same as the four words printed at the top

of the page. If the synchronising has been performed within RECORDS by the subroutine NEWREC, then the words at the top of the page will differ from those in the records. The next eight fields of the output line contain representations of the frames of the word. Only the six data bits are represented. If the parity bit was incorrect, and the error cannot be corrected, the field is followed by an asterisk. The tenth field in the line is an error indication. If the field is zero, then no error was detected. If a single error was detected and corrected, then the field contains the number, in octal, of the frame in which the error occurred. If more than one error was detected in the word, the number in the field, converted to binary, will indicate the columns in which errors occurred and the field will be followed by an asterisk. The last three fields give the measurements, in volts, made by the two LPADC's and the HPADC for that word.

The program RECORDS stores the readings from the ADC's as each record is decoded. At the end of the record, it calls the subroutine CALIB which performs the calibration of the ADC's. The calibration values required, and which are printed by RECORDS, are the conversion factors of the two LPADC's, the values of the positive and negative twelve volt supplies (which are used to off-set the LPADC's for some of their measurements) and the conversion factor of the HPADC. All ADC's measure a calibration voltage, which is assumed to be constant. The actual value is

compared with the value calculated by the old calibration factor and an estimate of the new calibration factor found. If this estimate varies by more than ten percent of the old value, it is assumed to be in error and ignored. Otherwise a new calibration factor is found. The new value is 0.95 of the old value plus 0.05 of the new estimate. In this way, the calculated value of the calibration never varies by more than half a percent between any two records. Since the major source of changes in calibration is changes in temperature, and calibration is performed once every 12.8 seconds, this is a reasonable maximum variation to permit. The effect of a single calibration is small, but the effect of many successive calibrations, all tending in the same direction can be large, so that short term variations in the calibration are averaged out and long term variations remain.

The subroutine CULP converts the readings of the low precision ADC's into the voltage values. The routine corrects many of the faults of the electronic circuits. Firstly, the counters of the LPADC's are not cleared before a conversion. CULP keeps a record of the previous count in each ADC and subtracts this from the current count. The difference, modulo sixty-four is the number of pulses received during the conversion. Secondly, the ADC's always add one extra count at the beginning of the conversion so that CULP must subtract one from the value found. Thirdly, the diode switch which multiplexes the ADC

inputs introduces a non-linearity in the conversion. This non-linearity depends on the current going into the ADC input amplifier. Since it is this current which the ADC measures directly, the diode correction is given as a function of the number of pulses received from the ADC. The corrections are given in the array D which is indexed by the number of pulses and contains the measured voltage drop across the diodes. It is assumed that the voltage drop is the same for all diodes and experiment confirms that this approximately so for diodes of the one batch. Finally, CULP, uses the values of gain and offset voltage calculated by CALIB and the known values of the gain and offset resistors to calculate the value of the voltage which is being measured.

All data input is handled by the subroutine NEWINP. There is a common region named BUFFER which contains space named UF, for two data records of fifteen words each one, one binary record named BF of 512 words and two counters. One counter points to the next word to be accessed. The other counter contains the number of the current binary record. When NEWINP is called, the words of BF which have not yet been accessed are copied into the underflow region UF and the word counter is set to point at the copy of the next word in UF. (This is a subterfuge to get around the fact that in FORTRAN the lower limit of array indices is restricted to value one. Effectively, the array UF acts like elements BF(-29) to BF(0).) A new binary record is read into BF

and the record counter incremented by one.

Subroutine NEWREC finds the next record of data in the buffer BF and assembles it in the fifteen word array KR, which is the first parameter. The second parameter given is LR, which initially contains the number of the last record found by NEWREC and finally contains the number of the new record. NEWREC always checks that the word counter is more than thirty words from the end of the buffer. If not it calls NEWINP to refill the buffer. In normal circumstances NEWREC finds the record number of the next fifteen words in the buffer using RECNO and copies the record into KR and the record number into LR. Occasionally, RECNO may find a flag. If the flag is -2, indicating the end of the data then the flag is returned as LR. Otherwise NEWREC starts again from the word immediately following the flag. This allows NEWREC to take advantage of the fact that normally one data word is stored in one computer word. If the end of record bit is missing the new record number is checked to see if it is one more than the last number. If it is then it is assumed that a single error has occurred and the record returned normally. If it is not then MATCHBT is used to check for the probable presence of a record. If a record is not found straight away then the data is searched, one frame at a time until a record or a flag is found. If a record is found it is copied one frame at a time into the array KR so that the words of the record are correctly aligned in the computer

word. In practice, NEWREC has shown itself capable of recognising and synchronising with very badly garbled data. Such synchronising requires a lot of computer time and much of the complication of NEWREC is designed to avoid it unless absolutely necessary.

Subroutine RECNO scans through one record of data and obtains the record number. It assumes that the bits of the record number are found in bit fifty-one of the computer words. RECNO returns the record number found as its second parameter and the number one as the third parameter. It will check for the presence of the end of record bit in the last word of the record. If it is not present it will return zero as the last parameter. If in the course of forming the record number a negative word is found, then the number of that word is returned as the record number and the word itself as the third. A negative word is a flag indicating that the data has ended. If the flag is -2, then there is no further data. If it is -1 then a new record may be presumed to begin in the word immediately following the flag.

A number of the bits in every word of the data are not used, or have a fixed value. These bits provide a means of checking for the beginning of a word. The subroutine MATCHBT performs such a check. The first frame of every word contains the bits 1 1 1 x e 0, where x may be either 1 or 0 and e is 0 except in the last frame of the record. MATCHBT has three parameters. The first is a fifteen word array and the second is an

integer. There are eight frames to a computer word, numbered from 0 to 7. MATCHBT searches the array looking for the pattern of the first frame of a data word in the frame position indicated by the integer. It counts the number of bits in error and returns this value as the third parameter. It includes a check that the end of record bit e is zero except in the fifteenth word of the array. The routine which uses MATCHBT assumes that if there are three or fewer bits in error then a record begins with the indicated frame of the first word of the array.

The subroutine INFRAME separates a word of data into its constituent frames and if necessary corrects any single errors which may have occurred. The parameters of INFRAME are, the word of data, the name of an eight word array to contain the frames and a word which will contain the error indication. The data word is decomposed by shifting and masking. As each frame is obtained the number of ones in it is counted. If the result is even, that is, there is a frame parity error, then the byte is complemented and the address of the byte is saved. The number of frame parity errors is counted. Each frame is also exclusive-ored to a longitudinal error counter. When all eight bytes have been found the number of ones in the longitudinal parity counter gives the number of longitudinal parity errors. If there are no frame errors and no longitudinal errors, then the error indication is set to zero and the subroutine is left. If there are exactly one frame error and one longitudinal

error then the offending frame is recomplemented and the longitudinal parity check word is exclusive-ored to the frame. This has the effect of inverting the incorrect bit in the frame.

The subroutine returns with the ordinal number of the corrected frame in the error indication. In all other cases a multiple error, which is not correctable, has occurred and the subroutine complements the longitudinal parity check and returns it as the error indication. To summarise, a zero error indication means that no parity faults were detected, a positive value means that a single error was detected and corrected, and a negative value indicates that more than one error occurred. In the last case the rows in which errors occurred are negative and the columns in which errors occurred can be found by re-complementing the error indication word.

When printing out the frames, RECORDS appends an asterisk to the negative frames to indicate the error and then recomplements them to give the true value of the frame. RECORDS also handles the error indication in the same way.

Examples of the error indication in the print out and their meanings are

00 = No errors were detected.

04 = A single error in frame four was corrected.

00* = At least one frame parity fault was detected without a longitudinal parity fault.

04* = Column three has a longitudinal parity fault.

14* = Columns three and five have parity faults.

The subroutine BYTPAR handles the parity error printing. It scans the frames of data and when it finds a negative frame, complements it and sets an error indication word to an asterisk. BYTPAR is written in Compass, because it is not possible to distinguish between positive zero and negative zero in FORTRAN.

The subroutine TWOROW interleaves the bottom six bits of two words to produce a twelve bit number. The odd numbered bits and even numbered bits of the ADC counters are transmitted in successive frames of data. TWOROW sorts the bits into the correct order to recover the original value of the count.

GETBYT and PUTBYT are a pair of subroutines which handle individual frames of data. Both have four parameters. The second parameter of each is a word of data, the third is an index to that word and the last is the index of the required frame in that word. GETBYT reads the indicated frame and puts it in the first parameter. PUTBYT stores the first parameter at the indicated frame. Both subroutines then increment the frame index and, if necessary, the word index. The two subroutines are complementary. The following loop appears in NEWREC.

```
      DO 17 I=1, 120
    CALL GETBYT (CH,BF(IB),IB,J)
17  CALL PUTBYT (CH,KR(K),K,L)
```

This move frames one at a time from the array BF, which is the input buffer, to the array KR, which is the new record. This

loop is used whenever it is known that the telemetry words are not correctly synchronised in the computer words. GETCHR and PUTCHR perform similar actions within ACSIBCD. PUTCHR is identical to PUTBYT. GETCHR selects the frames stored five to a word by PTREAD.

CHAPTER SEVEN

R E S U L T S

Two flights were made with the equipment described in previous chapters. The first was made on July the 28th., 1971, to test the operation of the telemetry unit and the pointer. The second, made on the 17th. of January, 1972 tested the interferometer and the experiment as a whole. Both flights were made from the Department of Supply Balloon Launching Station at Mildura. In both cases, the experiment hitch-hiked on the payload of an American air sampling experiment named Hibal. This is unfortunate from the point of view of water vapour determinations, as it is believed that large balloons carry large amounts of water vapour with them into the upper atmosphere. For the first flight, this did not matter, as the flight was intended purely as an engineering flight. For the second flight, the inclement weather and pressure of time forced a hitch-hike flight.

7.1. The First Flight.

The first flight took place on the morning of the 28th. of July, 1971. It was intended purely as an engineering flight. The interferometer was not flown and its place was taken by a pair of sun-sensors mounted on the pointer. Other sun-sensors were fixed to the frame of the experiment and a shaft encoder measured the angular position of the pointer to verify the operation of the pointer at altitude. The account of this flight will treat the different units, particularly those which required modification.

7.1.1. The pointer.

The experiment was mounted on top of a standard Hibal 105,000 ft. air sampling package. This package includes a four feet high chimney which rose past the pointer. The telemetry record shows that the pointer control was turned on as the balloon passed five thousand feet. As the balloon had been launched before dawn in mid-winter, the pointer was still in darkness at this time. The pointer rotated, hunting for the sun until the balloon reached about 18,000 ft. At this time it appeared to oscillate about a single position. This had been observed during laboratory tests whenever it was illuminated with light which was almost sufficient to operate the photocells. It is believed that the pointer attempted to lock onto a bright cloud on the horizon. Shortly afterwards, a shadow passed over the pointer, probably cast

by part of the Hibal framework, and the pointer hunted for, and found the sun. Throughout the rest of the flight, the pointer continued to find the sun without the apparent hesitation. Frequently, during the flight, the chimney mentioned above cast its shadow across the pointer and the pointer would hunt until the balloon rotated sufficiently for the pointer to again be in sunlight.

Nevertheless, the pointer was locked onto the sun for continuous periods of up to twenty minutes. It was considered that this test verified the operation of the detector, since it was anticipated that the experiment would be flown on a balloon on its own, so that it would be arranged that no object could interfere with the pointer.

7.1.2. The Sun Sensors.

For this flight, there were two sun-sensors mounted on the pointer. One of them was open to the sun. The other received light from the sun through a low pass interference filter. The open sensor was sensitive to light in the range 0.3 to 1.3 microns. The filtered sensor was sensitive to 1.0 to 1.3 microns. It was expected that the difference between the two sensors would give some indication of the amount of absorption in the 1.1 micron band of water vapour. It was also expected that the outputs of both sensors would increase during the flight, so that both were adjusted to give about four volts output at ground level. During the flight, the open sensor did show a small increase over its ground level

output. It also confirmed that the pointer was aimed at the sun and that the frequent loss of lock was due to a shadow across the pointer photocells. When the balloon was rotating in a particular direction the shadow passed over the sensor first and its output dropped to zero suddenly. When the sun came out of eclipse, the output of the open sensor rose slowly until the pointer locked onto the sun again.

The filtered sensor did not show an output greater than 0.1 volts throughout the whole flight. It did show a variation in output while the pointer was hunting for the sun. It showed maximum output immediately before the open sensor began to rise. This was interpreted by assuming that the filter holder had moved during the launch so that the sensor was shielded by the holder rather than the filter and that the increase in output observed was caused by light coming from an oblique angle past the filter. Because of the violent landing, it was not possible to verify that this was the case during the flight, but when the assumed conditions were set up on a ground test afterwards, the same results were obtained.

Figure 7.1 shows the kind of results obtained during one rotation of the balloon.

7.1.3. The Telemetry Unit.

The telemetry unit operated faultlessly until the balloon reached five thousand feet altitude when the pointer motors turned on. It was known that the motors were capable of generating

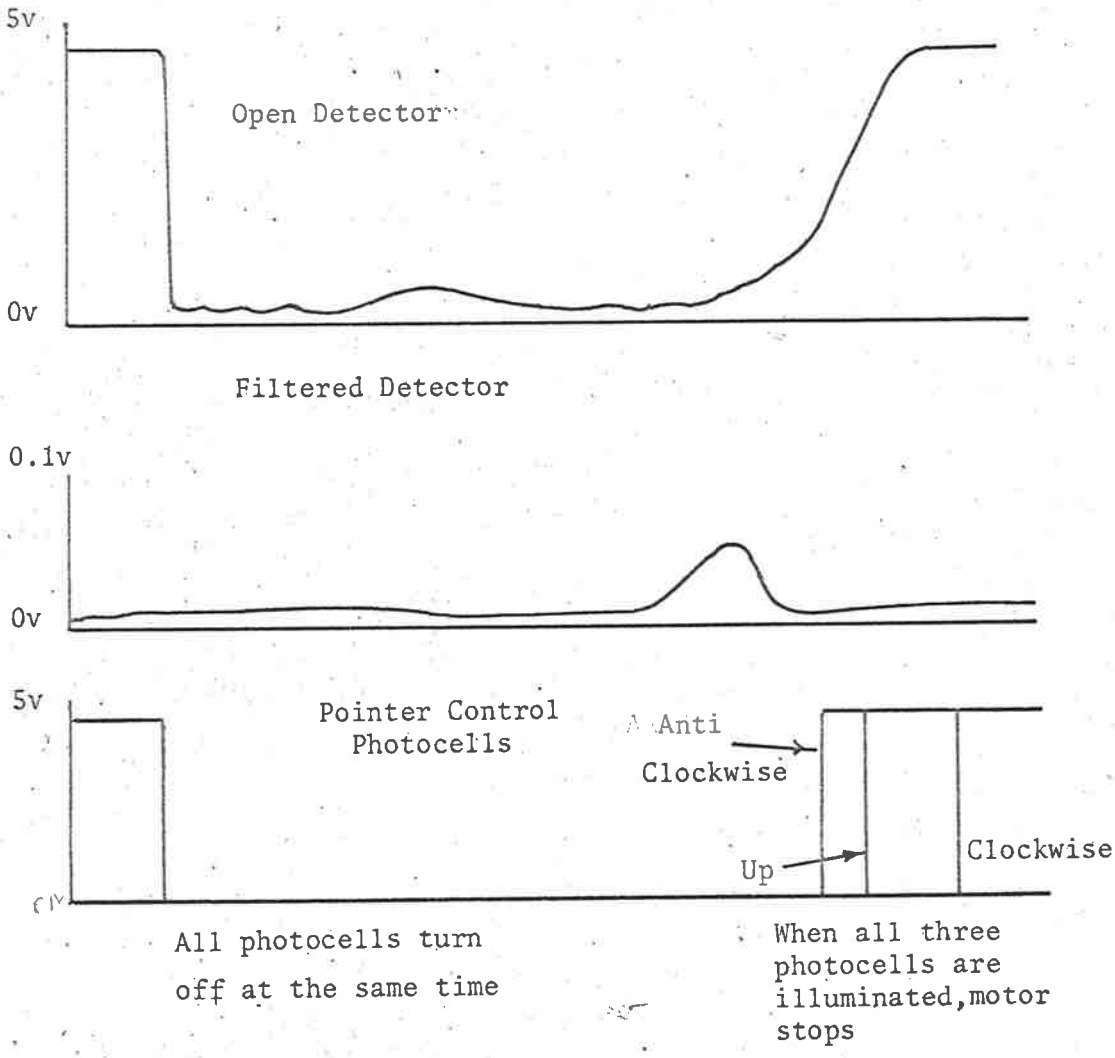

Figure 7.1

One Rotation of Pointer

noise pulses with an amplitude greater than seventy volts and rise times less than ten nanoseconds. These pulses had been suppressed by a pair of back to back zener diodes on each motor together with a large value electrolytic capacitor and a polyester one. In the laboratory these had successfully suppressed the motor noise. As the motors started, one of these diodes fused and the other diode on the same motor, being forward biassed also fused so that the motor noise was no longer suppressed. After the flight, the diodes were replaced with ones of higher power disipation rating, and the trouble never recurred.

The immediate result of the motor noise was that the various counters in the telemetry unit received extra pulses. Most affected were the longitudinal parity accumulators and the word counter. The extra pulses counted by the parity accumulators completely vitiated the error checking capability of the telemetry. The pulses in the word counter had a more serious effect. The most usual effect was to reset the word counter after the eighth word, thus repeating the first eight words of the record. It did not, however, restore the shift register of the record number counter to its initial value. Thus, the contents of the record counter were effectively multiplied by 256 each time one such event occurred. The record number was therefore useless as a time indicator. Towards the

end of the flight, one bit of the digital multiplexer failed, producing continuous ones. This proved to be caused by a dry joint which was repaired afterwards.

7.1.4. The Voltage Controlled Oscillator.

During the flight, the amplitude of the VCO output remained approximately constant. The modulation of the frequency showed a marked variation throughout the flight. The frequency corresponding to the logical zero remained constant and indicated a voltage of about zero. The frequency corresponding to the logical one varied so that at the beginning of the flight, the frequency indicated a voltage of about five volts. During the flight, the indicated voltage for a logical one decreased slowly and uniformly until at the end of the flight it was about - 3 volts. For a part of the flight, the indicated voltage was so close to zero that it was impossible to transcribe the data. In the latter part of the flight, the data had to be inverted before transcription. The digital part of the telemetry had evidently continued working through the whole flight, so that the indicated voltages could not be the actual ones. Not only will the digital circuits not work with negative voltages, they will be destroyed by them. It was therefore assumed that the VCO was at fault.

The VCO used in this experiment had been used for several years in other balloon experiments and this phenomenon had never been seen before. It was at first attributed to

temperature effects, but no mechanism for the observed fault could be suggested. Laboratory tests over a wide range of temperatures and supply voltages were unable to reproduce the effect. The manufacturers of the VCO claimed that the effect was impossible. In the absence of any theoretical or experimental explanation of the phenomenon, the only alteration made was to increase the logical one voltage input to the VCO to eight volts, in the hope that if the effect did recur the logical one voltage would remain positive. However, the effect was never seen again. Throughout all subsequent testing and the whole of the second flight, the indicated voltage of the logical one remained at eight volts.

7.1.5. The Landing.

The payload landed in a breeze, and the switch which released the parachute failed to operate, so that the payload was rolled over several times. This resulted in some damage to the experiment, none of it serious, but it did destroy much of the usefulness of the post-flight checks. The frame of the Hibal package, to which the experiment had been attached was damaged beyond repair.

7.1.6. Summary.

This flight brought to light a number of faults, all of which were successfully corrected. The major faults were the failure of the noise suppression on one motor and the peculiar effect of the VCO.

7.2. The Second Flight.

The second flight was made from Mildura on the morning of the seventeenth of January, 1972. This flight was intended as a complete test of the whole experiment, but an engineering failure prevented the correct operation of the interferometer, so that the value of the flight lies mainly in the confirmation of the correct operation of the rest of the system. It was intended to fly the experiment on its own on a small balloon, but adverse weather conditions delayed this flight and others which were scheduled for the same period. It was decided to combine this flight with a normal Hibal flight and use a larger balloon than usual. This has a number of disadvantages. Firstly, the ascent rate was the usual 1,000 feet per minute, rather than the 300 to 500 which is desirable for the interferometer. Secondly, the launch had to be delayed until such a time that the balloon would be in sunlight at 5,000 feet. Thirdly, it is believed that the larger balloons carry large amounts of water vapour into the upper atmosphere and so giving erroneous results to the experiment.

This account is divided into four parts, the preflight preparations, the flight itself, the descent and the post-flight checks. All the times are given in Universal Time. To relate these to time of day, note that the launch occurred at 0641 Eastern Australian Summer Time on January the seventeenth and the landing at 1141 EAST. The balloon travelled a distance of about 100 miles in a south-westerly direction, and the float altitude was about 71,200 feet.

7.2.1. Preflight Preparations.

The experiment was mounted on top of the Hibal package. This package, designed for air sampling at 70,000 ft. did not have the chimney which interrupted the pointer on the previous flight and the guy wires supporting the packages were sufficiently far from the pointer as to cast only the penumbra of their shadows onto the pointer.

The experiment was fixed in position by about 1745 UT the telemetry antenna was connected and the transmitter turned on. The receiver was tuned in to the transmission and it was verified that the digital bit stream was being transmitted through the whole data link to the tape recorder. All the ground station equipment was left with power on, but the telemetry unit was turned off. The whole payload was then taken out to the launching site. The launch program for the experiment was mapped out beforehand, but to handle possible emergencies, it was intended to communicate between the launch site and the ground station by means of hand-held radio transceivers. In the event, electrical noise from the launch vehicles limited the communication to one direction, so that communication from the ground station to the launch site was not possible.

The preparation of the telemetry was completed at about 1915 UT and the transmitter turned on. The first few seconds of the transmission were heard at the ground station and then

the receiver went dead. The student manning the ground station believed that the transmitter was faulty. The telemetry was switched to the run state at 1929.58 UT at the launch site, at which time the numbering of the records began. The telemetry unit was sealed and the balloon launched at 1941.30 UT. On return to the ground station the author determined that the receiver was faulty and repaired it. The first complete record received was number 131, transmitted at 1957.54 UT.

7.2.2. The Flight.

From the launch, the balloon maintained a climb rate of about 1,000 feet per minute. At 1958 when the telemetry record began, the altitude was about 16,000 feet. The infra-red detector output was zero and the linear transducer output was less than 0.1 volts. Both of these values were maintained throughout the flight. The interferometer was not scanning, although the power was being supplied to the scanning motor. The counter which controls the scanning motor was operating erratically. It was counting faster while the motor was turning in one direction than in the other. This had been observed during testing of the interferometer and was caused by electrical impulses from the interferometer drive motor entering the amplifier which sensed the position of the motor. These impulses were added to those derived from the position control photocell and caused the counter to change the direction of the motor too soon. The impulses were more effective at incrementing the

counter when the motor was moving in one direction than in the other, so that the length of time that the motor moved in the first direction was less than that in the other direction. The fault was cured in the laboratory by spark suppression diodes and condensers. It is believed that one of the electrolytic capacitors failed as the air pressure fell at the beginning of the flight. The interferometer had been operating correctly in vacuum tests in the laboratory, where the rate of change of pressure was much faster than on the balloon. It is probable that the damage to the capacitor occurred during transport to Mildura where there are no facilities for vacuum testing a large experiment.

The sequence of events leading to the observed results is believed to be as follows. The motor started when the pressure switch indicated 5,000 feet and the net result of ten minutes of faulty operation was to unscrew the micrometer until it became disengaged. In this position the output of the linear transducer was small, since the disengaged position was chosen as the zero of the transducer. The zero path difference position corresponded to about 3.9 volts output from the transducer. In the extreme position sides of the fixed and moving mirrors come very close, and it is believed that a particle of glue from the mountings was jammed between the two causing them to tilt so that the image of the sun and the interference pattern no longer fell on the detector.

The engineering data returned by the telemetry included information on the action of the pointer and battery voltages.

The nominally twenty one volt battery which supplied the twelve volt regulator declined from 18.5 volts at 2000 UT to about 16.4 volts at 2400 UT. The seven volt battery supplying the power to the five volt regulator declined from 6.45 volts to 5.65 volts in the same time. The seven volt battery supplying the motors started at about 6.66 volts, fell to about 6.15 volts around 2040, rose again to a maximum of about 7.04 volts around 2235 and varied erratically between 7.5 volts and 5.3 volts. This erratic behaviour is coupled with the erratic behaviour of the pointer described below. The transmitter voltage, nominally twelve volts, declined steadily from about 11.3 volts at 2000 UT to 10.3 at 2400 UT. The twenty one volt negative supply was not measured correctly due to a design fault.

The pointing control operated correctly for much of the flight. The indicators show that it was locked on to the sun at the first record received and remained locked on with very occasional movements until about 2206 UT when it started to indicate periodic hunting, as if a shadow was passing across it. At this time for the position of the balloon (approximately 141°E and 35°S) the altitude of the sun was about 75 degrees. Since the balloon subtended about 30° from the position of the pointer, the erratic behaviour can be interpreted as the sun being seen through the fabric of the balloon. As the balloon rotated, scattering by the balloon and reflections within it

provided sufficient light to simulate the presence of the sun until the angle between pointer and sun was large. When this happened, the pointer would rotate until it found some chance reflections which could operate the photocells. Further rotation of the balloon would repeat the actions. The measurements of the photocell amplifiers by the LPADC's frequently indicate voltages of between 0.5 and 2.5 volts at this time these being neither a logical one or logical zero. This would be caused by partial illumination of the photocells by a source too weak to operate them properly. Such a source would be specular reflection of the sunlight within the balloon. In laboratory tests it has been found weak sources do produce ambiguous voltages. These results in heavy battery drain, usually pulsed with frequencies of ten of Hertz and a corresponding oscillation of the pointer. It has also been observed during out of doors tests of the experiment. In one case the pointer attempted to lock on to the reflection of the sun seen in a window.

7.2.3. The Descent.

The payload of the balloon was cut down at 0009 UT, 17th. January. The telemetry signal was inaudible most of the time and the error rate in the recovered data averaged about three bits in error per word. Nevertheless, much of the engineering data was still readable. No alteration of the operation of the telemetry unit was observed at cutdown, or

afterwards, until 0017.20 UT. At this time, three sudden changes occur simultaneously. Firstly, the record counter contents shift, so that the time calculated from the counter was about five hours in error. The appearance is as if an extra clock pulse had been inserted so that the reading of the counter was doubled. Secondly, both the LPADC's failed. Most of the values read out correspond to an input of 8.67 volts. Thirdly, the pointer action changes. The action of the pointer corresponds to frequent periods of complete darkness with a few periods of full sunlight. These three events are interpreted as the opening of the recovery parachute, which is known to be a violent shock. The parachute usually opens at about 45,000 ft. altitude. The official altitude readings for this flight puts the 45,000 ft. reading at 0019 UT, but a smooth curve drawn through all the other readings suggests that the payload passed through 45,000 ft, at around 0017 UT and that the 0019 altitude reading is in error. This is not unlikely, since the altimeter is a mechanical device attached to an aneroid barometer. A sudden shock could cause the movement of the altimeter to stick, to be released as the force exerted by the barometer increased as the pressure increased. No further incidents were observed during descent. The telemetry signal was received until impact at 0041 UT.

7.2.4. Post Flight Checks.

The experiment was recovered without damage. The landing had evidently been gentle and it was believed that the state of the experiment as recovered was the same as that during the

flight. The interferometer was inspected to determine the cause of the failure. The micrometer was found to be disengaged and the fixed and moving mirrors were out of alignment, in agreement with the data recorded by the telemetry. In a subsequent test on the ground the interferometer appeared to work correctly. It was discovered that one of the electrolytic capacitors has an internal break. It is believed that at sea-level pressures, the mechanical strength of the container holds the break together, but at low pressures, the container expands and the capacitor no longer suppresses the interference sufficiently. The fault which appeared in the LPADC's after the parachute opened was due to a printed circuit coming loose in its socket. It is suspected that as the board moved it momentarily shorted the five volt power supply, causing the extra pulse which altered the record counter.

7.2.5. Summary.

The flight failed to show that the interferometer operated correctly. No information about the atmosphere was returned. All the data which was returned, however, verifies the correct operation of all of the rest of the experiment. In particular, the flight verified that the telemetry unit was capable of the high precision and high reliability necessary for the experiment.

CHAPTER EIGHT

C O N C L U S I O N

This thesis describes the design and construction of a novel form of interferometer. The interferometer is designed for use in situations where a robust, light weight Fourier transform spectrometer is required. It is capable of analysing radiation over a very large range of wave-lengths. The instrument described here was designed for a particular experiment and covers one decade of wavelengths, from two to twenty microns. Few laboratory instruments cover so large a wave-band and those that do are necessarily too large for balloon or space flight. By reducing the step size and the tolerances of the slits and mirrors, it is possible to construct an interferometer of the type described here which will operate over two decades, from about 0.3 microns to 30 microns.

The interferometer has been tested under a wide variety of conditions. The accuracy of the alignment was checked at a much shorter wavelength than it was designed for. It was found that the alignment remained stable to the extent that

the shift of the interference fringes was unobservable after five hours of vibration. No change in the interference pattern was observable during normal diurnal temperature changes. It has few moving parts and is capable of withstanding motions of a normal balloon launching. The weight of the interferometer is about two pounds. It has all the properties necessary for a wide band balloon borne spectrometer.

REFERENCES

The theory of Fourier transform spectroscopy is reviewed in:-

Vanasse, G.A., Sabai, H., Progress in Optics 6, 259, (1967)

Its use in astronomy is reviewed in:-

Connes, P., An Rev Astron., 8, 209, (1970)

The history of Fourier transform spectroscopy is reviewed in:-

Loewenstein, E.V., Ap. Opt., 5, 845, (May 1966)

The chapter on atmospheric absorption is largely based on:-

Goody, R.M., "Atmospheric Radiation", Clarendon Press, 1964.

Other papers cited are:-

Burch, D.E., Gryvnak, D., Singleton, E.B., France, W.L. and Williams, D., AFCRL Res. Rpt. 62-698 July 1962.

Burch, D.E., Howard, J.N., Williams, D. J. Opt. Soc. Am., 46, 452, (1956)

Connes, J., J. Phys. Rad., 19, 3, 197 (March 1958)

Connes, J., Connes, P., J. Opt. Soc. Am., 56, 896 (1966)

Cooley, J.W., Tukey, J.W., Math. Comp. 19, 296 (1958)

Ditchburn, R.W., "Light", Blackie (1963)

Elsasser, W.M., Harvard Met. Studies, No.6 Harvard University Press, (1942)

Fellgett, P.B., Ph.D. Thesis (1952)
also
Fellgett, P.B., Science J., 3, 58 (April 1967)

Fizeau, Ann Chim Phys., (3), 66, 429 (1862)

Gebbie, H.A., Phys. Rev., 107, 4, 1194 (Aug. 1957)

Gebbie, H.A., Delboulle, L., Roland, G.,
M.N.R.A., 123, 497 (1962)
M.N.R.A., 9, 125 (1964)
Astron. J., 69, 334 (1964)

Goody, R.M., Quart. J.R. Met. Soc., 78, 165 (1952)

Gush, H.P., Bruijs, J., Can. J. Phys., 42, 1037 (1964)

Hanel, R., Conrath, B., Science, 165, 1258 (1969)

Harwood, K., Honours Thesis (1966)

Hertzberg, G., "Molecular Spectra and Molecular Structure"
I Spectra of Diatomic Molecules (1950)
II Spectra of Polyatomic Molecules (1945)

Howard, J., Burch, D.E., Williams, D., AFCRL Res. Rpt. 39-41 (1955)

Jaquinot, P., Dufour, C., J. Rech. CNRS No. 6, 91 (1948)

Kaplan, L.D., Proc. Toronto Met. Conf., 43 (1953)

Ladenberg, R., Reiche, F., Ann. Phys., 25, 876 (1913)

Lipson, M., "Physical Optics"

Lorentz, H.A., Proc. Roy. Acad. Science (Amsterdam) 8, 591 (1906)

Michelson, A.A., Phil. Mag., (5) 31, 256 (1891)

Potter, J., Eisenman, B., Ap. Opt. 1, 567 (1962)

Raleigh, Phil. Mag., (5) 34, 407 (1892)

Rubens, H., Wood, R.W., Phil. Mag. (6) 19, 764 (1910)

Strong, J., J. Opt. Soc. Am., 47, 5, 354, (May 1957)

Strong, J., "Concepts of Classical Optics"

****